Transient suppression in hybrid electric ship power systems

by

Viknash Shagar

Australian Maritime College, University of Tasmania

Submitted in partial fulfilment of the requirements for the degree of

Doctor of Philosophy

University of Tasmania March 2019

Declaration and Copyright Statement

Statement of Originality

To the best of my knowledge, this thesis contains no material which has been accepted for a degree or diploma by the University of Tasmania or any other institution, except by way of background information and duly acknowledged in the thesis, and to the best of my knowledge and belief no material previously published or written by another person except where due acknowledgement is made in the text of the thesis, nor does the thesis contain any material that infringes copyright."

Viknash Shagar
2019

Statement of Authority of Access

I, the undersigned, the author of this thesis, understand that the University of Tasmania will make it available for use within the university library and by microfilm, digital or other photographic means, allow access to users in other approved libraries.

This thesis may be made available for loan and limited copying provided that the right of this author is identified/acknowledged in accordance
with the Copyright Act 1968.

Beyond this, I do not wish to place any restrictions on access to this thesis.

Viknash Shagar
2019

Statement of Ethical Conduct

"The research associated with this thesis abides by the international and Australian codes on human and animal experimentation, the guidelines by the Australian Government's Office of the Gene Technology Regulator and the rulings of the Safety, Ethics and Institutional Biosafety Committees of the University."

THESIS ABSTRACT

The requirements for power quality in ship power systems have been increasing over the years. This is an essential consequence of improving the efficiency of the onboard power network and reduce emissions in the long term. The connection of sophisticated navigation and measuring instruments into the grid has also necessitated a higher quality of power to ensure optimal operating conditions for all the loads and avoid malfunction of equipment onboard a ship. The most significant challenge to maintain power quality for the shipboard power system is to mitigate the transient conditions that arise due to the widely varying load conditions imposed by varying sea conditions as well as fluctuating onboard power demands.

This work has attempted to illustrate the extent of the transient phenomena due to load changes in the case of vessels with hybrid mechanical and electrical propulsion. Subsequently, control solutions to limit and reduce such transient conditions and their propagation that include energy storage devices such as the capacitor and battery have been developed.

A shipboard power system with hybrid propulsion has been modeled and the transient responses to various types of load changes during the course of different modes of operation possible for the hybrid system have been analyzed. An active damping strategy has been developed to reduce the torsional vibrations at the drive shaft of the thruster due to extreme load conditions while avoiding overdesign of the shaft itself. The strategy has been extended further to incorporate a capacitor clamped inverter to reduce the electrical transients that are caused by propagation of these transients from the mechanical portion of the hybrid propulsion system into the electrical system. A Model Predictive Control (MPC) strategy has also been developed for a Battery Energy Storage System (BESS) to mitigate the electrical transients arising as a result of propulsion and service load transients while keeping the main engine in the optimum operating range. The MPC power converter control allows for the battery to smoothen the electrical frequency profile during different types of extreme load change conditions and allows for charging and discharging the battery repeatedly. The findings of this research work have significant implications in defining the extent of transient conditions in hybrid power systems. In addition, the efficacy of integrating an energy storage system into the hybrid electric propulsion power network in order to reduce the transients has also been proven.

THESIS ACKNOWLEDGEMENTS

Sir Issac Newton once said '*If I have seen further than others, it's by standing upon the shoulders of giants*.' My giants would undoubtedly be my Academic supervisors Dr Shantha and Dr Hossein. I owe a huge debt of gratitude to my Academic supervisors for their invaluable support in every step of this long journey. They have given me a once in a life time opportunity to work in an area I have been interested in. I am grateful for the numerous one to one consultation as well as the long hours in the laboratory that Dr Shantha has spent with me to guide me through the entire course of study. I am sure that what I have learnt in those hours could not be measured by any means. Dr Shantha has also been a role model as a teacher and has inspired me to help my fellow course mates and students with the greatest dedication. I am also hugely appreciative of Dr Hossein for his encouragement and motivation during the challenging periods of my candidature. He has taught me to never lose sight of the big picture and always stay focused on what I have wanted to achieve.

In addition, I thank my Academic supervisors for their enthusiasm and encouragement in activities that have taken place outside the University such as conferences and collaboration with fellow researchers. A great deal of resources such as their time and finances have been invested in these endeavors. Through these efforts, I have been exposed to not only a huge variety of ideas in my field of study, but these have also widened my outlook of life. I am also fortunate to have received their expertise for their review of every aspect of my work throughout these years. I am also thankful for their unwavering patience and their belief in me over the years. I would also like to take this opportunity to express my gratitude to the Australian Maritime College – University of Tasmania for their financial support during my candidature.

I have been fortunate to have met Professor Tomasz, Dr Rose and Dr Kayvan at various points of my candidature and have received valuable guidance from them. I am grateful for their time despite their very busy schedules. Their enthusiasm in welcoming me to their home cities and Universities has certainly enriched my experience. Finally, I recall with fond memory the amazing discussions and activities that I have engaged in with my fellow course-mates Monaaf, Kutaiba and Gimara.

To my teachers

Contents

LIST OF ACRONYMS

AGPC:	Adaptive General Predictive Control
AVR:	Automatic Voltage Regulator
BESS:	Battery Energy Storage
ECA:	Emission Control Area
GA:	Genetic Algorithm
HESS:	Hybrid Energy Storage System
HV:	High Voltage
IEC:	International Electrotechnical Commission
IEEE:	Institute of Electrical and Electronic Engineers
LNG:	Liquefied Natural Gas
LV:	Low Voltage
MAIB:	Marine Accident Investigation Branch
MET:	More Electric Technology
MPC:	Model Predictive Control
PI:	Proportional – Integral
PMSG	Permanent Magnet Synchronous Generator
PMSM:	Permanent Magnet Synchronous Motor
PTH:	Power Take Home
PWM:	Pulse Width Modulation
PTI:	Power Take In
PTO:	Power Take Out
SCESS:	Super Capacitor Energy Storage System
SES:	Shipboard Electric Technology
SMES:	Super-conducting Magnetic Energy Storage
SOC:	State of Charge
UPS:	Uninterrupted Power Supply
ZEDS:	Zonal Electric Distribution System

LIST OF FIGURES

Page

LIST OF TABLES

Page

CHAPTER 1

INTRODUCTION

This chapter introduces the study, the result of which forms the basis of this thesis. It gives a background of the topic that the thesis focusses on, states the outcomes to be attained as well as the significance of the work undertaken in this area. The scope of work covered as well as its limitations are also presented in this chapter. The chapter concludes with a description on how the rest of the thesis has been organized.

1.1 BACKGROUND

Technological advancements have affected many sectors in today's world and the shipping sector is no exception. Electrification of the ship is a key component of this as the ships of today have a higher power demand and have loads that are highly variable in nature. In addition, shipping companies are under more growing pressure than ever to comply with Environmental Emission standards, especially when entering emission controlled areas (ECA) (McCoy, 2015). Similar to the automobile industry, all-electric ships are being considered as a promising solution to reduce or eliminate emissions. So far, only cruise ships have been successfully electrified while there are a large number of cargo ships and other types of commercial vessels that use the conventional mechanical power transmission based propulsion. Converting them into all-electric propulsion based ships is not practical. Therefore, hybrid electric ships have emerged as an alternative fully mechanical propulsion or all-electric ships. In hybrid electric ships, the traditional mechanical propulsion is combined with electrical propulsion for fuel efficiency, thereby, reducing the maximum power consumption. This leads to a decrease in the size of engines and an increase in efficiency, thus, leading to reduced emissions and lower fuel costs in the long term (Jayasinghe S. L., 2015; Li S., 2012). The combination of electrical and mechanical propulsion enables better flexibility of operation for the hybrid shipboard power system depending upon the propulsion as well as service load requirements for the system while at the same time increasing the complexity of the power system. Thus, the power system has to be capable of handling different load conditions involving both propulsion and service loads with minimal impactson the various key electrical and related mechanical parameters of the power system.

1.2 OBJECTIVES OF STUDY

The objectives that this study aims to achieve eventually are as follows:

1. Determine the level of electrical transients present in a hybrid shipboard power system due to a comprehensive variety of changing load conditions
2. Assess the effectiveness of conventional Proportional-Integral (PI) based Active Damping control in reducing the mechanical oscillations at the propeller shaft and subsequently using capacitors as energy storage devices in a clamping capacitor based inverter to absorb the resulting electrical transients in an Azimuth thruster drive system. As this portion of the study

relates to the electrical drive train of the ship, it is applicable to fully electrified ships as well as ships with hybrid propulsion

3. Assess the effectiveness of more advanced control technique such as the Model Predictive Strategy in reducing the frequency transient in the hybrid shipboard power system during load change conditions

1.3 LIMITATION OF STUDY

This study investigates the transient effects that load changes have on the electrical parameters of the hybrid shipboard power system and the potential for an energy storage system to reduce this transient phenomenon. Simulation models have been created to analyze the transient phenomenon caused by load changes of the hybrid shipboard power system. However, due to the limitations in modeling the power system structure of a ship and the environmental conditions that it operates in, some assumptions and reductions in the representations of the hybrid ship have to be made. These are as follows:

1. Actual environmental condition modelling that the ship encounters such as wind and waves would not be undertaken in this study. Instead a worst case step profile of the additional load that they represent to the hybrid shipboard power system will be used to demonstrate the effect that these load change phenomena have on the key parameters of the power system
2. Only 1 auxiliary generator will be used in this study for the hybrid shipboard power system although there are usually multiple auxiliary generators for redundancy purposes in a typical ship. As this study aims to show the dynamics between the electrical and mechanical components of the propulsion system and other loads, the power flow between the main generator and one auxiliary generator in addition to the energy storage system would be sufficient to illustrate the concept.

1.4 SIGNIFICANCE OF STUDY

The existing problem that has been identified is the large variation in key ship mechanical and power system parameters such as shaft torsional oscillations, DC link voltage, input current profile to the

thruster drive system, Main engine speed profile and electrical frequency in the shipboard power system that occurs in transient conditions when there are frequent and large amounts of load changes added to the network.

Conventional solutions to reduce shaft oscillations such as bigger and stiffer shafts connecting to the propeller as well as passive damping have often been found to add significant cost and weight to the system. These issues can be avoided by adding active damping control to the existing system that minimizes the additional hardware needed. Electrical transients on the DC link voltage and distortion experienced by the input current is a common phenomenon during variations in the loading conditions of a ship. This has been shown to be significantly reduced by adding clamping capacitors on the existing inverter of the thruster drive system. The addition of this capacitive energy storage element can be a more desirable alternative as compared to other commonly employed solutions such as adding a much larger DC link capacitance or other energy storage solutions which can be bulky and costly.

The frequency transient effects that occur due to load variations has also not been sufficiently studied in hybrid propulsion based shipboard power systems in existing literature. This problem has been made more complex due to the fact that hybrid shipboard power systems can operate in multiple modes due to the flexibility in using either mechanical or electrical or both kinds of propulsion according to the operational needs. In addition, due to insufficient research in hybrid electric ships, a complete modelling on the performance of advanced control techniques on Energy Storage elements in the hybrid electric ships for the purpose of mitigating transients arising from load changes has not been comprehensively reported so far. The aim of this research is to fill a part of the abovementioned research gap in evaluating hybrid propulsion system response to changing load conditions for the operation of the hybrid ship mainly from the control point of view and also develop more advanced control algorithms for the Energy Storage System to improve transient system performance that is essential for blackout prevention capability and increasing the reliability of the power system.

The findings of this study have quantified the transients caused by the various types of load change fluctuations. There has been an attempt to reduce the mechanical transients caused by propeller shaft vibrations. Electrical transients caused by load changes and propagation of disturbances from the

mechanical portion of the hybrid electrical system to the electrical portion has been decreased through the use of energy storage control measures. Conventional as well as advance control techniques have been applied to minimize the transient phenomena that occurs in the system to good effect.

1.5 LIST OF PUBLICATIONS

The University of Tasmania (UTAS) allows the presentation of a thesis by incorporating published or submitted papers for the Degree of Doctor of Philosophy that have taken place during the period of candidature. This thesis consists of five papers all of which have been accepted for publication and have subsequently been published.

Published Peer Reviewed Journal Articles:

1. **Shagar, V**.; Jayasinghe, S.G.; Enshaei, H. Effect of Load Changes on Hybrid Shipboard Power Systems and Energy Storage as a Potential Solution: A Review. Inventions 2017, 2, 21
2. **Shagar, V**.; Jayasinghe, S.G.; Enshaei, H. Frequency Transient Suppression in Hybrid Electric Ship Power Systems: A Model Predictive Control Strategy for Converter Control with Energy Storage. Inventions 2018, 3, 13

Published Peer Reviewed International Conference Papers:

1. Jayasinghe S. G, **Shagar V**, Enshaei H, Mohammadi D and Vilathgamuwa M, "Capacitor-clamped inverter based transient suppression method for azimuth thruster drives," 2016 IEEE Applied Power Electronics Conference and Exposition (APEC), Long Beach, CA, 2016, pp. 2813-2820
2. **Shagar, V** and Bandara, D and Jayasinghe, S and Enshaei, H, A capacitor-clamped inverter based torsional oscillation damping method for electromechanical drivetrains, MATEC Web of Conferences, 13-14 January 2016, Singapore, pp. 1-5. ISSN 2261-236X (2016)
3. **Shagar V**, Gamini S and Enshaei H, "Effect of load changes on hybrid electric ship power systems," 2016 IEEE 2nd Annual Southern Power Electronics Conference (SPEC), Auckland, 2016, pp. 1-5

1.6 STATEMENT OF CO-AUTHORSHIP

The following people and institutions contributed to the publication of work undertaken as part of this thesis:

Name and School = **Viknash Shagar, Australian Maritime College – University of Tasmania**
Name and institution, Supervisor = **Dr Shantha Jayasinghe**
Name and institution, Supervisor = **Dr Hossein Enshaei**
Name and institution = **Professor Mahinda Vilathgamuwa**
Name and institution = **Mr Danyal Mohammadi**
Name and institution = **Mr Doubadi Bandara**

Author details and their roles:

***Paper 1*, Effect of Load Changes on Hybrid Shipboard Power Systems and Energy Storage as a Potential Solution: A Review*:**
Located in chapter 2
Candidate was the primary author while Author 1 and Author 2 assisted with refinement and presentation.
[Candidate: 80%, Author 1: 10%, Author 2: 10%]

Paper 2, Effect of Load Changes on Hybrid Electric Ship Power Systems:
Located in chapter 3
Candidate was the primary author while Author 1 and Author 2 assisted with refinement and presentation.
[Candidate: 80%, Author 1: 10%, Author 2: 10%]

Paper 3, Capacitor – Clamped Inverter Based Transient Suppression Method for Azimuth Thruster Drives:
Located in chapter 4(A)

Author 1 was the primary author and conceived the idea and did the simulations while the Candidate wrote the manuscript. Author 2, Author 3 and Author 4 assisted with refinement and presentation.
[Candidate: 35%, Author 1: 50%, Author 2: 5%, Author 3: 5%, Author 4: 5%]

Paper 4, A Capacitor-Clamped Inverter Based Torsional Oscillation Damping Method for Electromechanical Drivetrains

Located in chapter 4(B)
Candidate was the primary author while Author 1 and Author 2 assisted with refinement and presentation.
[Candidate: 70%, Author 1: 10%, Author 2: 10%, Author 5: 10%]

Paper 5, Frequency Transient Suppression in Hybrid Electric Ship Power Systems: A Model Predictive Control Strategy for Converter Control with Energy Storage

Located in chapter 5
Candidate was the primary author while Author 1 and Author 2 assisted with refinement and presentation.
[Candidate: 80%, Author 1: 10%, Author 2: 10%]

We the undersigned agree with the above stated "proportion of work undertaken" for each of the above published (or submitted) peer-reviewed manuscripts contributing to this thesis:

Signed:

Dr Shantha Jayasinghe
Supervisor
Australian Maritime College

Professor Shuhong Chai
Principle
Australian Maritime College

University of Tasmania	University of Tasmania
Date: 06 April 2019	08 April 2019

OVERVIEW OF CHAPTERS AND RESEARCH OBJECTIVES

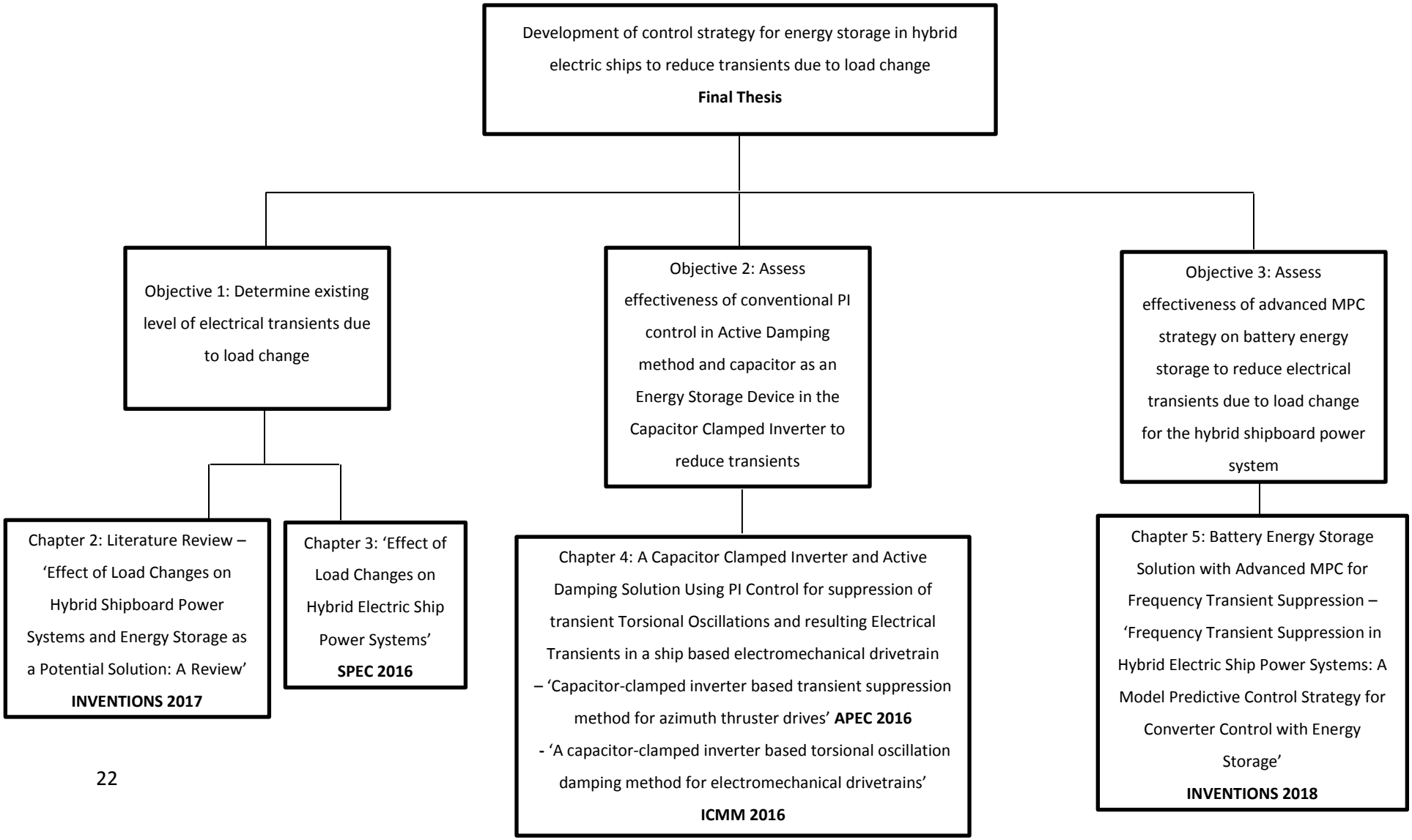

1.7 METHODOLOGY USED FOR THESIS

Due to the technical nature of the thesis and specific area of research that the work done focusses upon, models that represent the shipboard power system have been developed as the means of studying the system behavior in detail and building it further as appropriate to satisfy the objectives of the study. The models used in this study have been constructed using the MATLAB-Simulink platform. The two main models used for this study have been the Thruster Drive Train model and the Hybrid Shipboard Power System model. In light of the various models used in the different chapters of the thesis, these will be explained in greater detail in the relevant chapters.

1.8 ORGANIZATION OF THESIS

The thesis is structured into six chapters along with appendices. Chapter One introduces the topic of hybrid shipboard power system and the motivation to investigate the transient phenomenon that occurs due to the load changes. The limitations of the study have also been stated. In addition, the significance of the work done and its contribution to existing research done in the area of hybrid shipboard power system has been mentioned. Existing works on the state-of-the-art Energy storage technologies used for the purpose of reducing transient conditions in shipboard power systems including hybrid propulsion are reviewed in Chapter Two. A thorough review of advanced control techniques for Energy Storage systems has also been done. Chapter Three illustrates the modelling aspect of the hybrid shipboard power system. Furthermore, the existing levels of transient conditions that occur due to load change scenarios without any control measures being implemented are illustrated and discussed. Chapter Four explains the modelling of a ship thruster drive train and how active damping and clamping capacitors using conventional Proportional – Integral (PI) control can reduce torsional oscillations of the shaft that occur when load conditions change. The capacitive energy storage element of the drive train inverter has also been shown to reduce the resulting electrical transients in the DC link voltage and drive input currents. Chapter Five introduces the more advanced Model Predictive Control (MPC) strategy developed for the Battery Energy Storage System to reduce electrical frequency transients due to different load change conditions. Chapter Six concludes the study and states the key findings and contributions of the thesis while outlining opportunities for further work in this area.

CHAPTER 2

LITERATURE REVIEW

Viknash Shagar, Shantha Gamini Jayasinghe, Hossein Enshaei

Australian Maritime College, University of Tasmania, Launceston, TAS 7250, Australia

Published as *'Effect of Load Changes on Hybrid Shipboard Power Systems and Energy Storage as a Potential Solution: A Review.'* in '*Inventions 2017, 2, 21'*

In this chapter, a review of possible shipboard power system configurations with a focus on hybrid propulsion systems has been covered. The transient conditions that have been experienced by power systems due to load changes have been described. Conventional and novel solutions to the transient phenomena that have been used traditionally as well as those that have been more recently proposed have been discussed. In addition, the literature review includes possible control strategies for energy storage that can limit the transient phenomena.

Abstract - More electric technologies (METs) play an important role in meeting ever-growing demands for energy efficiency and emission reduction in the maritime transportation sector. As a result, ships with electrical power transmission are becoming popular compared to traditional mechanical power transmission based ships. Hybrid electric propulsion is an intermediate step in this trend where both mechanical and electrical propulsion technologies are combined to get the benefits of both technologies. In this arrangement, both propulsion and non-propulsion loads are connected to a common electrical power bus that could lead to serious power quality issues due to disturbances such as large load changes. This paper presents a comprehensive review on energy storage-based solutions that have been proposed to reduce their effects. The important aspects of existing as well as emerging energy storage control techniques and challenges in reducing transient effects in hybrid shipboard power systems with the use of energy storage are discussed in the paper.

2.1 INTRODUCTION

Technology advancements have affected many sectors in today's world and the shipping sector is no exception. Electrification of the ship is a key component of this as the ships of today have a higher power demand and have loads that are highly variable in nature. In addition, shipping companies are under growing pressure to comply with emission regulations, especially when entering emission control areas (ECAs) (McCoy, 2015). Therefore, following the trend in the automobile industry, hybrid electric ships, as an intermediate step towards all-electric ships, have emerged as an alternative to fill the need so as to reduce emissions caused by the ships of today. In hybrid electric ships, the traditional mechanical propulsion is combined with electrical propulsion for fuel efficiency thereby reducing emissions. Even though the retrofitting requires an initial investment, it can be compensated through the reduced cost of operation in the long run.

However, there is a noticeable gap in the existing knowledge of hybrid ships, especially in the electrical aspects of hybrid ships, such as understanding the behavior of the shipboard electric system (SES) in various operating conditions and severe load transients. Hence, the existing problem that has been identified are the large variations in power demand and hence the voltage and frequency fluctuations in the shipboard power system that occur in transient conditions when there are frequent and large amounts of load changes added to the network. This issue of voltage and frequency transients onboard mechanically driven or electric ships due to these load changes have been widely discussed in the literature (Miroševic´ & Maljkovic´, 2015; Radan, Sorensen, Adanes, & Johansen, 2008; Mindykowski, Szweda, & Tomasz, 2005; Prousalidis, Hatzilau, Michalopoulos, Pavlou, & Muthumuni, 2005). However, this effect has not been sufficiently studied in hybrid propulsion-based shipboard power systems. This problem has been made more complex due to the fact that such power systems can operate in multiple modes due to the flexibility in using either mechanical, electrical or both kinds of propulsion according to the operational needs. However, there has been ample evidence in the literature to suggest that energy storage can be a viable option to reduce these transients in a power system for other related applications. An effective control system for energy storage elements has the potential to counter the effect of load changes to a large extent (Bø & Johansen, 2017; Al-Barazanchi & Vural, 2015; Hou, Sun, & Hofmann, 2014; Arani & El-Saadany, 2013; Wenjie, Ådnanses, Hansen, Lindtjørn, & Tang, 2010; Lopes, Moreira, & Madureira, 2006). This

paper reviews the possible energy storage control systems that can be adopted onto ships to reduce the transient conditions in the shipboard power system due to load changes. This is particularly applicable to hybrid propulsion electric ships as their electrical system behavior has not been documented widely in the literature.

The following section gives an overview of shipboard power systems and the different architectures that are used in electric ships and the functions of the different components of the system that can potentially be used in hybrid propulsion ships. Section 2.3 describes the nature of loading conditions of ships and its effects on system voltage and frequency. It discusses the existing shipboard voltage and frequency control measures and also explores the potential for energy storage control techniques as a solution to mitigate the voltage and frequency fluctuations due to the transients caused by changing loading conditions. Section 2.4 introduces some thoughts on the challenges that might be encountered in implementing energy storage solutions onboard ships. Finally, Section 2.5 provides the summary and conclusion for this review.

2.2 SHIPBOARD POWER SYSTEMS OVERVIEW

The most common configuration of the shipboard power network is the radial power network where multiple generators supply power to switchboard panels, which subsequently are connected to the distribution system that serves most loads (Shen, Ramachandran, Srivastava, Andrus, & Cartes, 2011; Butler & Sarma, 2000). This has been used traditionally in both mechanically driven ships as well as in the electric ships. High Voltage (HV) equipment like large motors for pumps or propulsion are directly connected to the main switchboard or connected through step down delta-connected transformers. A floating delta configuration is essential for the transformer to increase survivability after the first single line to hull fault, loss of one phase of a transmission line or one leg of transformer winding. These, together with weapons systems, emergency lighting and communications are termed as the essential loads. Step down transformers connect the 6.6 kV HV switch board to the 440 V Low Voltage (LV) switchboard. LV equipment such as those used for lighting and other hotel loads are non-essential loads and are usually connected via the LV switchboard. A typical schematic for a shipboard radial power system of a ship employing electric propulsion as explained in (Bennabi, Charpentier, Menana, Billard, & Genet, 2016) is shown in Figure 2.1(a).

Modern shipboard power systems are moving towards the Zonal Electrical Distribution System (ZEDS). This system could have an AC or a DC main bus. An illustration of the AC zonal electrical distribution system (ACZEDS) and DC zonal electrical distribution system (DCZEDS) are shown in Figure 2.1(b) and 2.1(c) respectively. An ACZEDS system would be similar to DCZEDS except that there would not be any AC–DC rectification from the AC sources into the main busbar. The main advantage of the ZEDS configuration is that it compartmentalizes the power system into separate zones thus improving reliability in the event of a fault in any section of the system. Also, faults can be easily identified and isolated in a ZEDS through the use of local zone-based and global system-wide communication and protection networks that coordinate information between different zones. The hybrid electric ship power system configuration (Nielson, 2009; MAN Diesel & Turbo, n.d) was developed to combine the advantages of both electrical and the mechanical propulsion so as to supply power efficiently when there is a big variation in the power demand especially during maneuvering operations. Hybrid ships provide better energy efficiency and a reduction in emissions. Due to multiple energy sources, although the existing recommended level of redundancy is preserved, the reliability of the propulsion system is improved due to using two different propulsion systems that have a lesser chance of failing due to the same technical problems. A typical power generation and distribution system of a hybrid ship is depicted in Figure 2.1.

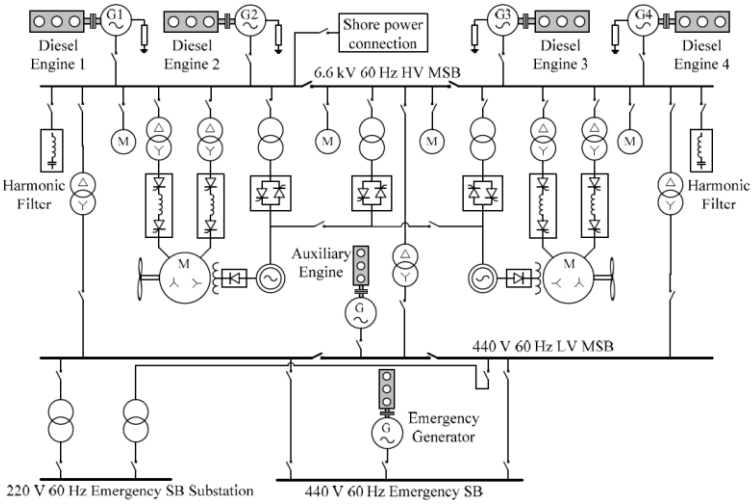

(a)

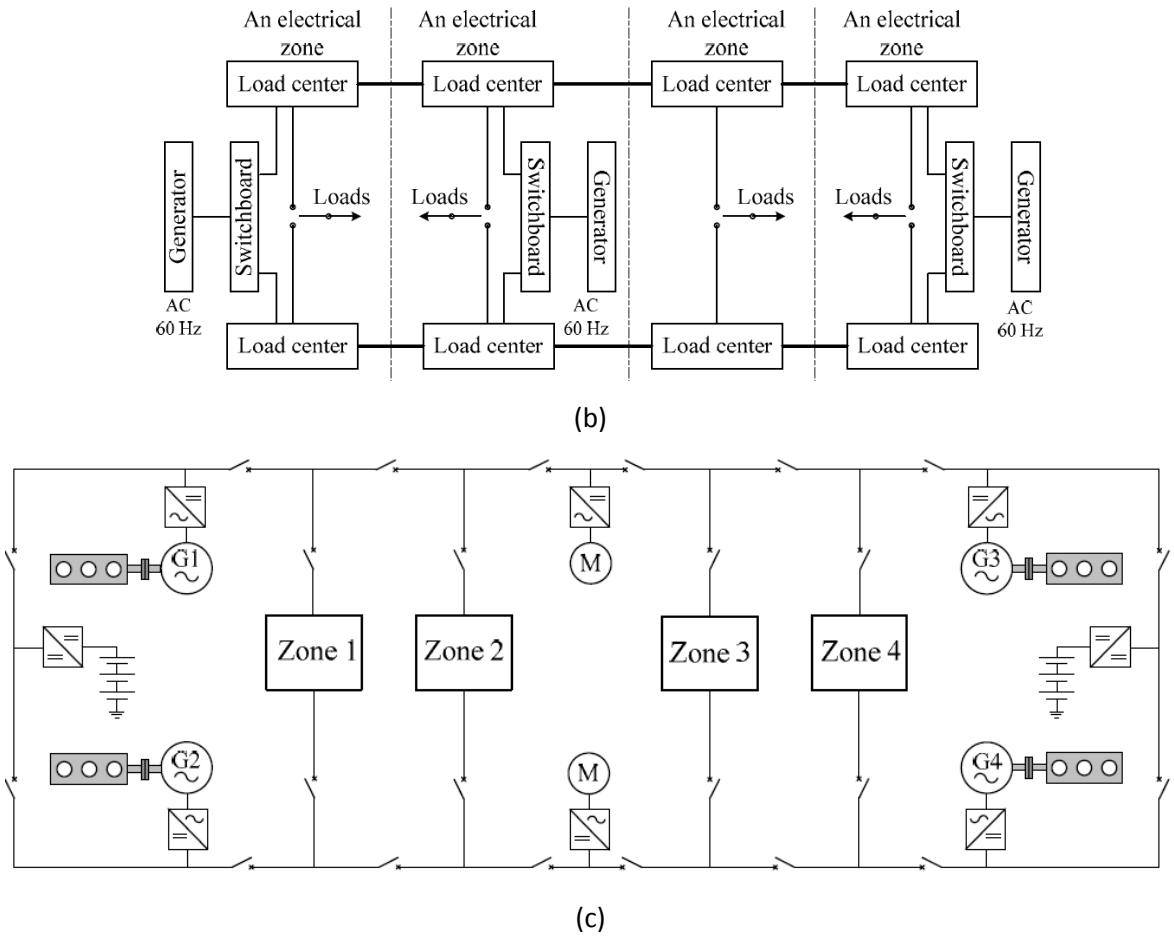

Figure 2.1. (a) High voltage/low voltage (HV/LV) Shipboard radial power system (b) AC zonal electrical distribution system (ACZEDS) (c) DC zonal electrical distribution system (DCZEDS).

Hybrid shipboard power system configuration can be classified as serial or parallel in nature as illustrated in Figures 2.2(a) and 2.2(b). In the former, the combustion engine and electric systems are in series and there is no direct mechanical connection between the engine and the propeller. The propulsion is only done by a variable speed electrical drive. Energy storage can be connected to the electrical drive. This improves the global efficiency of the system by optimizing the operating point of the combustion engine and the propeller. In the parallel configuration, the electric motors and combustion engines are mechanically joined using clutches and gearboxes by the same shafts. The electric motors are supplied by energy storage or other independent power sources. Hybrid vessels are already being tested for use in passenger ferries such as the Nemo H2 in Amsterdam and the tugboat RT Adrian in Rotterdam (MAN Diesel & Turbo, n.d.).

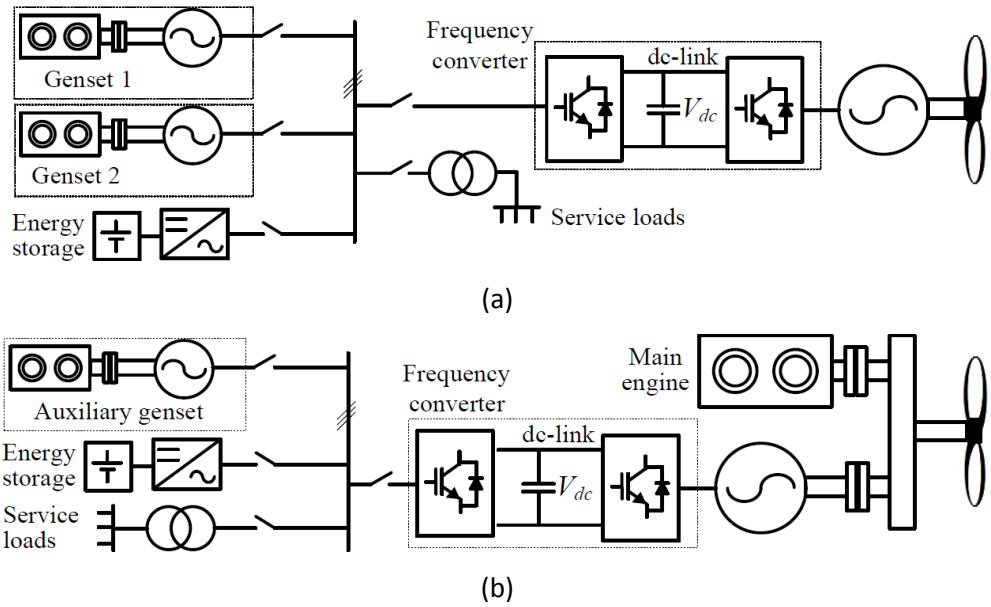

Figure 2.2. (a) Series hybrid ship architecture (b) Parallel hybrid ship architecture.

Current literature (Kim, et al., 2014; Prousalidis, Hatzilau, Michalopoulos, Pavlou, & Muthumuni, 2005) has covered various modes of operation that are possible for a hybrid ship electric system with a parallel architecture as shown in Figure 2.2(b). It is worth noting that usually the main (diesel) engine provides mechanical propulsion but auxiliary electrical generators which usually have a smaller capacity as compared to the main engine can also give power for electrical propulsion. A shaft machine connected to the electric generator and main engine can act either as an electric motor or an alternator according to the power demand of the hotel and propulsion loads. The most common modes of operation are outlined as follows.

1. Boost or Power Take In (PTI) Mode—Main Engine and Auxiliary Generators supply power to hotel and propulsion loads. Shaft machine acts as a motor to drive the propellers.
2. Parallel Mode—Power demand is more than that of the capacity of auxiliary generators but less than that of the main engine. The main engine thus runs at partial load and supplies power for hotel loads and propulsion with one auxiliary generator also supplying power to hotel loads. Shaft machine acts as an alternator and supplies electrical energy.
3. Transit Mode or Power Take Out (PTO) Mode—Only the main engine supplies power to propulsion and hotel loads. Shaft machine acts as an alternator.
4. Shore Connection or Cold Ironing Mode—Only port supply satisfies ship's power demand.

5. Power Take Home (PTH) Mode—Main Engine fails. Auxiliary Generators supply power for hotel and propulsion loads. Shaft machine acts as a motor.
6. Hybrid Mode or PTO/PTI Mode—Shaft machine acts as an alternator or motor in order to maintain shaft machine and main engine RPM in the range of 70–100% of full load to increase their efficiencies.

2.3 LOADING CONDITIONS AND ITS EFFECTS ON THE HYBRID SHIPBOARD POWER SYSTEM

2.3.1 Loading Conditions of ships

Knowledge of loading conditions is essential for any investigation on shipboard operation as it can determine the particular mode of operation that is optimal in terms of cost and efficiency. This is of great importance for Hybrid Ships due to the presence of various supply configurations mentioned above. Out of the various loads present in a ship, the propulsion load is the most dominant. This includes loading from heave compensators, wave induced thruster disturbance, thrust loss due to ventilation and interaction between thrusters (Kim, et al., 2014). Propeller load modeling is complex and is often specific to factors such as the number and design of propellers, hull design, wind strength, amount of exposure to air above the sea level and other environmental factors. However, existing literature (Journee, n.d.; Kristensen & Marie; Völker, n.d.) outlines algorithms that determine the resistive force needed to be overcome by the propellers for ship motion. This resistive force is assumed to be the propeller loading, which depends on the waves as they have the most effect on a ship at sea. The Douglas sea scale is used to classify the state of the sea based on the height of the waves. The thrust, R_T, needed for the baseline case of calm sea conditions based on the total ship resistance is to be calculated by Equation (2.1).

$$R_T = \frac{1}{2} C^T \rho S V^2 \qquad (2.1)$$

where ρ is the mass density of water, C_T is the coefficient of resistance for calm waters, derived by performing Computational Fluid Dynamics analysis on the hull form of a ship, V is the ship velocity, ∇ is the displaced volume, S is the wetted surface of the hull that is dependent on the draught amidship,

T, and the waterline length of the ship hull is denoted as L_{wl}. A rough guide of the calculation of *S* for the different kinds of ships (Völker, n.d.) is displayed in Table 2.1. Resistance on the propellers for calm waters is then calculated. This value varies as the square of the amplitude of the waves. Therefore, for any profile of wave conditions at sea expressed in terms of its height, the force exerted on the propeller for each discrete time interval can be calculated, summed up and averaged to determine the approximate mean propulsion loading on a ship. The power needed for the propellers can also be calculated, as it is proportional to the cube of the ship velocity.

Table 2.1. Wetted surface of hull reference table.

Type of Ship	S-Value Calculations
Bulk carriers and tankers	$S = 0.99(\nabla T + 1.9L_{wl} T)$
Container vessels (single screw)	$S = 0.995(\nabla T + 1.9L_{wl} T)$
Twin screw ships (Ro-Ro ships) with open shaft lines (and twin rudders)	$S = 1.53(\nabla T + 0.55L_{WL} T)$
Twin screw ships (Ro-Ro ships with twin rudders)	$S = 1.2(\nabla T + 1.5L_{wl} T)$
Double ended ferries	$S = 1.11(\nabla T + 1.7L_{wl} T)$

In addition to the propulsion loads of a ship, there exist other loads such as the hotel loads and reefer loads. An example of a complete load profile of a ship that takes into account all the different types of loads (Bennabi, Charpentier, Menana, Billard, & Genet, 2016) is the Post Panamax container carrier, the load profile of which, when at sea for 75% of the time in a year is shown in Figure 2.3 and Table 2.2. Note that ME refers to Main Engine while CSR is defined as the Continuous Service Rating, which is taken to be 90% of the maximum continuous power rating. The bar chart plots the Percentage of running hours against the Main Engine load. The exemplary load profiles of a harbor tug with two forward thrusters supplied by a 2040 kW diesel engine that tows container ships is shown in Figure 2.4 while that of a passenger motor ferry with a 50 kW service load, driven by 2 × 470 kW gas engines and does a 40-min to and fro journey (Jayasinghe, Meegahapola, Fernando, Jin, & Guerrero, 2017) regularly is as below in Figure 2.5. It is observed that the load variation has a more evenly balanced distribution approaching a typical normal distribution in the case of the container ships while smaller vessels such as tugs and ferries have a more skewed profile. This could be due to larger container ships undertaking longer journeys where the loading conditions are more numerous and random while smaller vessels undertake frequent and repetitive operations near the port or along a river. Also, extreme operating conditions are more prominent in the smaller vessels such as the tug and ferry as

compared to container ships. This could also be attributed to the long periods in oceanic voyages where container ships travel at a set speed with about close to 50% redundancy in power capacity while smaller ships operating closer to land have a higher proportion of activities that consume very high or a very low proportion of total power capacity such as berthing or maneuvering.

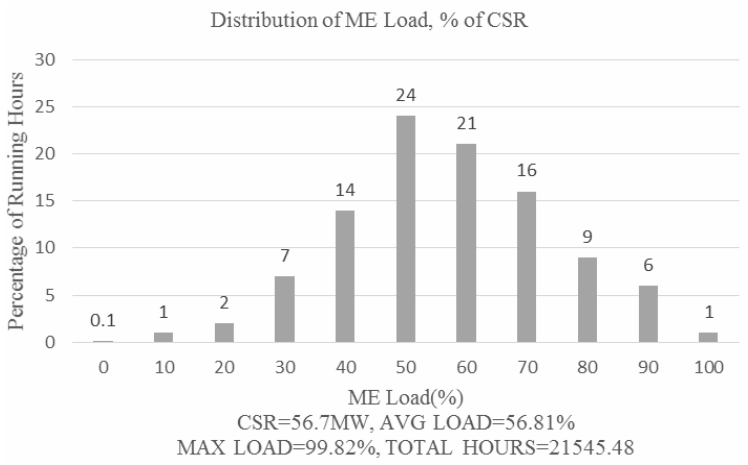

Figure 2.3. Load profile of a typical Post Panamax container ship. ME refers to Main Engine and CSR refers to Continuous Service Rating

Table 2.2. Hotel loading of Post Panamax ship at sea.

Ship Service	Electrical Loading Service
Normal service at sea, excluding shaft motor and reefers	1820kW
Normal service at sea, including shaft motor and excl. Reefers	up to 8590kW
Normal service at sea, excluding shaft motor and incl. 50% reefers	4100kW
Normal service at sea, including shaft motor and 50% reefers	up to 10,650kW
Normal service at sea, including shaft motor and 100% reefers	up to 12,870kW
Sea going average, excluding shaft motor, incl. 25% reefer loading	2960kW

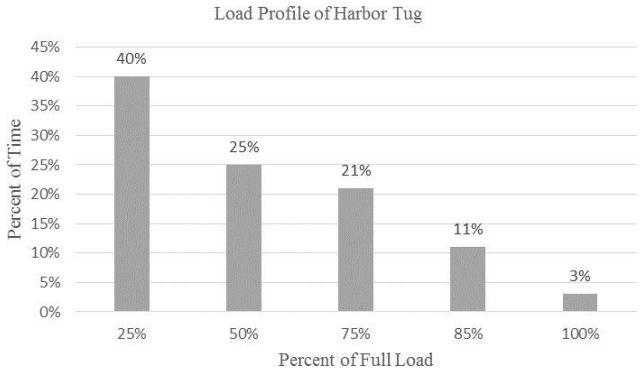

Figure 2.4. Load profile of a typical harbor tug

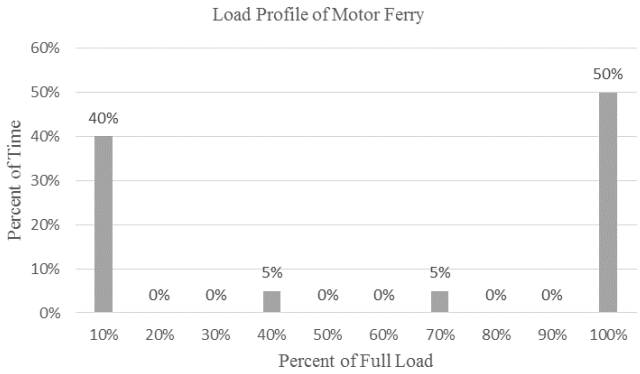

Figure 2.5. Load profile of a typical Motor Ferry

Another feature of the loading profile is that the load or the power demand profile of a ship can vary very quickly in a matter of minutes at sea because of the constantly changing environmental conditions influenced by the wind, wave and current. A typical load power demand and bus bar frequency profile, despite applying thruster power management algorithms and thruster speed control techniques can change by as much as about 40% of the nominal power in less than 10 s after employing power management algorithms (Tetra Tech, n.d.). The electrical frequency of the system can change by as much as 7% within 5 s under speed control, which in most cases is unacceptable for proper operation of sensitive loads connected to the system (Tetra Tech, n.d.). This highlights the need for further measures to be implemented in order to ensure that the voltage and hence the power as well as the frequency can be better controlled with lesser variation during load changes.

Once a ship is in harbor, there is a power demand for cargo operations as well as for some hotel loads on board. Some ports provide shore power connection at their berths while others do not, in which case, the ship has to plan to provide the required power. For example, the port of Los Angeles provides shore-side electrical power to the ships at its berth in order to reduce the emissions that might arise if the ships were to run on their diesel power. The average energy consumed by the different types of vessels berthed at the port (Jayasinghe, Meegahapola, Fernando, Jin, & Guerrero, 2017) is summarized in Table 2.3 below.

Table 2.3. Average energy consumed by different types of vessels at port

Vessel type	Port Call Frequency	Port Calls Year	Average Hours In Port	Estimated Annual Hours	Average Electric Load (MW-h/year)
Container ship	45	8	43	347	339
Tanker ship	15	24	30	734	976
Cruise ship	14	26	10	273	1911

It has also been found that a container ship can use as much as 4 MW of shore power at the berth. However, this is likely to be influenced by the size and amount of cargo operations required for the ship. The corresponding figures for Reefer ships, Ro-Ro ships, tankers and Bulk cargo ships are on average, 2 MW, 0.7 MW, 5 to 6 MW and 0.3 to 1 MW (Jayasinghe, Meegahapola, Fernando, Jin, & Guerrero, 2017) respectively.

2.3.2 Load Changes and its Effects on the Shipboard Power System

There is always a narrow range of values within which the frequency and voltage in a power system is allowed to vary despite any external disturbances such as load changes. Adding and removing the load from a power system causes transients that result in these parameters going beyond this range for some time period. Another important factor that influences the transient magnitudes is the time to start up the engines for the propeller and the ship. The startup time of the propeller can be between 1 to 60 s and that of the ship run up time is between 60 to 500 s. Electric machine dynamics have time constants between 1 ms to 1 s and thus their ability to cope with sudden load changes have a huge impact on the power system transient conditions. In addition, the type of shipboard power system configuration as covered in Section 2.2 and the distance and location of the load from the sources can

also influence the magnitude of transients experienced (Rolls Royce Power Electric Systems, 2010). Figure 2.6 illustrates an example profile of system parameter fluctuations such as those of frequency that can occur due to load addition and removal. Conventional control measures to reduce these fluctuations as described in Section 2.3.3, act after a delay to bring these parameters back to the acceptable range. However, in doing so, an over shoot is often observed and again the feedback system attempts to bring down the values resulting in a momentary dip. These oscillations continue for a period of time called the recovery time or settling time before the values settle within the acceptable range. The converse happens when a load has been removed from the system. It is obvious from the figure that the amplitude of the over shoot and dip as well as the length of the settling (recovery) time has to be reduced for a better transient response to load changes. The ideal response would be one where the frequency or voltage transients are virtually non-existent. The next paragraph explains in further detail how transients are created when a power system experiences a load change.

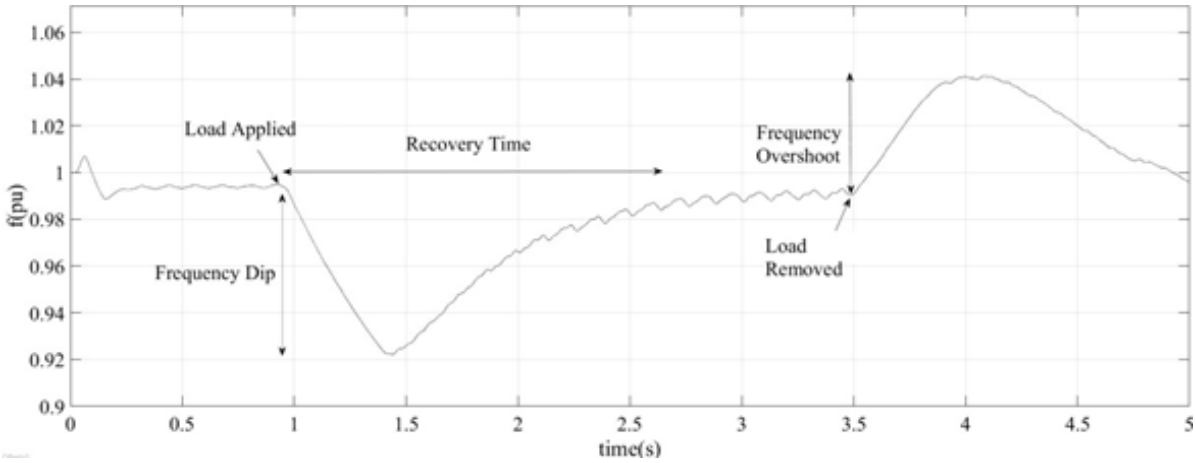

Figure 2.6. Typical frequency profile under load change.

When a load has been applied, the speed regulator of the engine of the generator injects more fuel into the cylinder but since the amount of air is not yet increased, the combustion is not complete and the frequency of the engine continues decreasing till the engine outlet temperature and air pressure increases at which point, torque production becomes more efficient and the frequency starts increasing. This process may take up to a few seconds till the frequency is stabilized. An increase of load in shorter period of time will result in a higher frequency dip. This is due to the limitation in the development of the mechanical torque as the rate of increase of the load becomes very high. When there is a load reduction, the fuel injection into the cylinder reduces but due to the large amount of air

mass still remaining, the combustion is complete and the frequency deviation is usually smaller than the case of a load increase. Frequent load fluctuations can result in a rise in the thermal load of the system because the air pressure decreases faster than it rises. This heating effect can result in burnt exhaust valves and hot corrosion. The voltage from a generator decreases when a sudden load is added and increases when a load is suddenly removed from the power network. Although the generator excitation system acts to restore the voltage to its nominal value, there is still a delay because of the response time of the Automatic Voltage Regulator in the excitation system to act during which period, the voltage will be fluctuating. Other factors that affect the voltage stability after a load change are the load current, power factor, generator transient and sub-transient reactance of the generator (Mindykowski, Szweda, & Tomasz, 2005). Such frequency and voltage transients result in inferior power quality for the system, which affects the operation of other loads connected to the same power network and can cause overheating of equipment thus presenting a fire hazard. There have been real-life instances of ships that suffer from such issues due to load changes. In (Nielson, 2009), the negative effects of long- and short-term deviations of frequency and voltage of shipboard power systems have been described. These can include overheating and energy losses as well as equipment malfunction. A case study of a ship with significant voltage dips highlights this issue. It was found that this only happens when the ship pulls in and out of port. Further investigation reveals that the inrush current during the starting up of a thruster motor during that ship operation has been the cause. The starting up of the thruster motor was necessary in order for the ship to perform maneuvering operation so as to navigate safely into or out of the port.

A similar issue for isolated power systems such as that of a ship has been discussed. Experimental results show that direct starting of induction motors which might be used for propulsion needs on board a ship can lead to an inrush current several times that of the rated value that can result in a voltage dip of up to 25% which is unacceptable for normal operation of other appliances connected to the power system. Conversely, disconnection of motor loads can mean an approximate 25% voltage overshoot of the grid voltage. Transient fluctuations of the system frequency have also been observed in both instances of adding and removing motor loads. If there are multiple motors to be started, since the starting torque of a motor is proportional to the square of the terminal voltage, a dip in the voltage due to other motors or other loads means that the motor takes a longer time to reach the required speed (Hall, 1999). The excessive current flow during this prolonged period of time will lead to a further

voltage drop and overheating. This chain effect might eventually lead to tripping of the motor(s). However, there are various existing conventional solutions to deal with the start-up effects of thruster motors in addition to inbuilt conventional control measures in the generator to deal with these voltage and frequency fluctuations. These will be described in the following section. There are standards defined by various bodies to stipulate the limits of the electrical parameters which if violated could lead to the above mentioned effects that could occur due to voltage and/or frequency dips. These standards could be applied as a general guideline to shipboard power systems as well. The IEC defines tolerance limits for voltage and frequency dips and spikes for both steady state as well as transient conditions. This is shown in Table 2.4.

Table 2.4. Acceptable ranges of voltage and frequency variation for AC distribution systems

Quantity in Operation	Permanent Variation	Temporary Variation
Frequency	±5%	±10%(5s)
Voltage	+6% to -10%	±20%(1.5s)

2.3.3 Conventional Shipboard Voltage and Frequency Control

The voltage and frequency of a power system is usually set by the generating sources. In a generator, the Excitation System controls the generator output voltage. It limits the magnitude of voltage dip or voltage rise within a fixed period of time. Typically, voltage change of 15% or less is usually brought back to nominal value within about 1.5 s (Prabha, 1993). The excitation system depends on an AC or DC exciter source to create a strong magnetic field at the field windings of the rotor when a DC current passes through it. The stator produces the generator terminal voltage when it cuts through the magnetic field of the rotating rotor. There is a feedback loop with an Automatic Voltage Regulator (AVR) where the generator output is measured and if there is a change from the nominal value, the field current is altered to maintain the voltage. Flexible AC Transmission System (FACTS) devices have also been traditionally used in power systems as voltage mitigation measures. FACTS devices principally use power electronic passive devices such as inductors and capacitors and active devices such as switches in various configurations to inject active or reactive power as needed to reduce the voltage error from the nominal value. Examples of FACTS devices are Static Synchronous Compensators and the Unified Power Quality Conditioner (Gayatri, Parimi, & Kumar, 2016; Jayawardena, Meegahapola, Robinson, & Perera, 2015; Srivatchan, Rangarajan, & Rajalakshmi, 2015).

In multi-generator systems, frequency control is usually implemented by the droop speed control settings of a generator. The frequency droop characteristic of a generator dictates that the system frequency drops as the active power of the system increases. The difference between the actual speed and the speed reference is used to increase the flow of fuel or steam into the prime mover so that the power output is increased. For a 100% change of the power loading of the generator of the system, the frequency at full load drops by a specific percentage from its no-load frequency. This percentage value is the droop setting value of the generator. The change in power output counteracts frequency fluctuations and allows the unit to settle into a steady state point in the droop characteristic. Droop control allows each of the generators that might have different speed settings to share a portion of the load without "fighting" for control over the load otherwise known as load hunting. Figure 2.7(a) shows a schematic of droop control implementation in a generating source (Prabha, 1993) while Figure 2.7(b) gives an example of a droop characteristic with a droop setting value of 5%. The start-up current of thruster motors is a key cause to transient conditions on the shipboard power system. Different combinations of options such as Direct-On-Line starting, Wye/Delta starting and a combination of autotransformer and capacitors are possible solutions to reduce the start-up current of squirrel cage motors in thruster motors as have been considered in (Sun, Wang, & Dai, 2011). However, these solutions, while reducing the starting currents of motors, do not eliminate the voltage and frequency fluctuations that come with adding or removing motor loads from the power network.

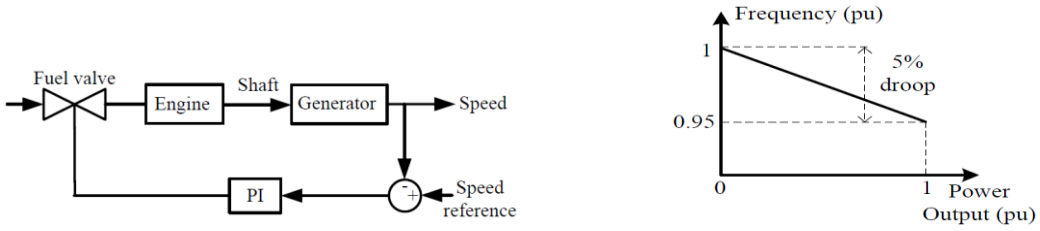

(a) (b)

Figure 2.7. (a) Frequency droop control (b) Frequency droop characteristic

Another key reason for voltage and frequency fluctuations in ships is the increasing proportion of loads that have a very short start up time. These are usually weapon loads or emergency service loads that demand a huge amount of power acting for a very short period of time. Pulsed loads have been added to two kinds of shipboard systems, which are that of the ferry and the Liquid Natural Gas (LNG) carrier. The step load nature of application of pulsed loads is another major cause of transients in ships. Conventional Proportional-Integral (PI) control solutions have been implemented on their ability to keep the voltage and frequency fluctuations down. Load dump tests in steps of 25% have been done in (Journee, n.d.) to simulate load changes on board a ship with a 2-steam turbine generator system. A two-layered control have been proposed by the authors to reduce frequency fluctuations. An adaptive P controller has been used as a primary frequency controller in order to deal with large frequency deviations. The second layer of control is the classical PI controller that aids in achieving the zero steady state error and provide identical power to both the units. The delay time between the actions of the two layers of control has also been optimized. Reference (Cupelli, et al., 2015) analyzes the stability of the rotor angle, frequency and voltage parameters of the MVDC network in an electric ship. The latter two parameters are directly related to the balance between power demand and power supply. The stability of the system has been mathematically defined. Different load side as well as generator side control techniques for stabilization of constant power loads fed by a DC/DC converter are analyzed. These include adding stabilizing state feedback on each individual load side converter and using active damping implementation on converters' interface to improve stability.

The effect of pulsed load on the frequency modulation of a ship electric network has been explored in (Kanellos, Tsekouras, Prousalidis, & Hatzilau, 2011). The expression for the frequency modulation has been derived as a function of pulsed load period, generator inertia, frequency droop and frequency controller gain. Each of these factors has been varied to investigate their effect in keeping the frequency fluctuation, active and reactive powers of the pulse load within limits. The study has been repeated for modulation of the voltage in the event of pulsed loads in (Kanellos, Tsekouras, Prousalidis, & Hatzilau, 2012). Here, the impact of the Automatic Voltage Regulator (AVR) gains, generator reactance cable reactance, base load and the pulsed load duty cycle in keeping the voltage variation within limits have been determined. This study gives the opportunity for optimization of the parameters to limit the transient effects of load changes on the key electrical parameters such as voltage and frequency.

There has been literature published in the area of load changes for the shipboard power system. However, the majority of them have focused solely on the thruster loads, neglecting the hotel and ship service loads that make up the total electrical load of any ship. Also, while there have been studies of the detrimental effects of thruster motor start-up on the voltage and frequency of the system, the effect of changing sea and wind conditions leading to frequent changes of the steady state load has not been explored fully in good detail. It has also been found in this section of the literature review that often, separate control strategies have been used to control the voltage and frequency fluctuations of the ship arising from load fluctuations. It might be more efficient from a control perspective to have a single control system to manage both of the parameters. Energy Storage solution is one such system where the active and reactive power supplied by the Energy Storage sources can be simultaneously controlled. Due to their additional capacities, they can also be used to reduce the reserve margins of the existing generation sources in the system. Energy storage has been widely studied in the Renewable Energy sector as such sources can be used to smoothen the system parameter fluctuations that occur due to the varying nature of power available from Renewable Energy Sources such as wind or solar power. The control strategies used in regulating the power and frequency to the grid in renewable power system applications could be applied with appropriate modifications to shipboard power systems that experience variable power demand conditions at sea due to the harsh environmental conditions or have the need for special applications such as weapons. The control solutions of these systems will be covered in the following sub-section. Also, other novel control techniques used in other areas of Power Engineering will be reviewed for potential application in the hybrid shipboard Energy Storage control system.

2.3.4 Energy Storage Systems

2.3.4.1 Energy Storage Devices

Energy storage has been reported in the literature as a means to improve the power quality of a network and increase the reliability of the system due to the additional energy capacity that can be supplied to the network when needed. Additional energy might be needed for a variety of reasons such as to meet fluctuating power demands, smoothen power supply from intermittent sources and

improving the voltage and frequency profiles that have been distorted due to transient conditions. The types of energy storage used in shipboard power systems can be broadly classified into 4 types. They are electrochemical devices that include batteries, electrostatic devices such as supercapacitors, electromechanical devices of which the flywheel is a common example and finally, the most recent technology, which is electromagnetic devices. The superconducting magnetic energy storage device (SMES) is an emerging example of an electromagnetic device. The two forms of energy storage elements widely used today in shipboard power systems would be the battery and the super capacitor. This is due to the ease in accessibility to this rapidly advancing technology and the modular nature of batteries and capacities, which makes it easier to change their capacities. Li-ion batteries technology is the preferred battery technology today as it has the longest lifetime and the highest power and energy density compared to other commercial battery types such as NiCad and NiMH. Due to the nature of their structure, batteries have high energy densities but low power densities while super capacitors have a high power densities and low energy densities (Prabha, 1993). Combining the different types of energy storage elements gives rise to a hybrid energy storage system and this is becoming more widely used due to the combination of the favorable qualities of the different energy storage elements that make up the system. A common example of hybrid energy storage systems would be one integrating batteries and super capacitors. Choosing batteries or supercapacitors as energy storage depends on the needs of the system and it is not unusual to have both of these energy storage elements integrated into the system. Both of these elements can be recharged continually when they are not supplying energy thus making them ideal for long-term usage.

The advantages of adding energy storage devices in stabilizing the power system as compared to conventional measures has been investigated in the literature mainly in the areas of microgrids and renewable energy system to increase the power reserve capacity and smoothen the power fluctuations arising from unpredictable power demand and supply.

A combined super capacitor and lithium ion battery Energy Storage System has been proposed in (Hou, Sun, & Hofmann, 2017) so that the torque and power fluctuations in an electric ship due to changing load demands can be mitigated effectively. A complete modeling of the propeller has been done by designing the mechanical power, thrust and torque coefficients in terms of the number of blades, blade area ratio, pitch ratio and loss factor arising from the propellers in and out of water

motion. Wave field motion models have also been employed to simulate the effect of waves on the propeller. The aim of the modeling is to minimize the speed variations of the propeller, which implies that the load torque and power will vary widely, which in turn are to be managed by Energy Storage System. The Energy Storage model is represented as a linear state space model with different states of charge being introduced and the control variable being the battery and super capacitor currents. A Model Predictive Control strategy have been applied in this study where the cost function developed is with the twin objectives of firstly, improving the power trading between power demand, generation, battery power and capacitor power and secondly minimizing charging and discharging current while being constrained by battery and super capacitor state of charge and other current level limitations.

Battery storage has been extensively used in the literature to improve the voltage and frequency voltage profiles in power networks. In addition, it is already considered as possible additional energy storage for emergency power in the relevant standards such as the IEEE Std 45-2002 (IEEE, n.d.), the IEEE recommended practice for electrical installations on shipboard. Here, it is stated that the emergency storage battery "should be capable of carrying the emergency load without recharging while maintaining the voltage of the battery throughout the discharge period within +5% and −12% of its nominal voltage". In the case of lighting and power, the battery capacity "at the rated rate of discharge should be a maximum of 105% of generator voltage when fully charged, and a minimum of 87.5% of generator voltage at the end of rated discharge". The reader is urged to refer to Section 6.6 of the IEEE Std 45-2002 Standard for the list of emergency load services (IEEE, n.d.). The supply capacity for the emergency services is also stipulated in Section 6.9 of the abovementioned Standard (IEEE, n.d.) for different tonnage of ships with various running times and distances. The American Bureau of Shipping (Roa, 2009) has also given recommendations for Uninterrupted Power Supply (UPS) where batteries are usually used and the related redundancies necessary for the different ship systems. Therefore, in view of the above, it is worthwhile looking into extending this usage of battery energy storage from emergency purposes into improving the key electrical parameter profiles due to electrical transient conditions that can be considered as a less impactful condition to the system as compared to emergency conditions. Further work in this area can include setting aside a dedicated portion of battery energy storage for mitigating transient effects due to load changes with the possibility of reusing this storage during an emergency as well.

Battery systems have been recommended to improve transient conditions due to load changes because they have the ability to exchange active and reactive power. Due to the coupling of these quantities with the frequency and voltage, they are effective in voltage sag correction and frequency control. However, for such parameter regulation, the battery system parameters like battery capacity, charging rates and state of charge have to be considered. In (Zarghami, Vaziri, Rahimi, & Vadhva, 2013), the battery energy storage system is modeled like a static compensator. However, unlike the static compensator, there is no voltage inverter in the battery system and the DC link capacitor has now been replaced by the battery.

2.3.4.2 Energy Storage Control Systems

The control of these energy storage devices is crucial for their effectiveness in the power network. The dynamics of a system is continually changing and therefore, the energy storage requirement of the system is also continually evolving. This means that the operation of these energy storage elements have to be able to adapt to these changing conditions as rapidly as possible to effectively serve the system needs in a reliable manner. In addition, the increase in energy capacity offered by energy storage elements can lead to a reduction in the reserve margin needed for the main generating sources. There have been numerous studies done in the field of renewable energy for power grids on land where energy storage devices have been used to manage the fluctuations in power that arise from these energy sources. Through reviewing these literature, it is hoped that a better understanding of energy storage and its control strategies can be gained so that this knowledge can be transferred to other applications of power engineering such as the hybrid electric ship power system to improve the voltage and frequency fluctuations that occur due to changes in load power demand. It is also worth noting that dealing with electrical fluctuations on a ship brings about unique challenges. There are low frequency fluctuations due to the waves during the majority of the time of operation of a ship at sea and also the high frequency load fluctuations due to the propeller rotation. The torque and thrust can also vary in a wide range of up to 100% (Hou, Sun, & Hofmann, 2014). Due to these extreme operating conditions, it is believed that in addition to control techniques applied to the system in order to improve power quality, some degree of energy storage is also required to stabilize the parameters in a shipboard power network.

Batteries have been used in Energy Storage Systems for a ship grid in conjunction with band pass (Kalman) filters designed to smooth out power fluctuations. The filter parameters are tuned by a Model Predictive Control (MPC) algorithm based on the power spectral density of the power consumption during load disturbances. The need for a control algorithm was suggested because of the large charging and discharging battery currents that happen when the load variations are huge thus producing waste heat that can be detrimental to the lifespan of the device. The MPC control strategy for the filter removes the power variations based on their size and temperature of the batteries. The State of Charge (SOC) and battery temperature are the operational constraints. The SOC is to be kept between 0.5 and 0.9 while the temperature has to be equal to or below a maximum of 35 degrees Celsius (Bø & Johansen, 2017). The objective of the optimization process is to design a filter that has an optimal balance between the phase lag of the estimation and the size of the ripples due to the State of Charge variations. Two case studies based on step load changes and slow power changes have been simulated. In the first case, most of the peak State of Charge variations are filtered out with the average estimate being close to the middle of the peaks. However, it was noted that when the filter time constants are very low, these time scales are difficult for the diesel engines to react to but if they are very high, then the variations are difficult to be filtered out thus raising the battery temperatures close to the limits or slightly beyond those limits. The second case also gives favorable results of filter action with the battery temperature being within limits for the test duration. It is the authors' opinion that there is room for the filter to further reduce the ripples at the expense of a larger phase lag between the average and estimated average of the State of Charge (Bø & Johansen, 2017).

Independent as well as coordinated control strategies using batteries and super capacitors have been considered and their performance in four metrics have been evaluated for an electric ship propulsion system. They are the power tracking error, battery and capacitor power loss based on energy cycling and the time spent on charging or discharging. The study concluded that for all the cases, the power tracking error decreased which implies that the energy storage control system has successfully mitigated power and thrust fluctuations. The authors have added an extension to this study (Zarghami, Vaziri, Rahimi, & Vadhva, 2013) by comparing two Energy Management strategies to reduce power fluctuations in the electric ship propulsion system. The first strategy, called Prefiltering, separately utilizes supercapacitors to reduce high frequency power fluctuations and batteries to compensate for low frequency fluctuations. The second strategy, termed Coordinated Control, considers the batteries

and super capacitors as a single Hybrid Energy Storage System (HESS) entity and coordinates the operation of the batteries and supercapacitors. Model Predictive Control (MPC) is used for power tracking and thus energy saving measures. Power fluctuations arising from different sea conditions have been used. A sensitivity analysis based on the length of the predictive horizon has also been done for the MPC strategies. It was found that the Coordinated Control MPC-based approach was better than the Prefiltering MPC approach for power tracking and therefore mitigation of the power fluctuations at the various sea states and reducing energy losses. The sensitivity analysis of the length of the predictive horizon revealed that the longer the length, the better is the MPC performance but with added computation burden but the performance difference between using a shorter predictive horizon of *N* value between 5 and 20 and a longer one of 100 is not significant when using an offline block MPC. In fact one sea state condition has shown better performance with a shorter predictive horizon. From this result, it is evident that long term prediction horizon is not necessary for this problem. This gives further support to the possibility of developing a real time MPC strategy for this application.

The use of super capacitors to smoothen the power output of the Marine propulsion system has been successfully proven in (Wenjie, Ådnanses, Hansen, Lindtjørn, & Tang, 2010). A buck boost DC–DC converter for the super capacitor to absorb and discharge power to the network has been used. This ensures that the super capacitor voltage does not drift excessively leading to loss of control of the power system generation and demand balance. An improved average power flow control method has been used for the converter to regulate the super capacitor current and voltage. PI control has been used in an inner and outer loop configuration in order to control the current and voltage of the super capacitor in response to the power demands of the load. A schematic of the control loops is shown in Figure 2.8.

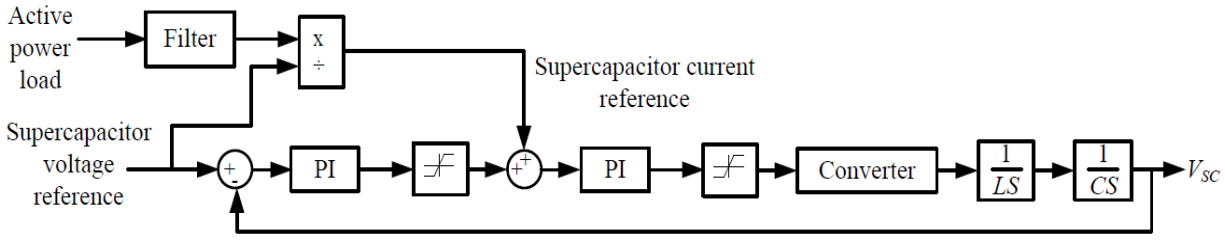

Figure 2.8. PI control of supercapacitor in energy storage system

In (Wenjie, Ådnanses, Hansen, Lindtjørn, & Tang, 2010), the electric propulsion system has been simply modeled using a generator, rectifier, super capacitor and a controlled current source that represents a motor. This simple system has been shown to make the load profile from the generating sources smoother despite thruster motor load variations of between 30% and 100% of the peak load.

Battery energy storage has also been shown to be effective in frequency application control. In (Mercier, Cherkaoui, & Oudalov, 2009), the battery energy storage system has been modeled as a first order transfer function with an incremental battery power to grid frequency relationship for use in a major synchronous grid such as the Union for the Coordination of Transmission for Electricity which serves continental Europe. A load frequency control dynamic simulator for the battery energy storage system and the generators has been modeled to get a single machine equivalent so as to determine the grid frequency. The remedial action of the battery energy storage system depends on the amount of frequency deviation from the nominal value. A deviation below 50 mHz for a 50 Hz system does not invoke any action but if the deviation is between 50 mHz and 200 mHz, then the battery would supply or absorb power in accordance to a linear power-frequency characteristic. However, if the deviation is beyond 200 mHz, then the full device power would be used to regulate the frequency. It was found that this strategy led to the battery eventually discharging itself in the long run. Therefore, the strategy was improved such that the battery recharges itself when the fluctuation in the frequency is lesser than 50 mHz. However, this led to overcharging and inefficiency because when there is an over frequency, the excess charge heats up the resistors resulting in losses. It is worth considering this well-established method of integrating energy storage on large land-based networks for ship-based power systems. The relatively basic proportional control used in this application can be a starting point for more advanced control technologies for hybrid electric ships.

Both voltage and frequency control can be achieved by using the battery energy storage described in (Lopes, Moreira, & Madureira, 2006). Here, battery energy storage has been used in the context of a Low Voltage land-based microgrid. High and low load scenarios have been simulated. In addition, faults have been simulated into the system with load shedding taking place as a consequence if the frequency deviations are too high. The loads are then re-connected in steps. Throughout this process, the voltage and frequency fluctuations are to be kept to a minimum. The voltage source inverter is controlling the active and reactive output from the energy storage device so that the frequency and

voltage parameters are kept constant. This is done by Frequency-Active Power and Voltage-Reactive Power droop controls. Two strategies are explored here. The system can either be in Single Master Operation or Multi Master Operation. The former mode of operation is one where only one inverter sets the voltage reference when the main supply is lost while the latter mode of operation allows all the voltage source inverters to operate based on their own pre-defined reactive and active power characteristics. A secondary load frequency controller is also activated for each micro source after a disturbance. This uses open loop PI control to bring the frequency back to the nominal value. The isolated and low voltage nature of this microgrid can be related to a shipboard power system, which is also isolated and has a limited capacity and can have integrated energy sources such as batteries.

A combination of battery and supercapacitors have been used as a Hybrid Energy Storage System (HESS) in (Hou, Sun, & Hofmann, 2015) to reduce the power and torque fluctuations on the drive shaft of a ship due to the effect of waves and other hydrodynamic forces. Four different strategies have been devised and compared to select the best control strategy for the HESS system. The first strategy would be the baseline condition without energy storage capability. The second strategy would be HESS control with Motor Load Following where a predictive load following strategy with receding horizon has been used given the motor load information. However, bus voltage and motor power information are not used. The third strategy is based on Bus Voltage Regulation where PI control is used for maintaining the bus voltage. Here, only the bus voltage information is needed. The final strategy is the system level Integrated Energy Management System which is built using an optimization-based control to minimize the DC bus voltage variation, power tracking error and eliminate high battery current operation with constraints imposed on the State of Charge and currents of the battery and the Supercapacitor. The best strategy was found to be the Integrated Energy Management System strategy based on the following parameters. They are the DC bus voltage variation, diesel energy power fluctuations, power loss for batteries and supercapacitors due to energy cycling and time spent charging and discharging the battery with high currents.

PI and fuzzy logic control have been used in voltage and frequency controllers for a standalone Photovoltaic-Wind-Diesel-Battery system in (Al-Barazanchi & Vural, 2015). A battery system with a voltage source converter and frequency regulation that acts in accordance to load variation has been implemented. The controller for the converter injects or absorbs the active and reactive power necessary to minimize the parameter variation. The PI control is used to generate the synchronous

reference frame control signals, i_d and i_q, that are related to the active and reactive power levels of the system respectively. The errors from these quantities would be the frequency and voltage errors, which are then sent to the fuzzy controller that reduces these fluctuations. The fuzzy logic employed is found to be effective in non-linear systems such as this. The system has been implemented and simulated in MATLAB using the Fuzzy Toolbox. This PI-Fuzzy control was found to be effective in controlling voltage and frequency fluctuations during fluctuations of the load as well as the renewable sources, which comprised of solar and wind power. Particle Swarm Optimization (PSO) has been used in (Das, Roy, & Sinha, 2011) to get the optimal gains for the PI controllers that regulate the frequency in a wind-solar-diesel hybrid system with batteries and super capacitor energy storage. PI controllers are used for the generation sources, super capacitor and battery system to balance the power output with the power demand. The objective function of the PSO algorithm in this case, is to minimize the squares of the frequency from the nominal value. The PSO-based PI controller registered lower frequency deviations as compared to classical PI controllers during varying wind, solar and load conditions. A similar control system employing fuzzy control or PSO has potential to be applied to a hybrid battery-supercapacitor energy storage system on board ships as a further step to traditional control technologies.

PSO has also been used in (Zhang, Li, Cong, & Zhang, 2015) to control a battery and supercapacitor energy storage system termed as the Active Parallel Hybrid Energy Storage System (APHESS) for an LNG ship in order to reduce the power fluctuations in the integrated electric propulsion system caused by Motor Starting and Pulse Weapon Load. In the optimization algorithm, the constraints of operation are the generator output power limit, the ramp rate of generator output power, energy storage capacity limits for batteries and supercapacitors, state of charge and current through the batteries and supercapacitors. The PSO method has been found to be very effective in such an application to find a suitable mathematical solution to a nonlinear optimization problem with multiple ranges. As a DC propulsion motor is being used, there is a common DC bus for the Energy Storage and the motor. The APHESS, in addition to combining the Batteries and the Supercapacitors into a single Energy Storage unit, realizes real time adjustment for output power fluctuation and uses two DC–DC converters. One of the converters controls the charging and discharging of the total power to the AC side. When the generator output power is greater than the maximum allowable power of the generators, the converter releases energy. When the DC motor brakes, the converter absorbs power from the motor back to the

grid. The second converter adjusts the size and orientation of the battery charge to share it between the batteries and supercapacitors. When the power demand is higher than the power supply from the generator, the batteries charge the supercapacitors to supply power from the APHESS to the loads and when the power demand is lesser than the supply, the supercapacitors in the APHESS absorbs power and charge the batteries (Zhang, Li, Cong, & Zhang, 2015).

An Adaptive General Predictive Control (AGPC) Scheme has been used as supervisory control for a Super Capacitor Energy Storage System (SCESS) in a multi area power network (Mufti, Iqbal, Lone, & Ain, 2015). The energy storage system is designed to be modular such that it can be added to any part of the power network that needs voltage and frequency support. There are two layers of control. The first layer is the inner control loop. This loop converts the power command from the outer AGPC control loop to a current command. The PI controller in the inner control loop forces the DC–DC buck boost converter to supply the desired output capacitor current. This is shown in Figure 2.9. The PI controller is tuned by the Genetic Algorithm (GA) with the integral square error being used as a fitness function.

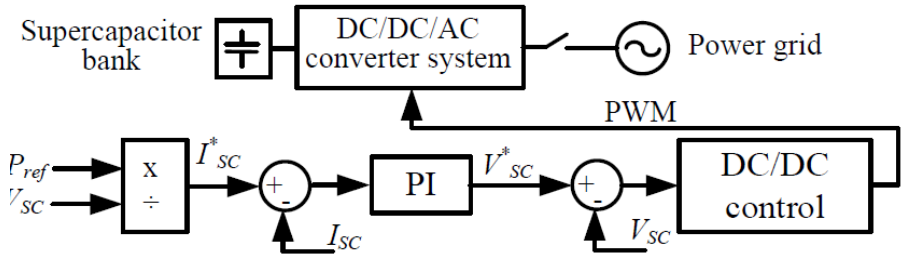

Figure 2.9. SCESS configuration.

The supervisory outer loop control is responsible for passing the signal for the amount of power to be supplied during a load disturbance and the amount of power to be absorbed from the network for recharge. The AGPC is able to do these tasks by estimating the plant parameters using a Recursive Least Square Identification algorithm and then computing the controller parameters by means of the normal state space representation of the process developed based on the estimated plant model. The functional block diagram of the AGPC (Zhang, Li, Cong, & Zhang, 2015) is shown in Figure 2.10. The control problem can then be expressed as a minimal cost function for the SCESS energy and voltage prediction with constraints of the converter capacity and capacitor charging and discharging

characteristics being imposed on it. Upon applying step load changes to the network, it was observed that the frequency and tie power deviations have been reduced drastically by the SCESS module.

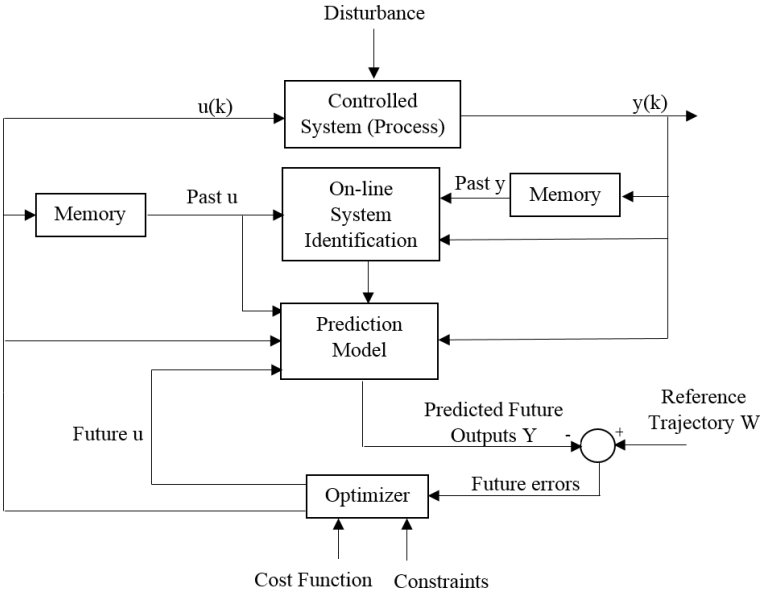

Figure 2.10. GA for PI controller tuning

Some of the main control methods for energy storage systems that reduce power, voltage or frequency fluctuations reviewed in this section as well as their advantages and disadvantages have been summarized in Table 2.5 below.

Table 2.5. Summary of advantages and disadvantages of energy storage control methods

Types of Control	Advantages	Disadvantages
Battery energy storage system with Kalman filters tuned by Model Predictive Control (MPC)	- Filter successfully removes power variations passed to batteries - Applied to ship grid - Charging and discharging current for batteries reduced +6% to -10%	-Compromise between slow engine reaction and big variations in power demand for batteries involved when setting filter constants ±20%(1.5s)
Coordinated supercapacitor-battery storage with MPC power tracking	- Power tracking error proven to be lesser compared to independent and separate supercapacitor and battery control strategies - Applied to ship grid	- Added computation burden for longer prediction horizon for MPC algorithm
Supercapacitor-based hybrid converter with Proportional-Integral (PI) control	- Supercapacitor voltage fluctuation minimized -Simple modeling of converter system with conventional PI control for higher loading conditions	- Effectiveness in reducing power variation in light loading condition of lesser than 30% not proven
Battery Energy Storage System for frequency control using load frequency control dynamic simulator	- Different strategies for energy support used within the same control method depending upon the level of frequency deviation resulting in increased effectiveness	- Overcharging of battery observed leading to heating - Modeling of battery and generators as a single machine equivalent might have to be modified to represent them in a hybrid propulsion power system
Battery and supercapacitor hybrid energy storage system with motor load following for torque and power fluctuation reduction	- Bus voltage information not required - Predictive load model developed from current motor load information - Applied to ship grid	- Not effective for high frequency load changes such as in high sea states

Types of Control	Advantages	Disadvantages
Battery and supercapacitor hybrid energy storage system with motor load following for torque and power fluctuation reduction	- Low and high frequency load changes reduced - Motor load information not required - Applied to ship grid - Simple voltage architecture without voltage measurement and feedback - Optimization method minimizes DC bus variation, power tracking error and high battery current operation simultaneously - Generator found to provide almost constant power leading to high fuel consumption efficiency	- Sum of generator and hybrid energy storage system currents can lead to high currents for the system if they are of opposite directions - Full system information required including voltage measurements and motor loading conditions
Photovoltaic (PV) Wind Diesel battery hybrid system with PI and fuzzy logic control	- Fuzzy logic is very effective in regulating both source and load variations for both voltage and frequency fluctuations	- PI control used to generate synchronous reference frame signals for *dq*-axis currents would introduce delay to overall control strategy
Wind-Solar-Diesel hybrid energy storage system with PSO-based frequency controller	- PI controllers tuned by PSO reduced frequency deviations to a greater extent than classically tuned controllers	- Online tuning of PI controllers has not been implemented for real time tuning of controllers
Active parallel hybrid energy storage system with Particle Swarm Optimization (PSO) control of battery and supercapacitor to decrease power fluctuations	- PSO method is very effective for non-linear optimization problem with multiple constraints on generator output power limits, generator ramp rate and energy storage capacity as well as its state of charge and current - Applied to Liquefied Natural Gas (LNG) ship grid - Real-time adjustment for output power fluctuation done	- Overcharging of battery observed leading to heating - Modeling of battery and generators as a single machine equivalent might have to be modified for representing the energy sources in a hybrid propulsion power system

Types of Control	Advantages	Disadvantages
	- Motor braking energy is gainfully absorbed back to grid	
Adaptive general predictive control used for Supercapacitor energy storage system in multi-area network	- Frequency and tie power deviations reduced significantly by more than 80% and 60% using adaptive predictive control - Power handled by the supercapacitive energy Storage was 0.01pu or lesser, thus, reducing heating effect and minimizing detrimental effects to lifespan to system	- Shipboard power systems might not be large enough to be multi-area networks - Load change cases considered a maximum of 0.02pu load addition which may not be applicable for application to seaborne vessels where the load changes are expected to be much higher at sea

2.4 CHALLENGES OF IMPLEMENTING ENERGY STORAGE IN SHIPBOARD POWER SYSTEMS TO REDUCE LOAD CHANGE TRANSIENTS

There have been numerous instances of Energy Storage implementations to reduce the effects of load changes on key parameters of the power system in the literature. However, the shipboard power system presents a unique environment, where such techniques have yet to be applied in a convincing manner, especially in areas such as the hybrid electric ships. Such power systems are of lower voltage than the land-based systems and tend to be more resistive resulting in conventional P/f and Q/V control approaches not being suitable. In these cases, the active power can have a greater influence on the system voltage with the reactive power needing to be controlled to regulate frequency (Roa, 2009). The nature of the load-changes also varies from that observed in the microgrids, where majority of the Energy Storage applications are in use. Due to the limited capacity of a shipboard power system, the power demand can change by up to 100% in a very short period of time during load demands such as pulse loads, those for weapons capability and the harsh environmental situations like wave induced load and hydrodynamic forces. In the long term, these cause excess wear and tear to the mechanical components in addition to unpredictable power demand. This results in low energy efficiency of the electrical sources and poor power quality. Therefore, Energy Storage solutions should be rapid acting and of sufficient capacity to avoid the damaging transient conditions. Control algorithms should be more robust to enable faster response in engaging the Energy Storage devices. There is already a trend of such systems moving away from traditional control methods like PI techniques towards modern and advanced approaches such as Genetic Algorithm, Adaptive Control, Model Predictive Control and Particle Swarm Optimization. Moreover, in power system configurations such as those in a hybrid electric ship, the response characteristic of the different modes of operation incorporating Energy Storage action should be carefully analyzed before the design of systems. In view of these, it might be necessary to combine different sources of Energy Storage as well as modify the proposed advanced control algorithms to develop a customized solution with properties that suits the operational needs of a particular marine power system. It should certainly take into consideration its size, extreme operating conditions and regulatory requirements such as energy efficiency and power quality standards.

2.5 SUMMARY

This paper introduces the shipboard power system with hybrid propulsion and the challenges it faces due to load changes arising from harsh environmental conditions at sea so as to maintain key electrical parameters within acceptable limits. The possibility of applying energy storage systems adapted from various other applications to reduce the transients arising from these load changes have been explored. It is found that battery and supercapacitor energy storage devices have been the most commonly used energy storage devices in related applications such as microgrids and renewable energy power systems. These are accompanied by a vast array of control strategies that have the potential to be modified to tailor the needs of the hybrid shipboard power system.

CHAPTER 3

EFFECT OF LOAD CHANGES IN HYBRID ELECTRIC SHIP POWER SYSTEMS

Viknash Shagar, Shantha Gamini Jayasinghe, Hossein Enshaei

Australian Maritime College, University of Tasmania, Launceston, TAS 7250, Australia

Partly published as '*Effect of load changes on hybrid electric ship power systems*' in the '*2016 IEEE 2nd Annual Southern Power Electronics Conference (SPEC), Auckland, 2016, pp. 1-5*'

This chapter looks at defining the severity of the transient phenomena in the hybrid propulsion shipboard power system due to load changes. The hybrid shipboard power system has been modeled and simulation studies have been carried out to investigate the effects of different types of load changes on the power system. The extent of the resulting transient conditions as well as their key properties on both the mechanical and electrical portions of the hybrid system have been analyzed and the findings have been presented.

Abstract – Load transients are often the cause of power failures leading to blackouts or malfunction of sensitive equipment on-board electric ships. Having a number of operating modes, hybrid electric ships face the same issue at a higher probability. This paper focuses on assessing the effects of load changes on hybrid electric ship power systems. Hybrid electric propulsion and the different modes of operation are first described in detail. Subsequently, the modelling of the hybrid shipboard power system using the MATLAB/Simulink platform is done. Different load change conditions are applied to this system in order to investigate the transient effects on the mechanical speed and the electrical frequency of the system caused by varying the magnitudes and types of loads that occur in the Power Take Out mode of a hybrid ship's operation. This study has attempted to find the nature of the load as well as the hybrid ship operating modes that have a greater effect on the engine speed and main busbar frequency transient conditions resulting from load variations. These findings give an overview of the severity of mechanical and electrical transient conditions that might arise for a hybrid propulsion system in the different loading scenarios at sea as well as other characteristics of the transients so that mitigation measures can be undertaken to reduce the effects of transients on key electro-mechanical parameters in future works.

3.1 INTRODUCTION

Similar to the automotive industry, new technologies have affected the shipping industry in many ways. Out of these technologies electric propulsion has created a significant change in the course of the shipping industry and becoming norm for propulsion in future ships. As a result, more ships are expected be fitted with electric propulsion systems. Even though electric propulsion has its advantages like improved memorability, increased fuel efficiency and flexibility in engine placement, it suffers from the drawback of getting load transients propagated into the electrical power system (McCoy, 2015). As mentioned above, following the same trend in the automobile industry, hybrid electric ships have emerged as an intermediate step towards fully electric ships to fill the need of reducing emissions caused by the ships of today. In hybrid electric ships, the traditional mechanical propulsion is combined with electrical propulsion for better fuel efficiency, thereby reducing emissions. Although the retrofitting requires an initial investment, costing can be compensated through saving fuel for the operation in the long run.

Currently, there is a noticeable gap in the available knowledge on hybrid ships, especially in the electrical aspects, such as understanding the behavior of the shipboard electric system (SES) in various operating modes and load transients. The existing problem that has been identified are the large variations in voltage and frequency in the shipboard power system that occur in transient conditions, where frequent and variable amounts of load-changes are added to the network. This effect has not been sufficiently studied in the hybrid propulsion based shipboard power systems. This problem is even more complex due to the fact that such power systems can operate in multi-modes because of the flexibility in using mechanical, electrical or both types of propulsion according to the operational needs. To analyze the transient behavior of the power system in a hybrid electric ship, a complete modelling of the electrical system would be necessary. By applying the various load-change scenarios for the system under different modes of operations, the transient levels of frequency and voltage can be measured. Hence the relationship between the magnitudes of the load-change and the resulting voltage and frequency fluctuations for each mode of operation can be determined. As a result, control measures such as energy storage systems can be designed to supply or absorb active and reactive power at appropriate times to reduce the magnitude and duration of these fluctuations.

With the aim of covering the aforementioned areas the paper is organized as follows. Section 3.2 of the paper describes the structure and different operating modes of a hybrid electric ship. System modelling and associated control parameters are presented in Section 3.3. Test cases, load profile and simulation results are presented in Section 3.4. Section 3.5 provides a discussion on the results obtained. Section 3.6 summarizes and concludes the study.

3.2 HYBRID SHIPBOARD POWER SYSTEM CONFIGURATION AND MODES OF OPERATION

Single line diagram of a hybrid electric ship power system is shown in Figure 3.1 where an electric motor, also known as a shaft machine, and a main engine are coupled through a gear box to drive the propeller. This particular combination allows the ship to operate in a number of different operating modes to suit given condition. For example, under light load conditions some of the auxiliary engines can be turned off and the main engine can be loaded to supply both propulsion and service loads by operating the motor as a generator. This flexibility can be used to optimize the fuel efficiency of the ship.

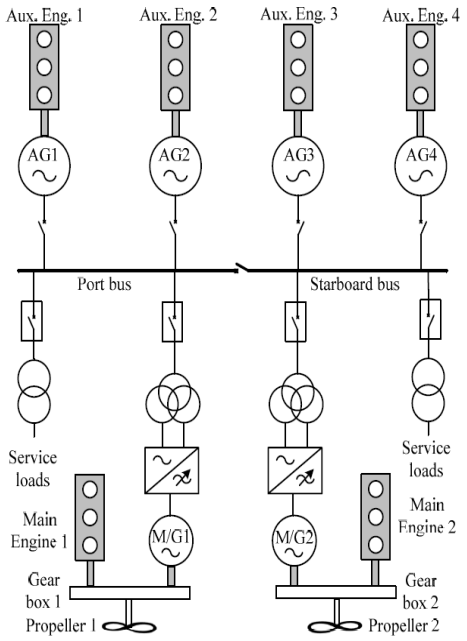

Figure 3.1. Hybrid ship power supply

The most common modes of operation covered in current literatures for the hybrid ship (MAN Diesel & Turbo, n.d.) are outlined as follows:

1. Boost or Power Take In (PTI) Mode – Main Engine and auxiliary generators supply power to service and propulsion loads. Shaft machine acts as a motor to drive the propellers.

2. Transit or Power Take Out (PTO) Mode – Only the main engine supplies power to propulsion and service loads. Shaft machine acts as an alternator to supply power to the service loads.

3. Power Take Home (PTH) Mode – Only Auxiliary Generators supply power for service and Propulsion loads. Shaft machine acts as a motor driven by the electrical power supplied by the generator.

4. Hybrid or PTO/PTI Mode – Shaft machine acts as an alternator or motor to maintain main engine RPM in the range of 70 – 100% of full load in order to increase their efficiencies. This makes flexible use of the electrical generators and the main engine.

5. Parallel Mode – Power demand is more than that of the capacity of auxiliary generators but less than that of the main engine. The main engine thus runs at partial load and supplies power for hotel and propulsion loads with one auxiliary generator supplying power to hotel loads. Shaft machine acts as an alternator.

6. Shore Connection or Cold Ironing Mode – Only port supply satisfies ship's power demand. All the engines can be shut down when the ship receives the shore power.

This portion of the study focuses only on the PTI mode of operation as the PTI mode utilizes both the main and auxiliary power generation sources and hence, this allows for a study of transients arising from the operation of both the power sources separately and in conjunction, due to events of various load changes. In addition, the largest fluctuations in loads for the ship are likely to occur during the PTI

mode as it can cater for the largest power demands possible for the vessel. Thus the worst case transients can be deduced by setting the configuration of the propulsion system of the hybrid vessel to PTI. Finally, in view of subsequent studies considering the incorporation of energy storage capability into the hybrid propulsion system, the severity of transients encountered during the high power demand conditions during the PTI mode would give information justifying if an energy storage system is necessary and if so, quantify the capacities of energy storage elements such a batteries and super capacities that might be required for the maximum generation capacity of the power system that includes both the main and auxiliary sources.

3.3 SYSTEM MODELLING AND CONTROL

In order to simplify the analysis, a simple hybrid electric ship with a main engine, an auxiliary engine-generator set, a shaft machine and a gearbox is considered in this study. The main and auxiliary engines have the same power capacities. The corresponding single line diagram is shown in Figure. 3.2(a). The conventional P/f and Q/V droop control is used for power sharing and control of the ship power system. The ship power system and its control is modeled using the MATLAB/Simulink software as shown in Figure 3.2(b) and Figure 3.2(c) (Patent No. Hybrid Shaft Generator Electric System for Shaft Generators Patent Number NO 332138, 2013; MAN Diesel & Turbo, n.d.). The control parameters and specification values for the generators, governor control and excitation system have been given in Tables 3.2, 3.3 and 3.4 (Rolls Royce Power Electric Systems, 2010; Saadat, 2004; Prabha, 1993; Krause, 1986; Caterpillar, n.d.; MarelliGenerators, n.d.; Murty, n.d.; MatLab , n.d.; Rolls Royce; MATLAB, n.d.).

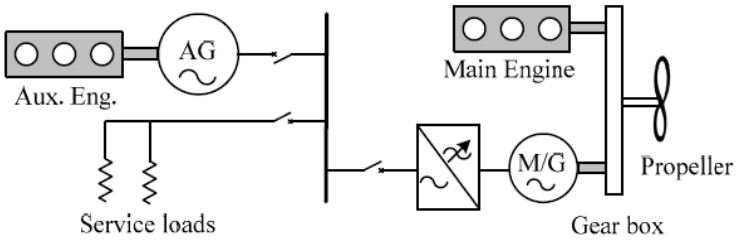

(a)

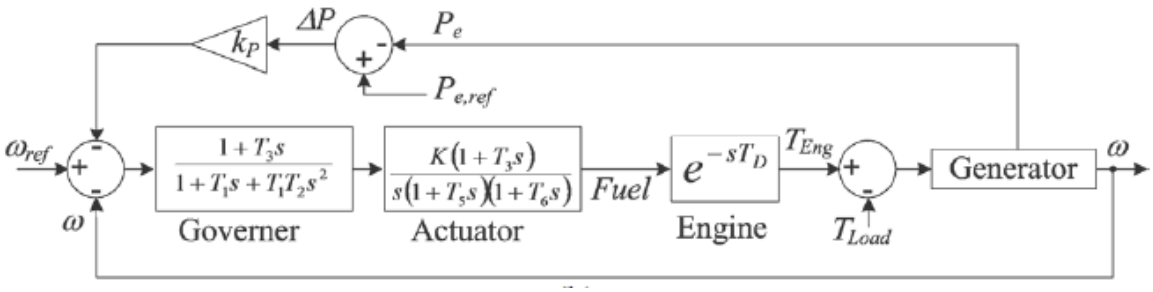

(b)

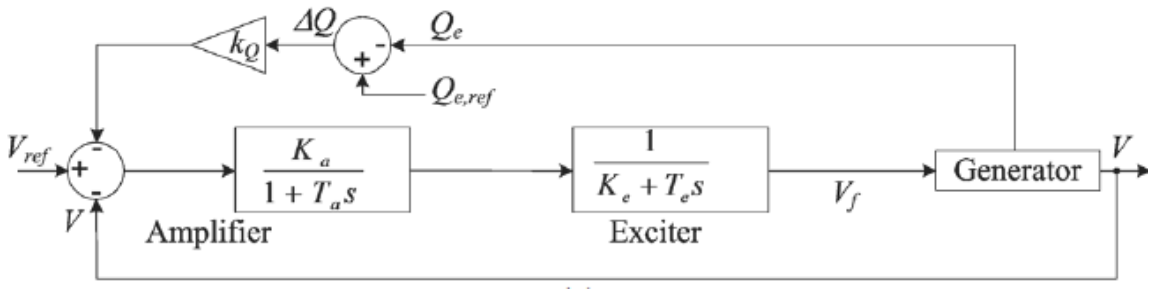

(c)

Figure 3.2. (a) Single line diagram of the hybrid electric ship power system used in this study (b) frequency droop controller (c) voltage droop controller

Table 3.1. System Parameters.

Parameters	Value
Bus voltage	230V
Base capacity	136kVA
Steadystate service RL load	50kW, 1kVAR
Frequency	50Hz
Base torque (Main engine)	8658NM
Setpoint torque	8500NM
Main engine (8 pole) reference speed	68rad/s
Main engine active power capacity	680kW
Main engine setpoint power capacity	578kW
Auxiliary generator (4 pole) power capacity	136kW

Table 3.2. Generator Parameters.

Parameters	Value
d-axix reactance	1.14pu
d-axis transient reactance	0.134pu
d-axis subtransient reactance	0.0694pu
q-axis reactance	0.643pu
q-axis subtransient reactance	0.0746 Ω
zero sequence reactance	0.0746 Ω
stator reactance	0.000614 Ω
open circuit transient time constant	3s
short circuit transient time constant	0.35s
short circuit subtransient time constant	0.029s
Inertia	218.3kgm^3
per unit inertia constant	2.7s

Table 3.3. Governor Control Parameters.

Parameters	Parameter description	Value
T_1	Electrical control box 1st time constant	0.01s
T_2	Electrical control box 2nd time constant	0.02s
T_3	Electric control box derivative time constant	0.2s
T_4	Actuator derivative time constant	0.25
T_5	Actuator 1st time constant	0.009s
T_6	Actuator 2nd time constant	0.0384s
T_D	Fuel Combustion delay	0.024s
K	Control gain	40
K_P, K_Q	Droop	5%

Table 3.4. Excitation System Control Parameters.

Parameters	Parameter description	Value
K_a	Controller gain	300
T_a	Controller time constant	0.001
K_e	Exciter gain	1
T_e	Exciter time constant	0
K_f	Damping filter gain	0.01
T_f	Damping filter time constant	0.2

The system parameters are shown in Table 3.1. A setpoint power capacity has been defined for the main engine, at 85% of the maximum power capacity to keep it constant as the main engine is not fast acting in response to changing power demands. Therefore the torque delivered by the propellers is also fixed at a set point if the main engine reference speed is a constant. This torque setpoint is at a value of 8500NM. The capacity auxiliary generator is at 20% of that of the main generator. The steady state service RL load of the system is 50kW, 1kVAR. In this study, the base power capacity of the electrical portion of the hybrid propulsion system is taken to be 136KVA. Therefore the electrical load quantities can be expressed in per unit (pu) notation relative to this base capacity. The mechanical (propulsion) loads will be expressed in pu terms relative to the base torque value. The generator, governor control and the excitation control parameters used for the model are listed in Tables 3.2 to 3.4 respectively.

In the system shown in Figure. 3.2(a), the main engine provides mechanical power to the gear box. The shaft machine, M/G, can act as a motor to provide a power boost to the propeller or work as a generator to take out part of the mechanical power available at the gearbox and feed into the electrical power system. The auxiliary generator, AG, supplies power to the service loads as well as the propulsion load depending on the operating mode chosen. In the simulation model shown in Figure.3.2

(b) the propulsion load and service loads are represented as the load Torque, T_{Load}, which is varied to introduce load changes.

3.4 SIMULATION RESULTS

The electrical loads on a ship can change very quickly and by large amounts compared to the total capacity available at a given time. This can result in system instability due to transients that arise from these load changes. Therefore, load change should be investigated in order to determine the severity of the transient effects as a result of typical levels of load changes (Chin, Su, & C, 2016). This study particularly focusses on frequency transients following low load changes. Since the speed of the main engine is also linked to the electrical system, the former will also be a measured quantity in the following case studies. Analysis of the simulation commences after the first 10s to omit the transients due to initialization of the model in the software. The 5% and 10% thresholds for permanent and transient variations as stipulated in the relevant standards have been displayed in Table 2.4 and is calculated from the nominal electrical frequency value of 50Hz. These thresholds have been included in the subsequent frequency plots and have been marked at 45Hz, 47.5Hz, 52.5Hz and 55Hz by the colored lines. The parameters are considered to have reached steady state if they are within 2% of the steady state values of 68rad/s and 50Hz for the speed and frequency values respectively. A brief description of the test cases to be conducted is as listed in Table 3.5. It is to be noted that the Service load change only includes the change in the active power component of the loads. The reactive (inductive) power is assumed to be 2% of the active power loading at all times. All the load increments and decrements are applied as step changes to simulate the worst case loading scenario for the particular load levels. A sudden increase in load levels with a minimal ramp rate gives the system the least amount of time to evolve and change its state thus resulting in the highest transient levels. This enables an evaluation of the robustness of the existing system model without implementation of additional mitigation measures.

Table 3.5. Test Case Description Summary

Test Case	Load change [propulsion load change (pu), service load change (pu)]
1	[0,0] (base load cond.)
2a	[0.05,0]
2b	[0.1,0]
2c	[2*0.05,0] (multi step load cond.)
3a	[0,0.15]
3b	[0,0.3]
4	[0.1,0.3] (simultaneous load cond.)

Case 1 – Steady state loading conditions have been applied in this case. The torque setpoint to the propellers is set constant at 8500NM while the RL service load is also kept constant at 50kW, 1kVAR. The propulsion and service load profiles are shown in figures 3.3 and 3.4. The main engine speed and the electrical frequency at the main electrical busbar have been plotted in figures 3.5 and 3.6 respectively. The engine speed is found to be at a steady state value of 68rad/s while the electrical frequency is constant at 50Hz as expected. Thus the system is stable at initial load conditions.

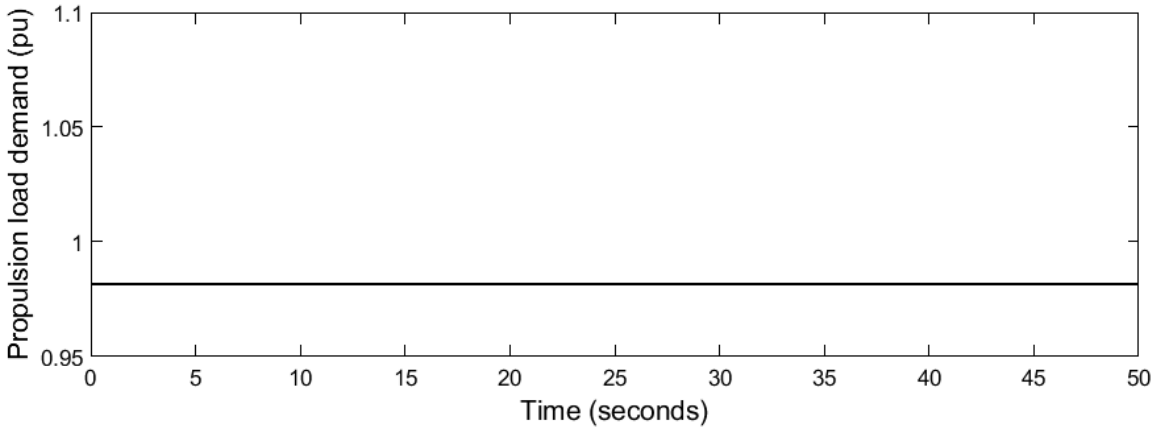

Figure 3.3. Propulsion load profile

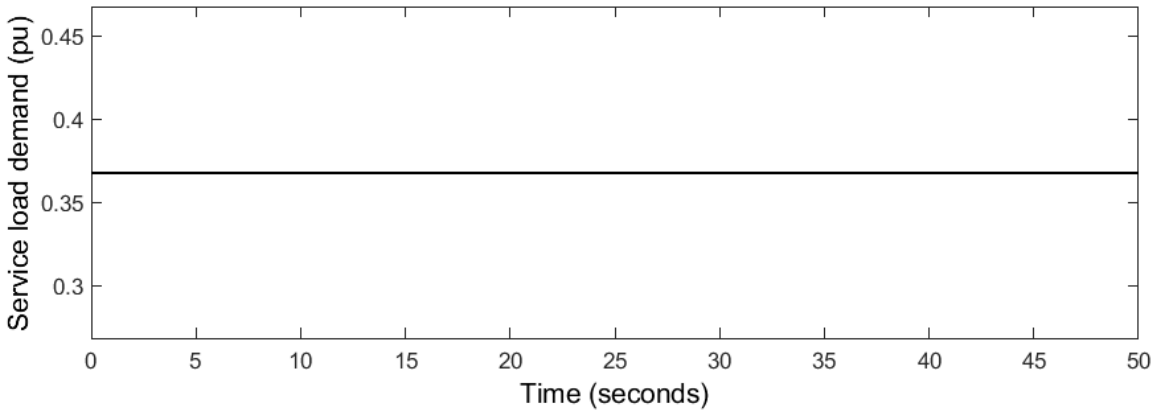

Figure 3.4. Service load profile

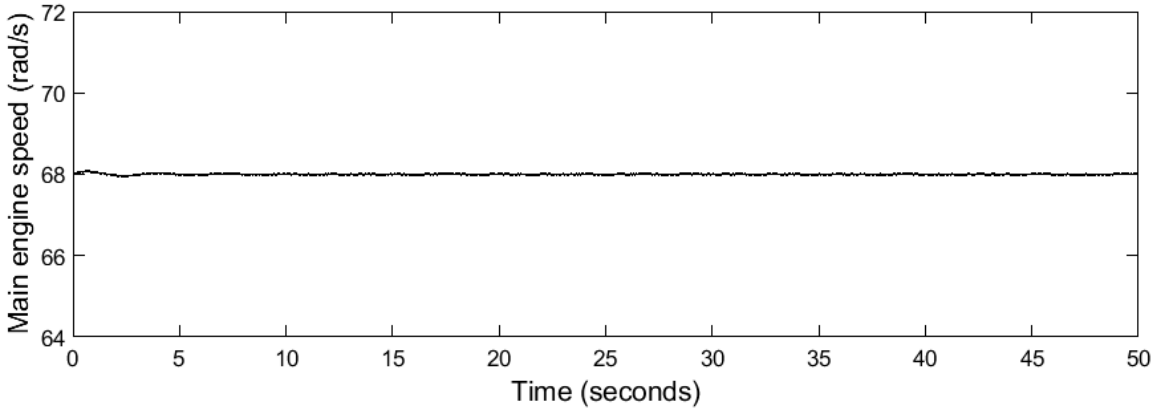

Figure 3.5. Main engine speed profile

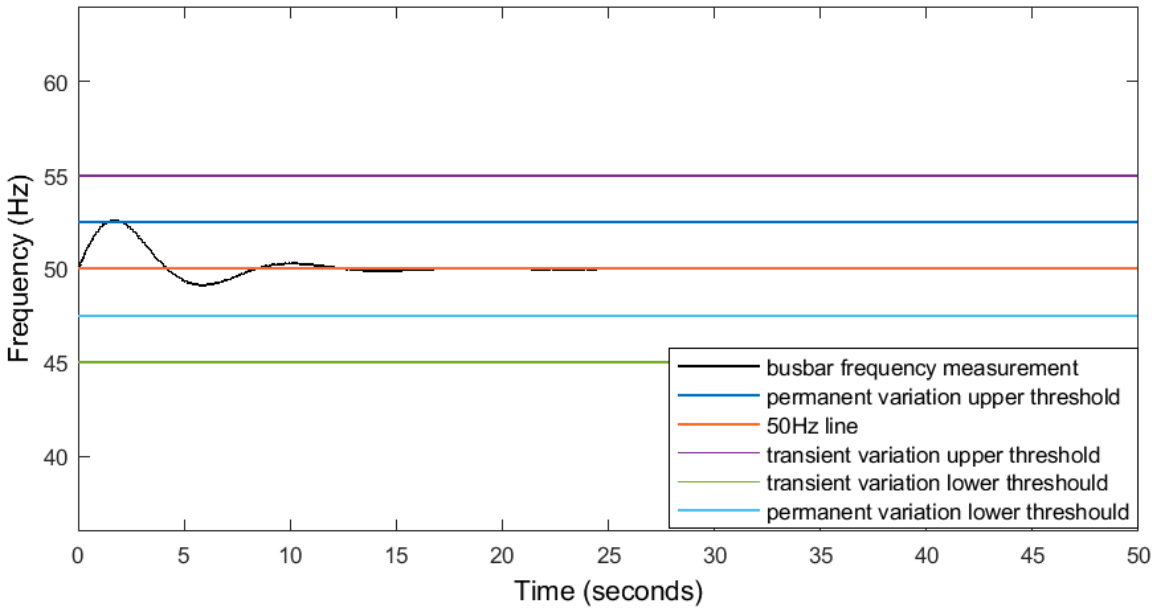

Figure 3.6. Frequency profile

Case 2 – Step changes to the propulsion load have been applied and removed in various levels of 0.05pu and 0.1pu in addition to the torque setpoint value while the service load is still kept at the steady state level.

In Case 2a, the propulsion torque load is increased by 0.05pu at 15s and removed at 30s.The load profiles are shown in figures 3.7 and 3.8 and the resulting main engine speed and main busbar frequency plots are shown in figures 3.9 and 3.10.

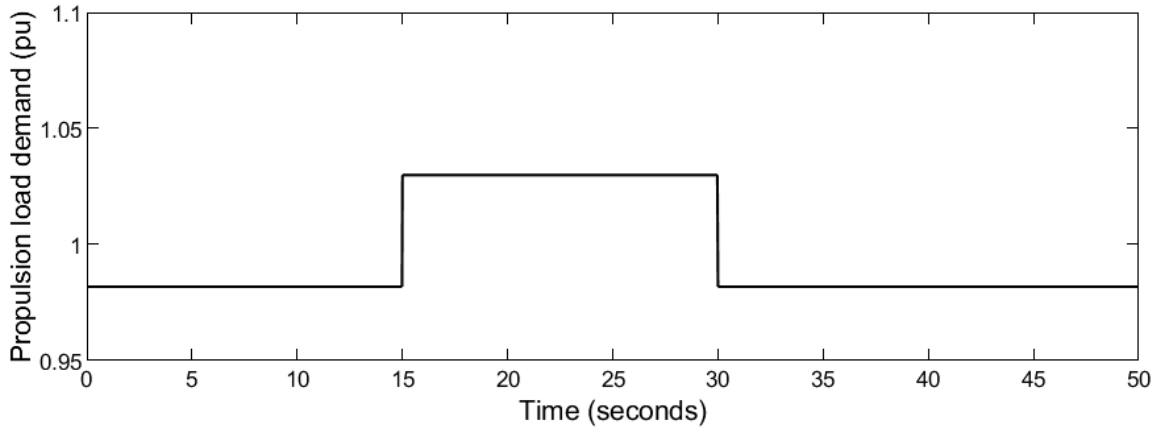

Figure 3.7. Propulsion load profile

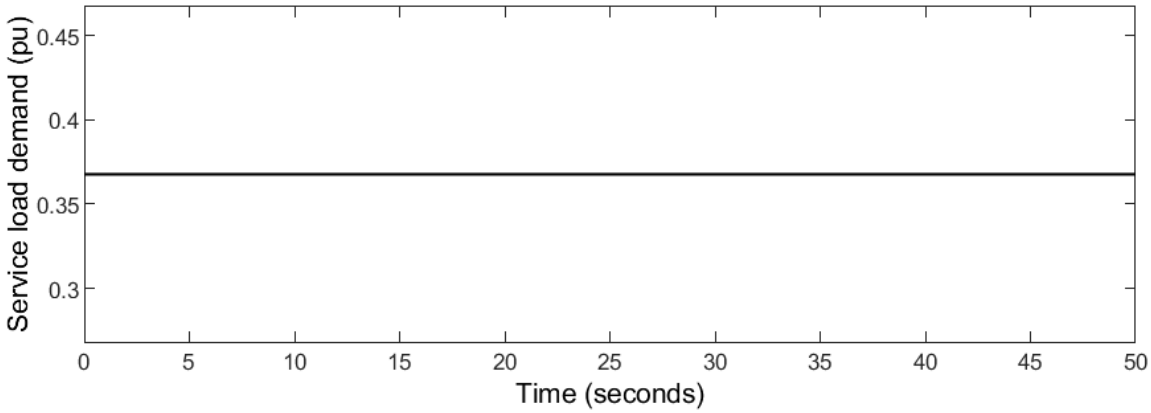

Figure 3.8. Service load profile

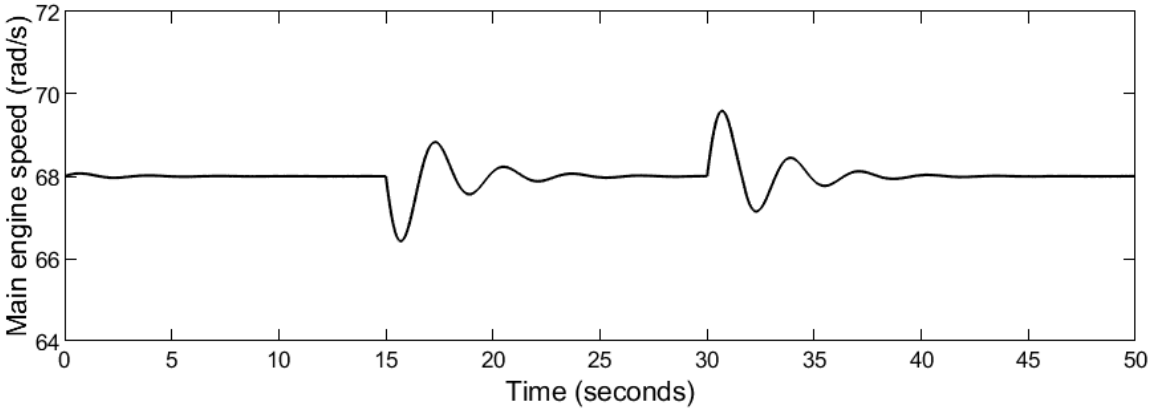

Figure 3.9. Main engine speed profile

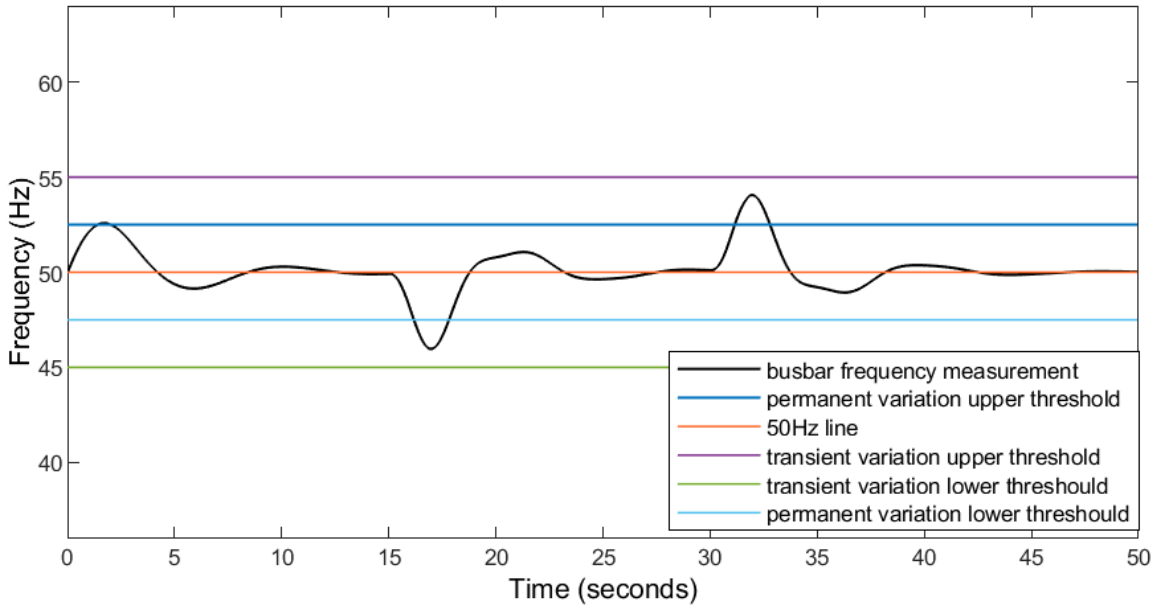

Figure 3.10. Frequency profile

The main engine speed has a maximum fluctuation of about 1.6rad/s and takes about 0.8s to reach the steady state value. The frequency fluctuates by a maximum of about 4.2Hz for a period of an estimated 6.6s before reaching steady state. For both parameters, the load application and removal have resulted in symmetrical transients.

In Case 2b, the propulsion torque load has increased by a step change value of 0.1pu at 15s and removed at 30s. The load profiles are shown in figures 3.11 and 3.12 while the resulting main engine speed and main busbar frequency plots are shown in figures 3.13 and 3.14.

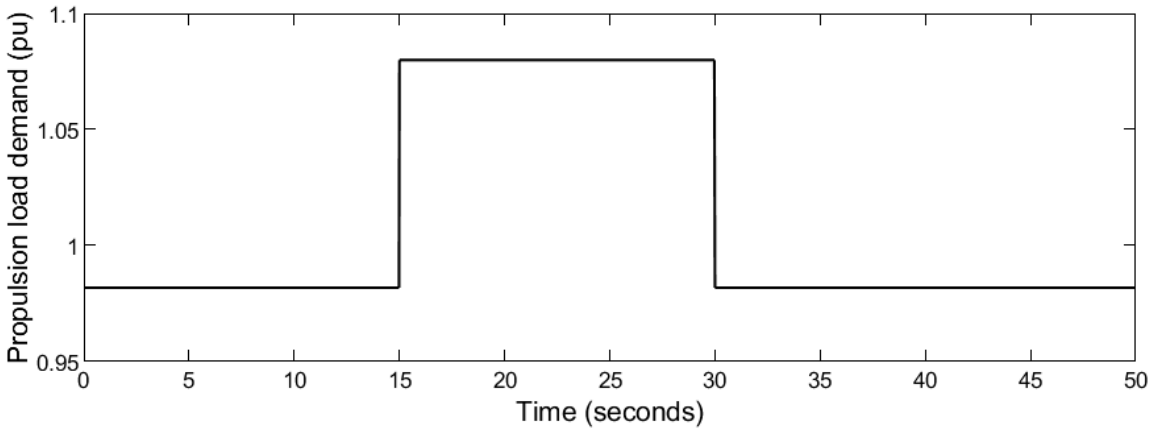

Figure 3.11. Propulsion load profile

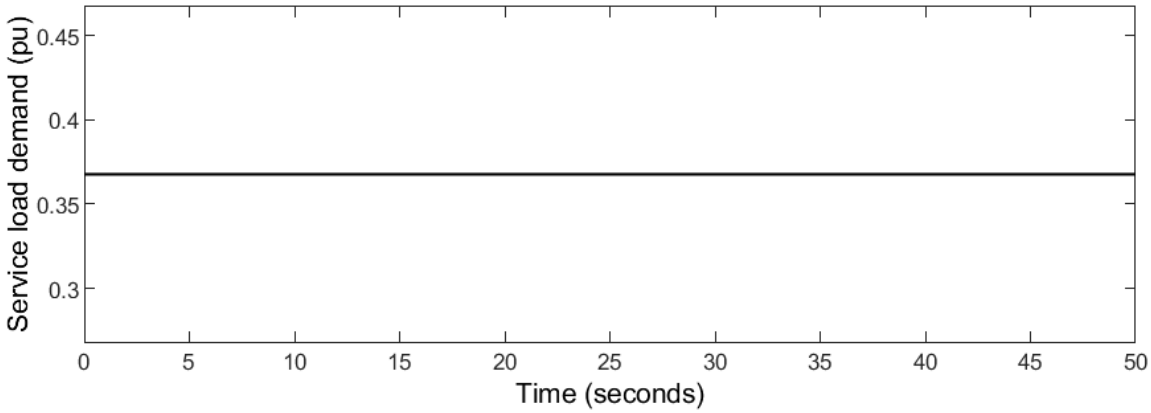

Figure 3.12. Service load profile

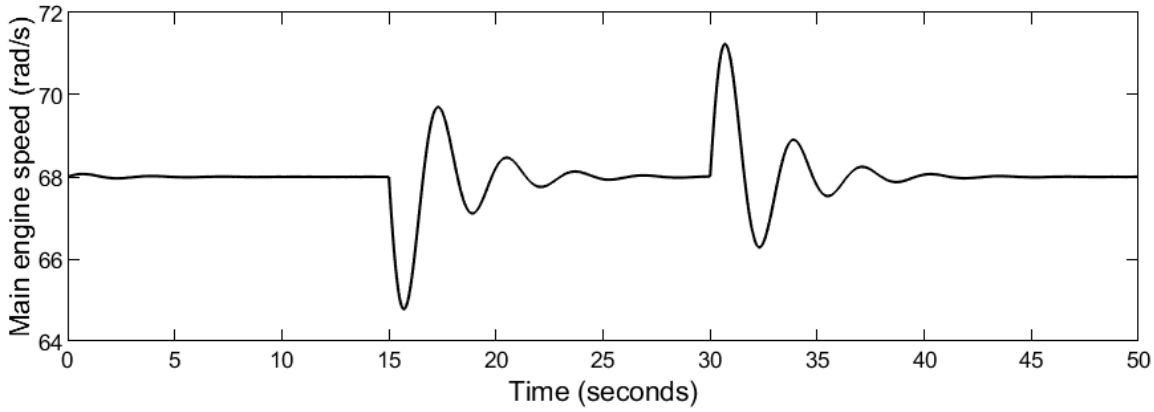

Figure 3.13. Main engine speed profile

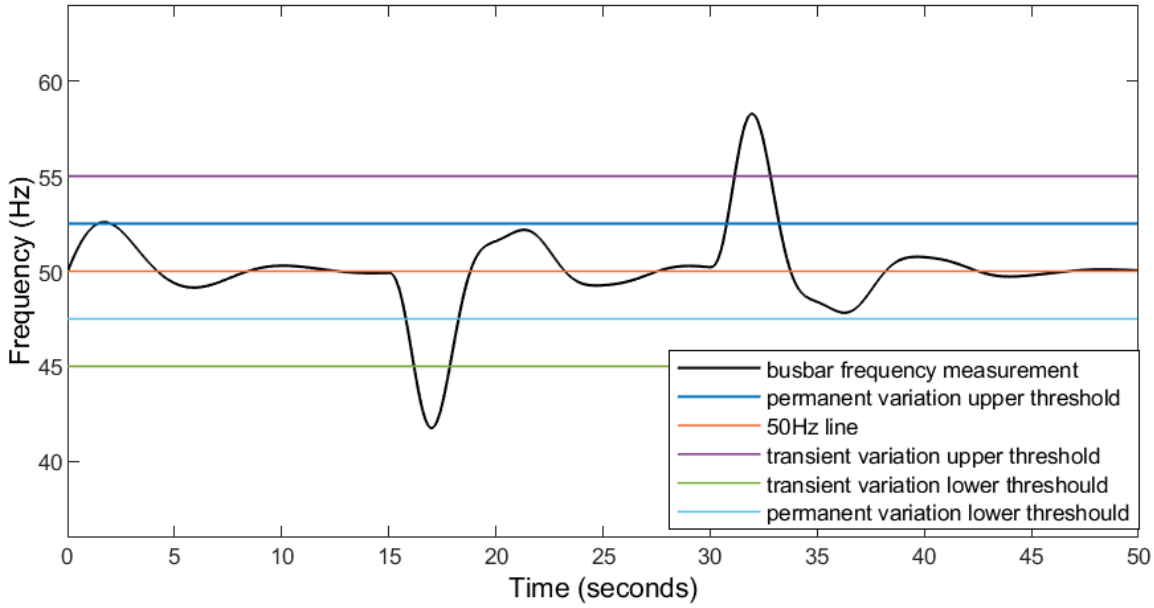

Figure 3.14. Frequency profile

The main engine speed has a maximum fluctuation of about 3.2rad/s and takes about 2.9s to reach the steady state value. The frequency fluctuates by a maximum of 8.6Hz for a period of 7.7s before reaching steady state. For the frequency profile, the load application event has resulted in more severe transients than the load removal event while the loading and unloading events produce symmetrical transients for the main engine speed profiles.

In Case 2c, multi-stage loading has been applied to the system. This profile type of load change is especially relevant for sea going vessels where extreme tidal and other environmental changes might result in successive step load events in close succession to each other and therefore it's crucial to understand the extent of such load changes.

The propulsion load has been applied and later removed by an amount of 0.1pu as in Case 2b. However, it has been done in in 2 steps of 0.05pu increments. The second increment of 0.05pu step load change has been applied before the main engine speed has reached steady state following the first step load increment. The second step load increment of 0.05pu has been applied and removed at 0.4s (ie. at the halfway point of the 0.8s settling time period from Case 2a) after and before the initial step load increment and decrement of the same load value at 15.4s and 30s respectively. This multi-step load profile is as shown on Figure 3.15. The torque loads values have been converted into per-unit (pu) terms for brevity in the figure. The service load, main engine speed and electrical frequency profiles resulting from this load change profile are as shown in Figures 3.16, 3.17 and 3.18 respectively.

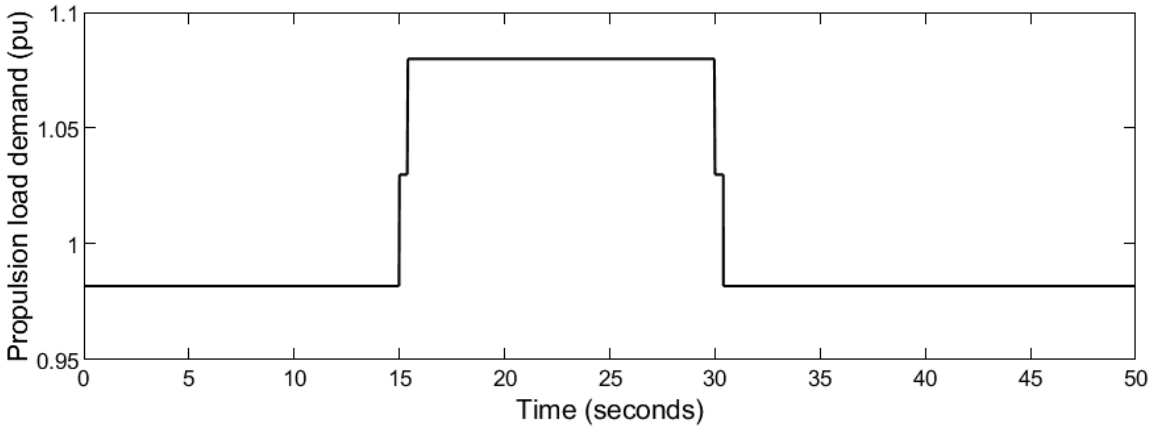

Figure 3.15. Propulsion load demand profile

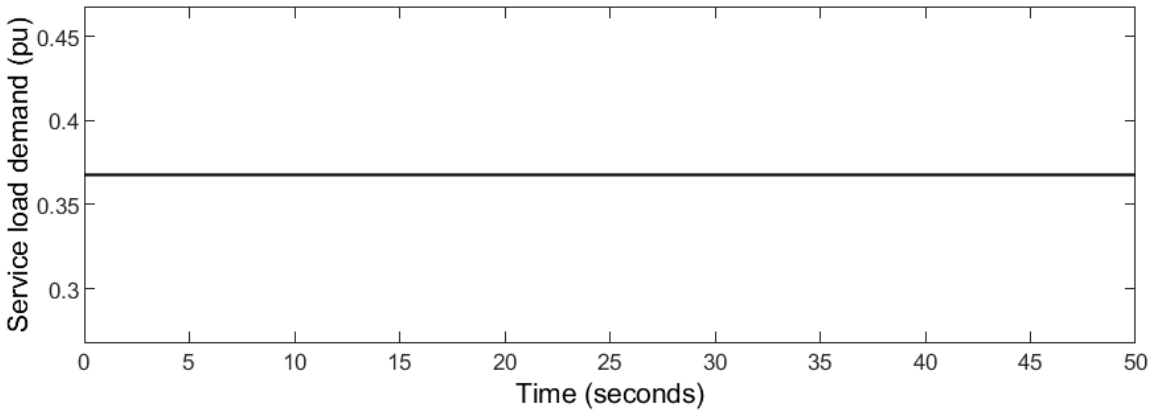

Figure 3.16. Service load demand profile

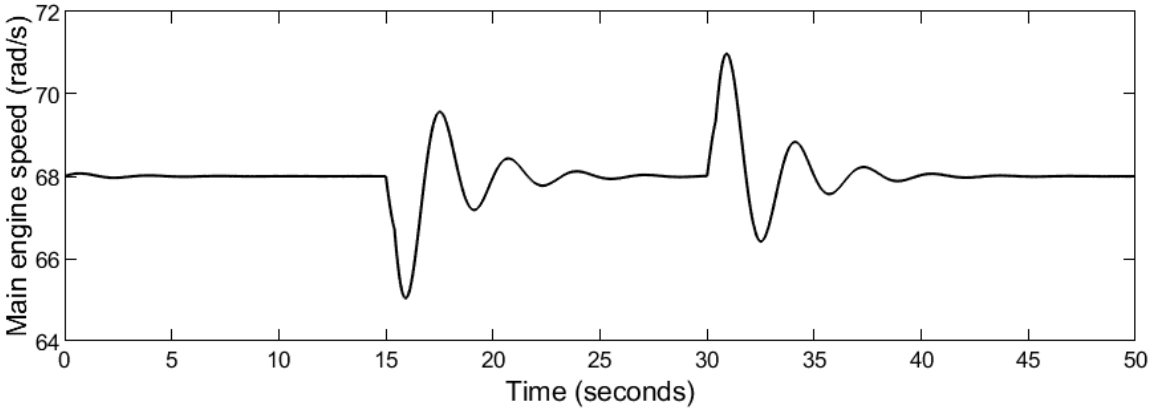

Figure 3.17. Main engine speed profile

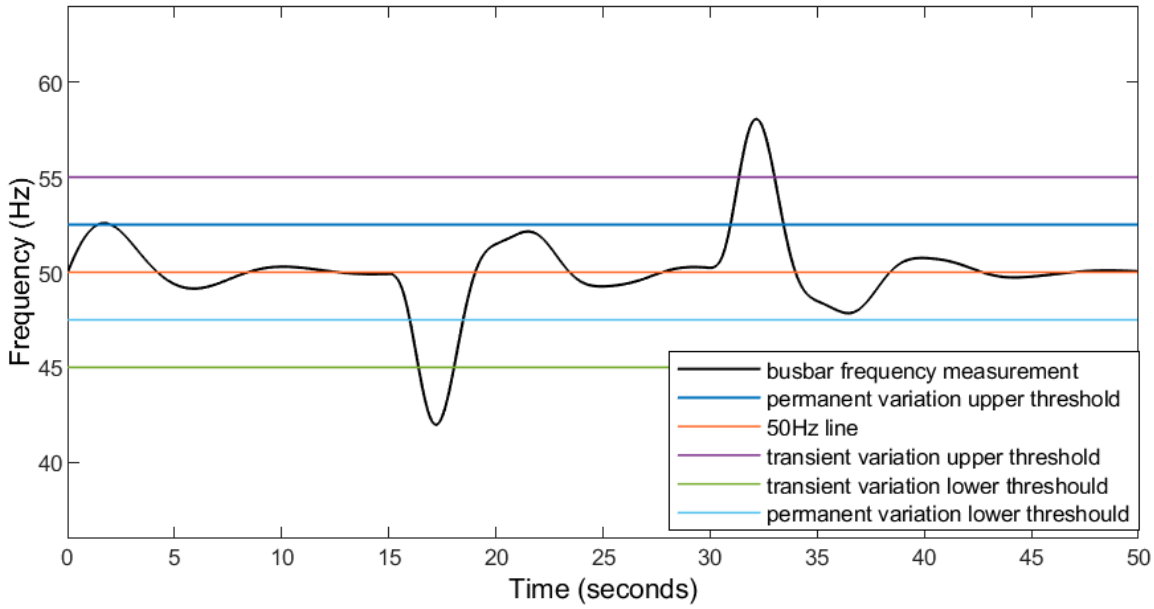

Figure 3.18. Frequency profile

The main engine speed has a maximum fluctuation of about 3.0rad/s and takes about 2.4s to reach the steady state value. The frequency fluctuates by a maximum of 7.7Hz for a period of 7.5s before reaching steady state. The speed profile is almost symmetrical for the loading and unloading events. However, the frequency profile is symmetrical for the load application and load removal events.

Case 3 - Step changes to the service load have been applied and removed in various levels of 0.15pu and 0.3pu in addition to the steady state resistive load value of 50kW while the propulsion load is kept at the steady state level. Circuit breakers have been used to switch the RL service loads in and out of the power system model. Thus, the service load changes can be considered to be step changes. Unlike *Case 2*, the multi-step load application will not be considered for service loads in this part of the study because they can largely be controlled by vessel operators and thus, a sufficient time interval between consecutive service load changes can be arranged to avoid transient conditions from successive loading conditions from interacting with each other. The inductive load has been kept at 2% of the magnitude of the active power loads. Henceforth, load change levels for the service loads would refer to the active power loads and the proportionate reactive power load changes is assumed to be a ratio of the active power load as described above.

In Case 3a, there has been a step change of the service load level. It has increased by 0.15pu from an initial level of 0.37pu at 15s and removed at 30s. The propulsion and service load profiles are depicted in figures 3.19 and 3.20. The resulting main engine speed and main busbar frequency plots are shown in figures 3.21 and 3.22.

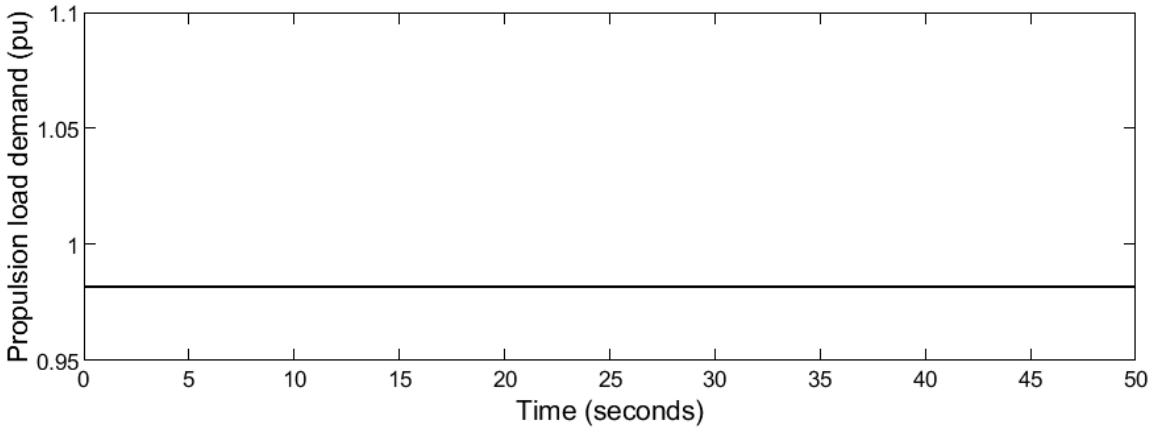

Figure 3.19. Propulsion load demand profile

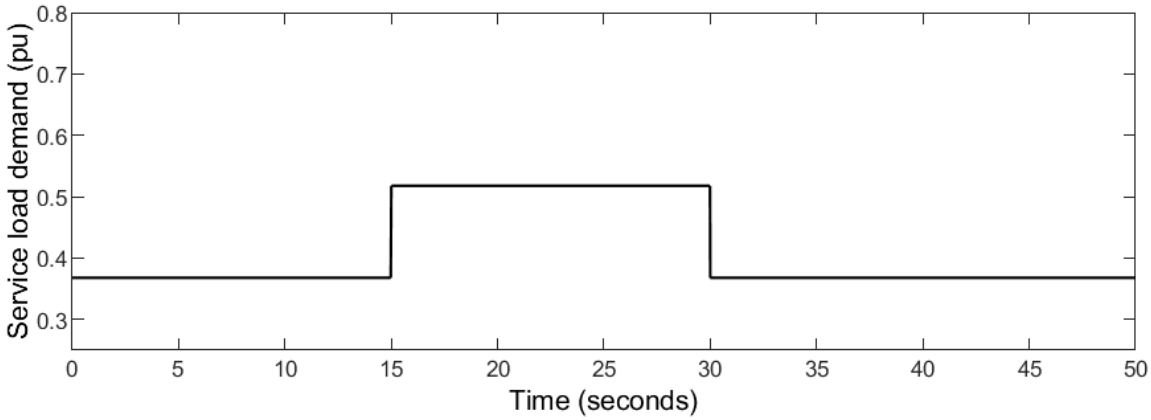

Figure 3.20. Service load profile

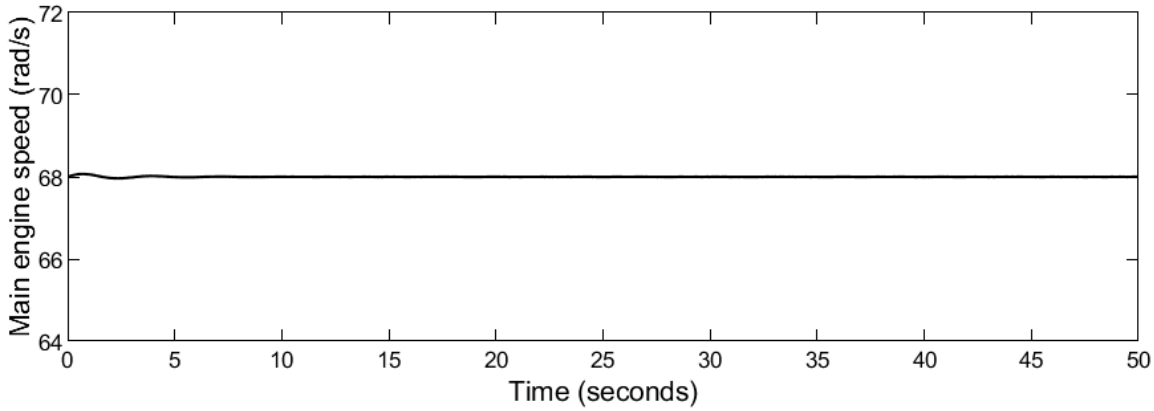

Figure 3.21. Main engine speed profile

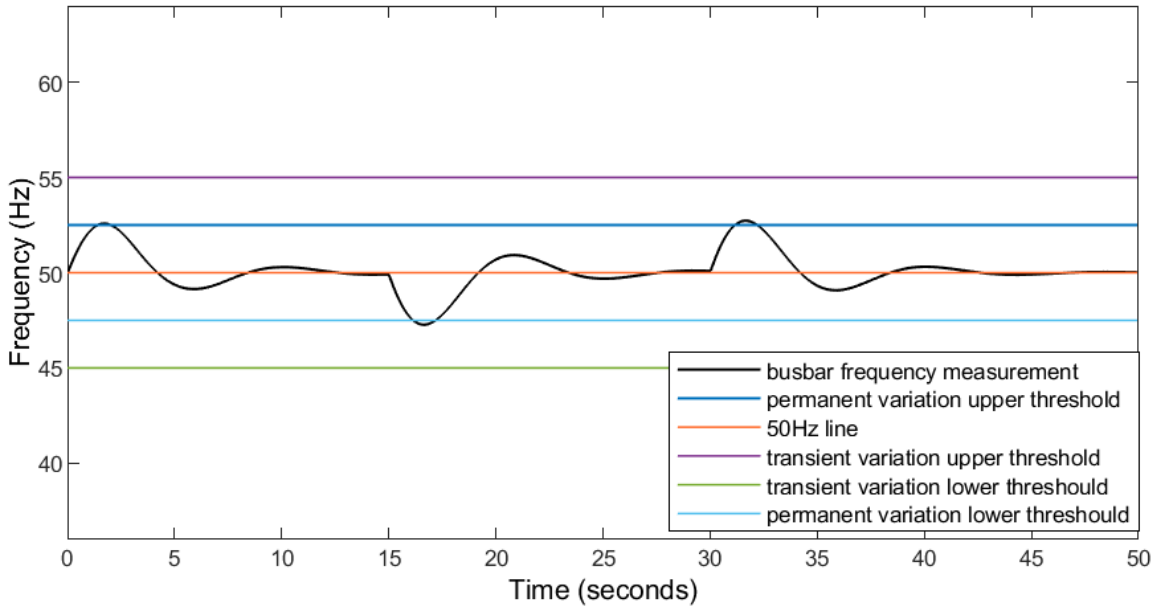

Figure 3.22. Frequency profile

The main engine speed has negligible transients in response to the service load changes and remains at its steady state value of 68rad/s. The frequency fluctuates by a maximum of 2.5Hz for a period of about 3.2s before reaching the steady state and the transients resulting from the load application and removal events are approximately symmetrical in nature.

In Case 3b, the service load has increased by 0.3pu from an initial value of 0.37pu at 15s and removed at 30s in a step load fashion. The propulsion and service load profiles are displayed in figures 3.23 and 3.24 while the main engine speed and main busbar frequency plots are shown in figures 3.25 and 3.26. The main engine speed has negligible fluctuation in response to the service load changes and remains at its steady state value of 68rad/s. The frequency fluctuates by a maximum of 5.5Hz for a period of about 7.2s before reaching the steady state and the transients resulting from the load application and removal events are symmetrical in nature.

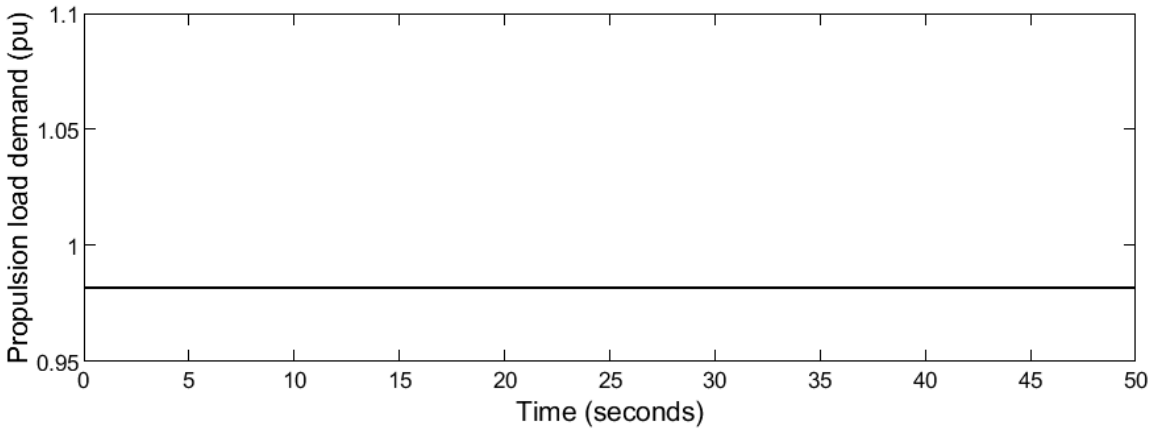

Figure 3.23. Propulsion load demand profile

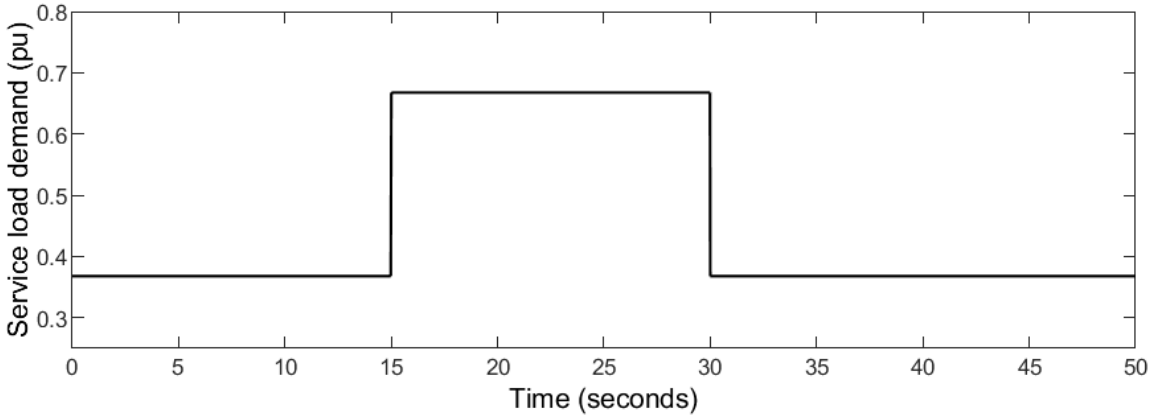

Figure 3.24. Service load demand profile

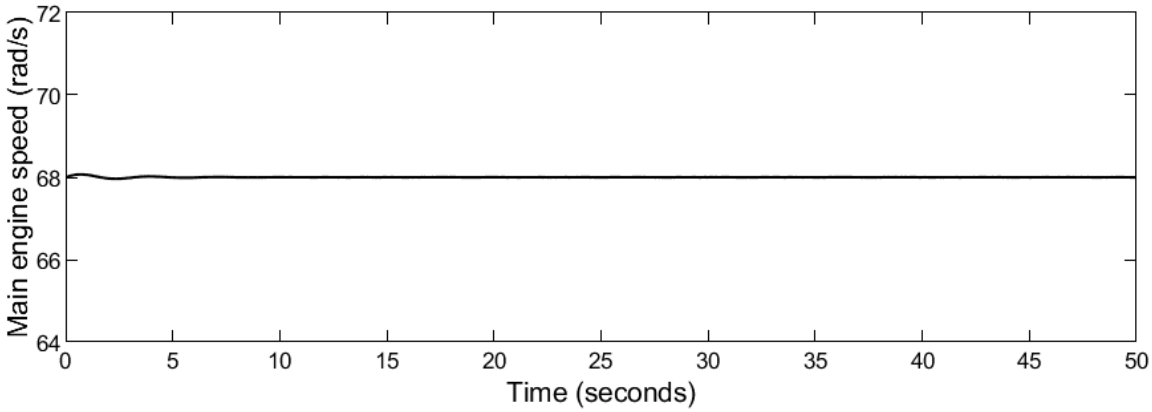

Figure 3.25. Main engine speed profile

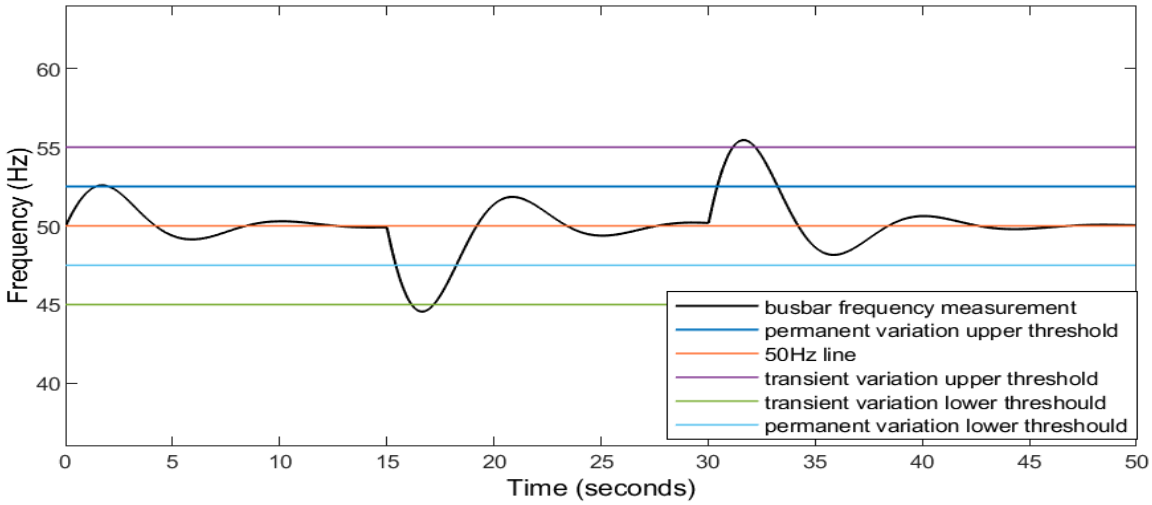

Figure 3.26. Frequency profile

Case 4 – The effects of simultaneous loading of propulsion and service loads would be studied in this case. This can illustrate a practical scenario in ship operations where the ship has to maneuver for berthing purposes. The main engines are still in operation, however, the bow and/or stern thruster motors have to be started at the same time that the main engine speed is to be altered to prepare for the operation. Electrical loads that are unrelated to ship propulsion purposes such as chillers may also happen to be started or switched off in coincidence to a sudden increase in loading to the propellers. In this case, a 0.1pu propulsion loading and a 0.3pu service loading has been simultaneously applied

at 15s to the system and removed at 30s in a step change manner. This set of loading conditions constitute the highest level of loading for the propulsion and service loads that has been applied thus far. The propulsion and service load profiles are depicted in figures 3.27 and 3.28 while the main engine speed profile is as shown in Figure 3.29 and the main busbar frequency is displayed in Figure 3.30.

The main engine speed has varied by a maximum of 3.3rad/s and the settling time of the transients is about 2.8s. On the electrical portion of the system, the busbar frequency fluctuates by a maximum amount of 13.5Hz. The settling time of the frequency transient condition to steady state levels is about 11.7s. From the plots, it's apparent that the main engine speed and the electrical frequency transient profiles are approximately symmetrical for the load application and the load removal events.

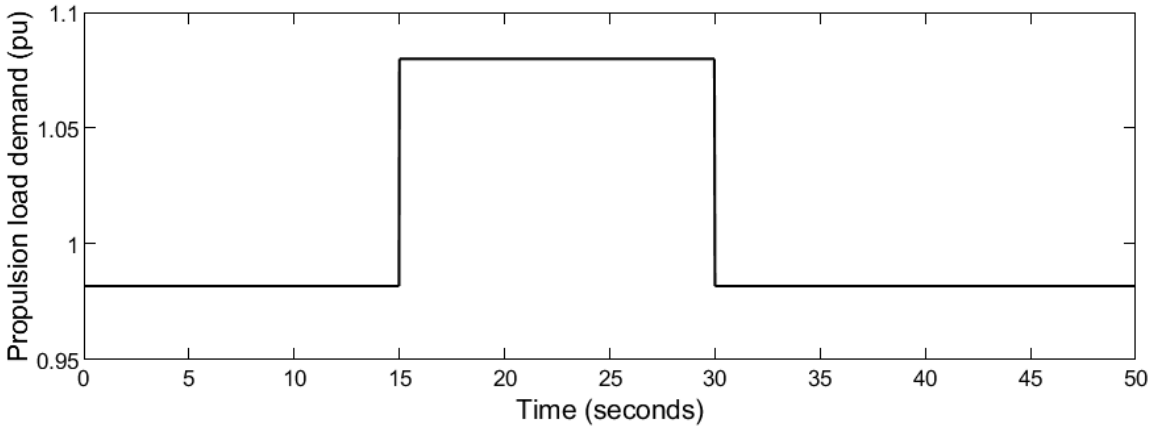

Figure 3.27. Propulsion load demand profile

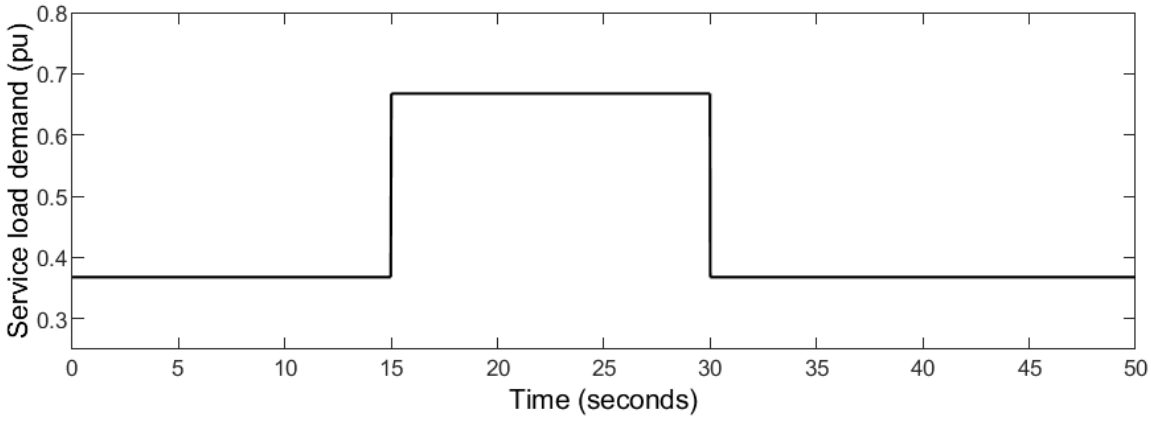

Figure 3.28. Service load demand profile

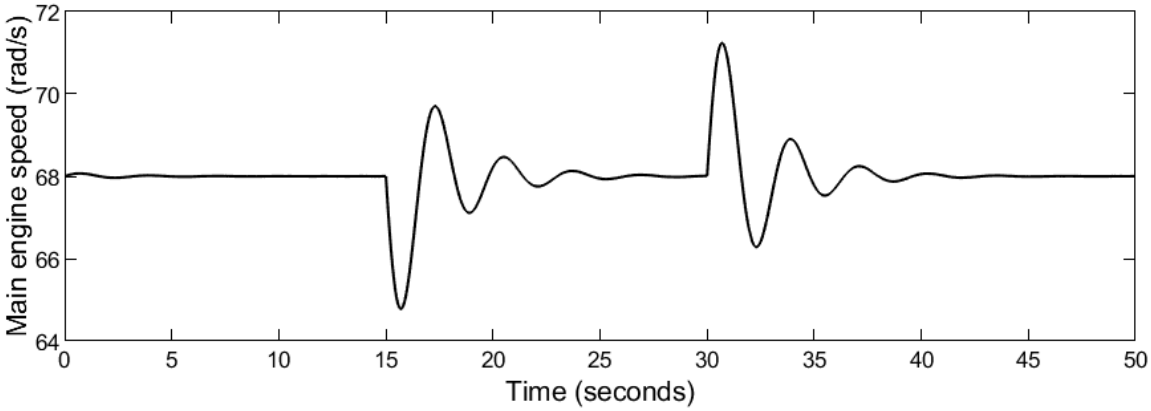

Figure 3.29. Main engine speed profile

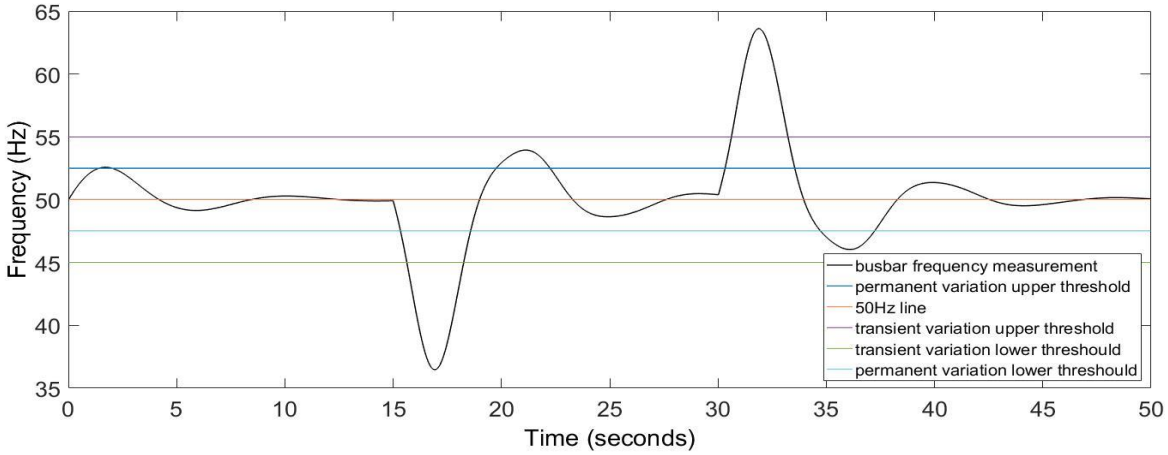

Figure 3.30. Frequency profile

Table 3.6. Test Case Results Summary

Case	Max. main engine speed transient magnitude (%)	Main engine speed transient settling time (s)	Max. main electrical busbar frequency deviation (%)	Main electrical busbar frequency deviation settling time (s)
1	-	-	-	-
2a	2.4	0.8	8.4	6.6
2b	4.7	2.9	17.2	7.7
2c	4.4	2.4	15.4	7.5
3a	-	-	5.0	3.2
3b	-	-	11.0	7.2
4	4.9	2.8	27.0	11.7

A summary of the key parameters quantifying the severity of transients during the load change cases is as shown in Table 3.6. The maximum magnitude of fluctuation of parameters are expressed as a percentage of the nominal values of 68rad/s for the main engine speed and 50Hz for the main electrical busbar frequency. It is to be noted that parameter values which are within 2% of the steady state values are considered to have reached steady state. It follows that if the maximum variation of the parameters is lesser than or equal to 2%, they would be considered to be negligible and would be marked with a '-' in the table.

3.5 DISCUSSION

The results across all the cases involving load-changes show that the electrical frequency experiences more severe transients than the main engine speeds. This occurs even in Cases 2a and 2b where there are no changes in the service load levels which are directly connected to the electrical system. Therefore, the transients experienced by the propeller shaft connecting to the main engine has been shown to propagate upstream into the electrical system, thus, causing distortion at the main electrical busbar.

The results from test cases 2a and 3a show that a 5% change in propulsion load level and a 15% change in the service load levels lead to transients that are well within the IEC standards for frequency transient conditions. However, doubling the load change levels to a propulsion load change of 10% or a service load change of 30% applied separately or in conjunction results in the IEC standards for frequency transient requirements of both the transient amplitude and the recovery (settling) time being violated as in Cases 2b, 2c and 3b. The amplitude of the frequency has gone beyond the 10% threshold limit for transient conditions. Likewise the settling time has also been greater than the transient recovery time limit of 5s in these cases. The permanent variation limits of the electrical frequency as stipulated by IEC and displayed as in Table 2.4, has not been violated in all the cases conducted during steady state conditions. Hence, it is clear that transients caused by relatively low load change conditions of between 10% and 30% has the potential to be huge in magnitude and therefore disruptive to the optimal operating condition of the entire power system. Such large transients lead to poor power quality that might result in malfunction of various equipment crucial to ship operation. In addition, they are a safety hazard as they can cause overheating and increase the risk of failed insulation.

The level of transients observed from the system operating conditions suggest that doubling the propulsion and service load change levels from 0.05pu to 0.1pu and 0.15pu to 0.3pu respectively (as in Cases 2a to 2b and 3a to 3b) results, in most cases, speed and frequency transient magnitudes being more than twice as severe, as quantified by the maximum fluctuation recorded. However, the settling time has not been affected to the same extent as the magnitude of the maximum fluctuation. This largely suggests the relationship between the amount of load change experienced by the hybrid

propulsion power system and the severity of the transients is not linear.. The robustness of such systems, can in fact, become much more degraded in comparison to the increase in load levels.

The multistep load change for propulsion purposes has been included in this study due to the higher power levels involved in operations for propulsion purposes as compared to service loads. The multistep load change sequence applied in Case 2c, where the second step of the propulsion load change takes place at the halfway mark of the settling time of the initial step, has resulted in milder transient conditions of up to 17.2% lesser settling time and a 10.5% reduction of the maximum amplitude of the fluctuation encountered, as compared to applying the equivalent amount of load change in a single step. This can be used in applications to reduce transients where the external propulsion load conditions experienced by the propellers can be approximated beforehand based on tidal and wind patterns or in ice-breaking operations where the thickness of the ice and the propulsion torque needed to break through it is known. The propulsion operation can then be undertaken in instances where the total load torque increases in stages rather than in one bigger step with the same overall propulsion load change.

The simultaneous propulsion and service load change has been investigated in Case 4. Case 4 also presents the heaviest load change scenario out of all the cases considered. It is observed that when the propulsion and service loads are applied and removed at the same instant, the effect on the main engine speed is only slightly worse off in terms of the settling time of the transients and almost similar for the transient amplitudes as compared to Case 2b which had the same propulsion load change but with no change to the service load change level. However, the transient levels in terms of the amplitudes of the fluctuations and the settling times at the electrical busbar is significantly worse when the loads are simultaneously applied as compared to applying the same quantity of propulsion or service load change separately as had been done in Cases 2b and 3b. This indicates that the transient conditions at the electrical portion of the hybrid propulsion power system can be reduced if service loads are added or removed at different times relative to the propulsion load changes experienced by the vessel.

In the vast majority of the cases studied, it is observed that the engine speed and electrical transients that occur during equal load application and removal events are almost symmetric in nature with two

exceptions. This implies that although the direction of the parameter changes are of opposite signs mathematically, the magnitude of the transient amplitudes and settling times are almost equal. This enables prediction of the transients for either the load application or removal event if the characteristics of the other event is known.

3.6 SUMMARY

This study is an introduction to studying the transient electrical conditions due to load-changes in a hybrid electric propulsion shipboard power system, particularly investigating the sensitivity of the main engine speed and electrical system frequency to load-changes. The power system has been modeled in MATLAB/Simulink and relevant mathematical equations described. The effects of service and propulsion loads-changes have been separately analyzed. It has been established that the magnitude of load changes as well as the timing sequence of simultaneous or consecutive load changes have a significant effect on the amplitude and duration of transients experienced by the hybrid propulsion power system.

This study has focused on low levels of load changes and the results have clearly shown that even at these low load conditions, considerable transients that exceed the threshold values stipulated by relevant standards can develop. Furthermore, it has been found that mechanical transients that arise from the propellers can propagate to the electrical system main busbar resulting in larger excursions in the electrical frequency leading to major power quality issues throughout the network. In addition, higher levels of propulsion load changes has been found to alter the symmetrical properties of the electrical transients that arise during the load addition and load removal phases, hence, presenting an additional challenge in predicting the extent of transients at high load conditions. Thus, mitigation measures to reduce and possibly eliminate the transients in the electrical portion of the hybrid propulsion system have to be developed in order to protect the entire hybrid propulsion power system against potentially unpredictable loading conditions of the vessel at sea.

This is of prime importance to maintain high reliability where more advanced equipment sensitive to power supply changes are being connected to the shipboard power system. A good example would be navigational equipment that have stringent power supply requirements. Energy storage is a viable

solution that can improve the speed and voltage transients in the system due to the additional supply of active and reactive power, which are tightly coupled with the frequency and voltage profiles of a power system. However, the control system of an energy storage system would be crucial to its effectiveness and speed in addressing the concerns during the transient period. It is the opinion of the authors that in the next stage of the research being undertaken in this area of the hybrid propulsion shipboard power system, further work can be done in this respect to make the hybrid shipboard power system more robust and reliable. Subsequent work can consider integrating an Energy storage system as part of the Hybrid propulsion power system and a possible solution to absorb these electrical transients.

CHAPTER 4

SUPPRESSION OF TRANSIENT TORSIONAL OSCILLATIONS IN THE ELECTROMECHANICAL DRIVETRAIN USING A CAPACITOR CLAMPED INVERTER WITH ACTIVE DAMPING CONTROL SOLUTION

In this chapter, an active damping method has been developed to reduce the mechanical speed transients at the drive shaft that occur due to the changing propulsion load conditions. Furthermore, capacitive energy storage feature has been integrated into the inverter side of the motor drive to absorb the resulting fluctuations in the DC link voltage and the drive input current while at the same time limiting the propagation of these electrical transients.

CHAPTER 4(A)

CAPACITOR CLAMPED INVERTER FOR TRANSIENT SUPPRESSION IN AZIMUTH THRUSTER DRIVES

Shantha Gamini Jayasinghe[1], **Viknash Shagar[1]**, Hossein Enshaei[1], Danyal Mohammadi[2] and Mahinda Vilathgamuwa[3]

[1]Australian Maritime College, University of Tasmania, Launceston, TAS 7250, Australia

[2]Deparment of Electrical and Computer Engineering Boise State University, 1375 University Drive, Boise, USA

[3]School of Electrical Engineering and Computer Science, Queensland University of Technology, Gardens Point, Brisbane QLD 4001, Australia

Published as *'Capacitor-clamped inverter based transient suppression method for azimuth thruster drives*' in the '*2016 IEEE Applied Power Electronics Conference and Exposition (APEC), Long Beach, CA, 2016, pp. 2813-2820'*

Abstract—The more-electric trend is there in almost all the corners of the automotive industry. The same trend is followed by the maritime transportation industry as well and as a result, conventional mechanical transmission based propulsion systems are gradually being overtaken by electric power transmission based propulsion systems. An azimuth thruster driven by an electric motor is a common configuration found in systems that include electric propulsion. Due to the tight speed control and stiff drivetrain in these propulsion systems, load transients easily get propagated into the dc-link of the motor drive and subsequently into the upstream power bus as well. These transients can cause disturbances to the other loads connected to the power system. In the worst case, stability of the shipboard power system gets affected by the transients. This paper proposes to use the capacitor-clamped inverter based motor drive itself to absorb such transients and thereby prevent the propagation into the power bus. The efficacy of the proposed concept is verified through computer simulations. Simulation results show that the capacitor-clamped inverter is capable of absorbing load transients without passing them to the upstream power bus.

4(A).1 INTRODUCTION

Shipping is considered as the linchpin of the global economy as it accounts for more than 90% of the goods transported locally as well as internationally (UN Framework Convention on Climate Change, 2011). This figure is on the rise as the world population and economies continue to grow. With this foreseeable growth, the demand for fuel oil increases and as a result its price is expected to show a steady rise in the long run. On the other hand, the global share of greenhouse gas emissions from ships is on the rise. In this context, more-electric technologies such as electric propulsion are widely adopted to improve the fuel efficiency and thereby reduce the fuel cost and emissions (Jayasinghe S. L., 2015). With this global trend, more and more ships are being fitted with electric propulsion systems such as azimuth thrusters and podded propulsion systems (Reusser, 2015).

Azimuth thrusters get the name from the fact that the housing where the propeller is being fitted can be rotated in any horizontal direction. The drivetrain of azimuth thrusters come in two forms as the L-drive configuration and the Z-drive configuration. The L-drive is generally chosen for electric propulsion where the motor is connected to the vertical shaft and the propeller connects to the horizontal shaft. There is a bevel gear to link the two shafts. The Z-drive is preferred in direct mechanical power transmission where the engine is mounted in the horizontal direction. In this configuration both the engine shaft and the propeller shaft are horizontal. There is a vertical shaft and two bevel gears to link the two horizontal shafts. The propeller experiences extreme hydrodynamic forces and transient conditions mainly caused by waves, ice-interaction, ventilation and propeller racing (Smogeli, 2006). The fatigue caused by the repetition of these conditions lead to premature failures in the mechanical drivetrain (Rauti, 2013; Fonte, 2011). In order to prevent such failures, shafts and gears of the drivetrain are designed to be stiff and thus transients acting on the propeller straightaway propagate into the motor drive. If the motor drive is not designed to absorb such transients they appear as distortions in the dc-link voltage of the power converter. This can cause instabilities, tripping and failures in the power converter. Moreover, the transients can propagate further into the upstream power bus. Given the fact that loads and generators in ships are comparable in size, this propagation can even lead to blackout in the shipboard power system. Therefore, it is important to contain transient energy within the converter with the use of a proper transient energy absorbing mechanism.

The simplest ways of absorbing transients are fitting passive dampers to the drivetrain or adding energy storage elements to the dc-link of the motor drive through interfacing converters. However, these additional hardware and power electronics to the system increase the losses, cost and complexity into the system. Therefore, in this paper, authors have explored the possibility of using the energy storage capability of the capacitor-clamped inverter to absorb transients. This approach eliminates the need for additional bulky energy storage elements, interfacing power converters and other associated hardware.

The advantages of the proposed system come with challenges and limitations as well, mainly due to the change in clamping-capacitor voltage with the absorption of transient energy. Pulse width modulation (PWM) of the converter is the major challenge which has been overcome in this study through modifications introduced to the sinusoidal PWM (SPWM) method. The modifications ensure the delivery of the required current without significant distortions even under varying capacitor voltage conditions. The proposed concept and modified SPWM method are verified through computer simulations. The results show that the capacitor-clamped inverter is capable of absorbing transients without passing them to the shipboard power system. Moreover, the modified SPWM method found to be capable of delivering required current even under variable capacitor voltage conditions without introducing significant distortions to the output current.

Section 4A.2 of the paper describes the proposed transient suppression method followed by the system modelling in Section 4A.3. The modifications introduced to SPWM are presented in Section 4A.4. Challenges and implementation issues of the proposed method are discussed in Section 4A.5 followed by the simulation results in Section 4A.6.

4(A).2 THE PROPOSED TRANSIENT SUPPRESSION METHOD

Over the last decade, there has been a steady growth in the interest among shipping companies for larger ships as compared to deploying more number of small ships (Review of Maritime Transport ., 2014). With the increase of the ship size, electrical power demand also increases and hence shipboard power systems move from low voltage systems to high voltage systems (Hall, 1999). The traditional two-level converter based electrical drives are not able to meet high voltage and high power levels of

the large vessels (Thantirige, 2015). Advanced converters technologies such as cascaded H-bridge converters, neutral-point-clamped converters and capacitor-clamped (flying capacitor) converters have emerged as promising alternatives. Out of these alternatives, capacitor-clamped converter topology has good dynamic performance and a relatively simple modulation process (Li W. L., 2016; Ashraf, 2015; Dargahi, 2015; Kumar, 2015; Ziyou, 2015; Zhang L. W., 2007; Jing Huang, 2006; Lin, 2006; Dae-Wook, 2005; Kang, 2004; Xiaomin, 2004). Moreover, due to the presence of capacitors, the capacitor-clamped converter has the capability to absorb transient energy itself (Jayasinghe S. V., 2013). The proposed concept is based on this special feature which has not yet been explored in relation to propulsion drive systems.

Figure 4.1 illustrates the schematic of the proposed azimuth thruster drive system where the clamping-capacitors of the inverter are supposed to absorb load transients. The challenge in letting the clamping-capacitors to absorb transients is the change of their voltages which in turn create unbalanced conditions. The obvious effect of unbalanced capacitor voltages is the increase in the total harmonic distortion (THD) in the output current. The solution to these issues is the incorporation of an appropriate compensation into the modulation scheme which is discussed in detail in section 4.4.

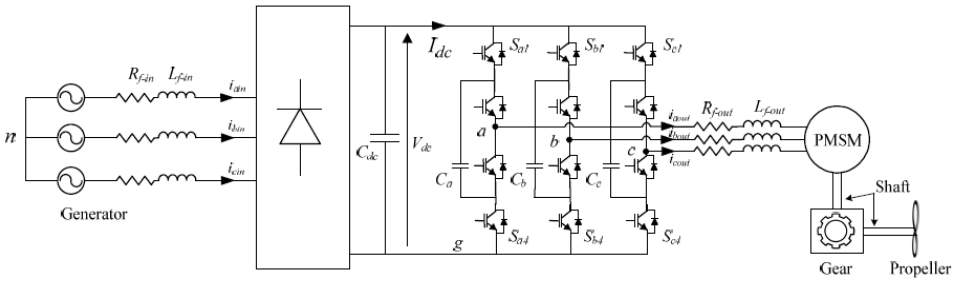

Figure 4.1. Capacitor clamped inverter based azimuth thruster system

4(A).3 SYSTEM MODELLING

4(A).3.1. System Modelling

A permanent magnet synchronous motor (PMSM) is used as the driving motor of the azimuth thruster considered in this study. The synchronous reference frame based PMSM model, shown in Figure 4.2,

is used in the simulation. Based on this model, two expressions can be derived for *d-q* axis voltages as in (4.1) and (4.2) respectively. The vector diagram showing zero direct axis current control of the PMSM using the *d-q* axis voltages is illustrated in Figure 4.3.

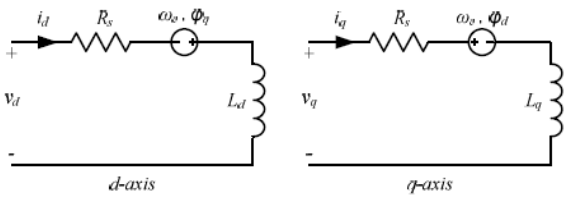

Figure 4.2. PMSM model in the synchronous reference frame

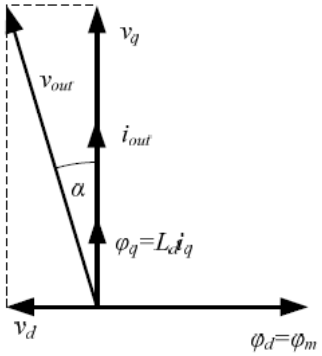

Figure 4.3. Vector diagram showing zero direct axis current control of the PMSM

$$v_d = i_d R_s - \omega_e \varphi_q + L_d \frac{di_d}{dt} \tag{4.1}$$

$$v_q = i_q R_s + \omega_e \varphi_d + L_q \frac{di_q}{dt} \tag{4.2}$$

where v_d and v_q are *d-q* axis voltages, i_d and i_q are *d-q* axis currents, R_s is stator resistance, L_d and L_q are *d-q* axis inductances, ω_e is electrical rotational speed and φ_d and φ_q are magnetic flux components in *d-q* axes respectively. Magnitudes of φ_d and φ_q are given in (4.3) and (4.4). φ_m in (4.3) is the flux produced by permanent magnets of the motor. The electric torque, T_e, produced by the motor is given in (4.5) where *p* is the number of pole pairs in the motor.

$$\varphi_d = L_d\, i_d + \varphi_m \tag{4.3}$$

$$\phi_d = L_d\, i_q \tag{4.4}$$

$$T = \frac{3}{2} p(\varphi_d i_q - \varphi_q i_d) \tag{4.5}$$

Angular acceleration of the rotor shaft and the relationship between the electrical rotational speed and the mechanical rotational speed are given in (4.6) and (4.7) respectively.

$$\omega_m = \frac{1}{J}(T_e - T_L) \tag{4.6}$$

$$\omega_e = p\omega_m \tag{4.7}$$

where J is the inertia of the load, ω_m is the mechanical rotational speed of the rotor and T_L is the load torque.

4(A).3.2. Drivetrain Model

The drive train of L-drive azimuth thrusters contain two shafts and a bevel gear. In order to simplify the analysis the shafts are assumed to be identical and the bevel gear is assumed to be an ideal gear with 1:1 gear ratio. The equivalent model of the two shafts can be expressed as in (4.8) where K_s and B are the stiffness and damping coefficient of the shaft respectively. The torque transmitted through the shaft varies with the angle of twist between the two ends, $(\theta_m - \theta_p)$, where θ_m is the angle at the drive end and θ_p is the angle at the load end. The corresponding block diagram is shown in Figure 4.4 which includes the inertia of the load, J_p, as well.

$$Tp = Ks \int (\omega_m - \omega_p)\, dt + B(\omega_m - \omega_p) \tag{4.8}$$

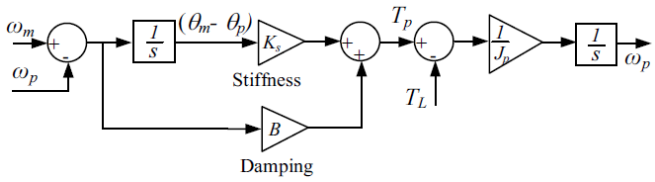

Figure 4.4. Drivetrain and load model

4(A).4 MODULATION AND CONTROL

4(A).4.1. Drivetrain Model

Modulation and control of capacitor -clamped three level inverters are comprehensively discussed in literature (Li W. L., 2016; Ashraf, 2015; Dargahi, 2015; Kumar, 2015; Ziyou, 2015; Zhang L. W., 2007; Jing Huang, 2006; Lin, 2006; Dae-Wook, 2005; Kang, 2004; Xiaomin, 2004). Nevertheless, in all these publications, balanced or equal conditions are assumed, or some techniques are used to balance capacitor voltages. Conventional carrier based PWM methods or space vector PWM methods can

directly be used as the modulation method in those systems. However, as explained in the Section 4(A).2, voltage unbalance is an unavoidable phenomenon in the proposed system. If the conventional modulation methods are directly used in such situations, output current get distorted.

In (Jayasinghe S. V., 2013) authors have proposed a modified Space Vector PWM (SVPWM) scheme to reduce the effects of unbalanced voltages and deliver required current even at unbalanced conditions. Similarly, the standard SPWM method can also be modified to suite unbalanced conditions (Vilathgamuwa D. J., 2011). The block diagram shown in Figure 4.5 summarizes the modifications introduced to the standard SPWM method. The fundamental concept of comparing the three-phase reference voltages generated by the controller against triangular carriers is common for the modified SPWM method as well. The difference comes in the way of generating carrier waveforms. Generally, only two symmetrical carriers are sufficient to implement SPWM for a balanced capacitor-clamped inverter. But, in the proposed system, each inverter leg require an individual set of carriers due to the dynamic changes in clamping-capacitor voltages. In addition to that, each set should consist of four carriers as shown in Figure 4.5. Therefore, altogether there should be 12 different carriers to implement the modified SPWM method. Modern processors that are tailored for motor drive applications generally come with large number of PWM units and thus the need for 12 PWM units does not create practical implementation issues.

The need for four carriers for each inverter leg can be justified as follows with reference to the leg '*a*' of the inverter. In the proposed system, a given reference voltage for the leg 'a' can be synthesized in two alternate ways. The first method uses the three voltage levels of 0, V_{Ca}, and V_{dc}. Similarly, in the second method, the voltage levels 0, $V_{dc} - V_{Ca}$ and V_{dc} are used (the corresponding switching states and gate signals are given in Table 4.1). Since there are three voltage levels associated with each method two carriers are required for each method. As a result, each leg of the converter requires four different carrier waveforms. In addition to that, amplitudes of these carriers should be varied according to the changes in capacitor voltages. The equations for calculating the corresponding carrier amplitudes are given in Table 4.2.

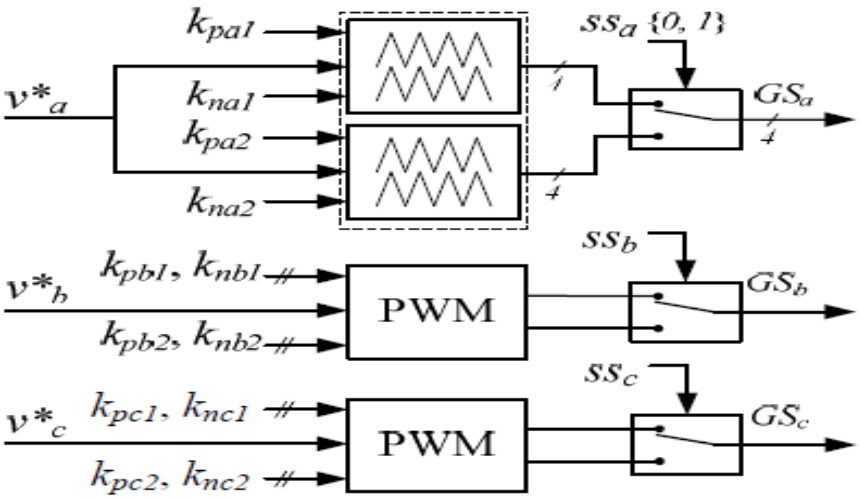

Figure 4.5. Block diagram of the modified SPWM method

Table 4.1. Switching states and Line to Ground voltages for Leg A.

Switching state (S_a)	Gate signals ($GS_{a1}...GS_{a4}$)	v_{ag}
0	0011	0
1	0101	V_{Cc}
2	1010	$V_{dc} - V_{Ca}$
3	1100	V_{dc}

Table 4.2. Amplitudes of modified carriers

Carrier amplitudes for leg 'a'	Carrier amplitudes for leg 'b'	Carrier amplitudes for leg 'b'
kpa1 = $2(1-V_{Ca}/V_{dc})$	kpb1 = $2(1-V_{Cb}/V_{dc})$	kpc1 = $2(1-V_{Cc}/V_{dc})$
kna1 = $2V_{Ca}/V_{dc}$	knb1 = $2V_{Cb}/V_{dc}$	knc1 = $2V_{Cc}/V_{dc}$
kpa2 = $2V_{Ca}/V_{dc}$	kpb2 = $2V_{Cb}/V_{dc}$	kpc2 = $2V_{Cc}/V_{dc}$
kna2 = $2(1-V_{Ca}/V_{dc})$	knb2 = $2(1-V_{Cb}/V_{dc})$	knc2 = $2(1-V_{Cc}/V_{dc})$

4(A).4.2. Capacitor charge/discharge control

Charge/discharge controller for the capacitor C_a attached to the leg 'a' of the inverter, is shown in Figure 4.6. The same controller and the following analysis can equally be used for the other two phases as well. The controller output SS_a selects the suitable output voltage synthesizing method out of the two possibilities shown in Figure 4.5. If SS_a is permanently held at '0', the capacitor C_a gets discharged during the positive half cycle of the a-phase current and get charged in the negative half cycle. Similarly, the opposite happens when SS_a is held permanently at '1'. Therefore, if SS_a is tied to 0 or 1, the average current flow through the capacitor is zero and hence the average voltage of the capacitor

will not get affected. This indicates that the controller output SS_a should be changed at each and every half cycle to obtain an average charging or discharging current. In order to obtain a net discharging current, SS_a should be held at '0' during the positive half cycle and '1' at the negative half cycle. Similarly, if SS_a is held at '1' during the positive half cycle and '0' at the negative half cycle, a net charging current can be obtained. These two settings would produce maximum rates of discharging and charging for the capacitor C_a respectively. An intermediate rate can be obtained by switching between the above two settings. This switching is achieved through PWM as shown in Figure 4.6.

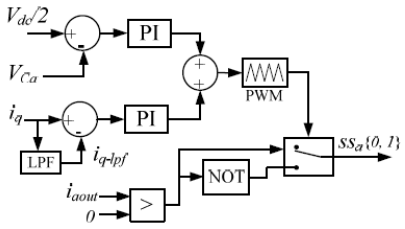

Figure 4.6. Charge/discharge controller for the capacitor C_a attached to the leg *'a'* of the inverter

As shown in Figure 4.6, a reference signal for the PWM unit is generated by adding the output of two PI controllers. The first PI controller sets the reference to bring the capacitor voltage to half of the dc-link voltage. The second PI controller adjusts the reference signal to absorb transients. As discussed in the following section, the *q*-axis current, i_q, varies with the load and thus changes in i_q reflect load transients. Taking this into account, the low pass filtered value of i_q is subtracted from the instantaneous value to obtain the error signal for the second controller. The gains of the two controllers are selected in a way that the second controller dominates during transients and the first controller dominates during the steady state. As a result, even if the clamping-capacitor voltages vary during transients they gradually return to the balanced condition during steady state operation.

4(A).4.3. Motor Controller

The synchronous reference frame based controller is used for the speed control of the motor. The corresponding controller block diagram is shown in Figure 4.7. The zero *d*-axis current control technique is used to control the speed of the PMSM. In this method the *d*-axis component of the stator current is maintained at zero. As a result, the *d*-axis component of the magnetic flux becomes equal to the flux produced by the permanent magnet of the motor as shown in Figure 4.3. As expressed in (4.9), this flux, together with the *q*-axis current, produces the electrical torque which is analogous to

the operation of dc motors. Therefore, in the speed controller shown in Figure 4.7, the *q*-axis current is controlled to control the speed of the motor. In the steady state operation, the speed controller compares the actual speed of the motor with the reference speed and the error is passed through a PI controller. The output of the PI controller is the torque reference which is used in (4.10) to derive the required *q*-axis current. The *d*-axis current reference is kept at zero. Based on these current references, required voltage components can be calculated using (4.11) and (4.12). Equations (4.13) and (4.14) are used to determine the amplitude and the angle of the inverter output voltage vector (Vilathgamuwa D. J., 2011). Equations (4.15 - 4.17) are used to generate three-phase reference voltages for the PWM unit. This is a standard speed controller for PMSMs. Apart from this standard controller there is an additional controller added in the speed controller shown in Figure 4.7 which alters the *q*-axis current reference (torque reference) to minimize the speed difference between the two ends of the shaft. This in turn reduces stresses in the shaft during load transients (Geng, 2011). However, due to the influence of this additional controller the transients straightaway get passed into the motor drive.

$$T_e = \frac{3}{2} p \varphi_m i_q \tag{4.9}$$

$$i_q^* = \frac{2T_e^*}{3p\varphi_m} \tag{4.10}$$

$$v_d^* = -\omega_e \varphi_q = -\omega_e L_d i_q \tag{4.11}$$

$$v_q^* = \omega_e \varphi_d + i_q R_s = \omega_e \varphi_q + i_q R_s \tag{4.12}$$

$$v_s^* = \sqrt{(v_d^{*^2} + v_d^{*^2})} \tag{4.13}$$

$$\alpha = tan^{-1}(\frac{v_d^*}{v_q^*}) \tag{4.14}$$

$$v_a^* = v_s \sin(\omega_e t + \alpha) \tag{4.15}$$

$$v_b^* = v_s \sin(\omega_e t + \alpha - (\frac{2\pi}{3}) \tag{4.16}$$

$$v_c^* = v_s \sin(\omega_e t + \alpha + (\frac{2\pi}{3}) \tag{4.17}$$

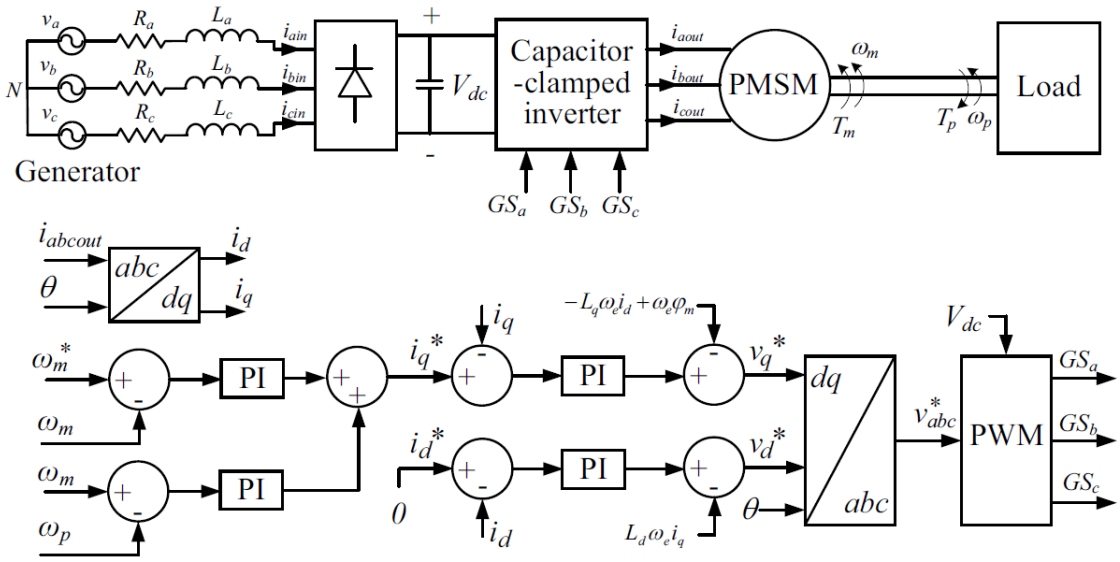

Figure 4.7. Block diagram of the speed controller

4(A).5 CHALLENGES AND LIMITATION

4(A).5.1. Challenges in capacitor implementation

The proposed transient suppression method requires the capacity of the floating capacitors to be increased to absorb transients in the system. This would imply that the capacitors would then be expected to be heavier and of a higher volume. The extent of this added weight and volume has to be carefully considered because in the case of marine applications, the space onboard a ship is extremely limited and costly. A survey on the capacitors rated for 600V indicate that the weight and volume of the capacitors experience a sudden increase above the 100KVar (General Electric, n.d.). The volume of the capacitor bank enclosure stays the same for KVar ratings from 50 to 100. However, this volume increases 8-fold for the capacitors rated from 100KVar to 150KVar (General Electric, n.d.).

The weight also doubles when capacity is more than 100KVar (General Electric, n.d.). These large changes in weight and volume can be attributed to the electrolyte material and arrangement of plates used for capacitors with higher capacitance. The weight of the capacitance bank increases by about 0.2kg for every 10mF increase in rating of the capacitance that supply 100KVar or less. The

corresponding value for capacitors supplying more than 100KVar is 0.19kg (General Electric, n.d.). In this study, the reactive power supplied by the capacitors is between 50KVar to 150KVar therefore the aforementioned weight and volume increases are significant. A table summarizing how the physical characteristics of capacitor banks vary with the electrical parameters can be found in Table 4.3.

Table 4.3. Capacitor parameters

KVar Rating	Capacitive Reactance (ohms)	Capacitance (mF)	Weight (kg)	Volume (m^3)
50	7.20	368	10.0	0.0289
60	6.00	442	14.5	0.0289
70	5.14	516	15.0	0.0289
80	4.50	589	17.3	0.0289
90	4.00	663	17.3	0.0289
100	3.60	737	17.3	0.0289
110	3.27	810	39.5	0.249
120	3.00	884	39.5	0.249
130	2.77	957	39.5	0.249
140	2.57	1032	40.8	0.249
150	2.40	1105	45.0	0.249

4(A).5.2. Trends in improving the reliability of capacitors

The reliability of capacitors is a major factor in the operation of the capacitor-clamped inverter. Therefore, any failure of capacitors can potentially cause a short circuit in the system which can lead to catastrophic results especially at high voltage levels. In addition to that, marine application involve strict safety regulations as well. Therefore, increased reliability of the capacitors is mandatory to promote capacitor-clamped converters as a competitive power converter for the motor drive in azimuth thrusters. Moreover, in order to bring down the maintenance costs of the system, it is desired that system components such as capacitors have longer lifetimes.

In view of this, there are a number of technologies designed to improve the lifetime of capacitors. Dry film technology for capacitors has recently entered the market and it has been touted to be self-healing. It is gradually replacing aluminum electrolytic capacitors at medium to high voltage levels. The voltage range of this technology is from 600V to 1350V and a dry film capacitor has a voltage gradient of up to 500V per micrometer during discharge. High capacitance values of up to 48mF have been reported

using this technology (Gilles, T., AVX, A Kyocera Group Company, n.d.). The self-healing is achieved by coating the di-electric film of a capacitor with a thin metallic layer that evaporates due to the heat produced when a defect in the film occurs, thus, isolating the defect from the rest of the capacitor and preventing its spread. This leads to reduced maintenance for the capacitors. It has been found that capacitors using dry film technology have only a 2% drop in capacitance after 100000 hours of operation. Also, a large voltage gradient means that the capacitor can handle high ripple currents and voltage surges up to twice the rated voltage (Gilles, T., AVX, A Kyocera Group Company, n.d.). In comparison, aluminum electrolytic capacitors suffer chemical breakdowns when the rated voltage has been exceeded by 50%.

Heat is often the most crucial factor for capacitor failure. Therefore, efforts have been underway to reduce the losses caused by current flow into a capacitor. One way is to reduce the equivalent series resistance of capacitors by using multiple laser welded electrode tabs. This is effective because a higher number of metal tabs connecting the outer electrodes to the capacitor winding using advanced laser welding reduces the resistance of a capacitor (EVOX RIFA PASSIVE COMPONENTS, 2001). This results in the capacitor experiencing lesser internal heating and a higher capability to withstand ripples.

Electrolyte evaporation has also been cited as a common cause for decreased lifetime of electrolytic capacitors. This problem has been tackled by reducing the evaporative capability of the electrolyte and improving the sealing of the electrolyte to reduce electrolyte loss. Solvents containing ethylene glycol have been found to reduce electrolyte evaporation at higher temperatures. Better compositions for the rubber sealant as well as double sealing have been explored. A combination of the above measures have been found to double the lifetime of capacitors from 10000hrs to 20000hrs (Dempa Shimbun, n.d.).

The above improvements in capacitor performance show that the reliability and longevity of capacitor can be enhanced in light of further advances in electrical and chemical technologies in the near future. This indicates that the use of capacitor-clamped inverter as part of the motor drive and integrating the proposed method into it is feasible from the practical implementation point of view

4(A).5.3. Trends in improving the reliability of capacitors

Maritime applications demand for enhanced reliability in power electronic converter systems which are used for powering up the essential loads such as propulsion systems. An investigation on power electronic converter failures has revealed that 60% of the failures are due to capacitor failures. Moreover, capacitor failure incidents and resultant damages to ship power systems are reported in marine accident investigation branch (MAIB) reports (Report on the investigation of the catastrophic failure of a capacitor in the aft harmonic filter room on board RMS Queen Mary 2. Dec. 2011, n.d.). This highlights the need for detection, identification and isolation of failures as soon as possible. In multilevel inverters such as the capacitor-clamped inverter, there are more switches which increases the availability and make the system more tolerable in case of a fault (Fuchs, 2003). There are several methods proposed in the literature to isolate faults such as IGBT short-circuit faults, thereby avoiding catastrophic consequences. Fast acting fuses and thyristors are key elements that are used in these methods to isolate the fault from the whole system (Welchko, 2004; Bolognani, Zordan, & Zigliotto, 2000). The advancement of fault detection, identification and isolation techniques together with the development of fault accommodation topologies help improve the safety and availability of capacitor-clamped inverter based motor drives.

4(A).6 SIMULATION RESULTS

A computer simulation on the MATLAB/Simulink platform was carried out to show the efficacy of the proposed transient suppression method. Two step changes are introduced to the load as shown in Figure 4.8(a) to create a load gain scenario and a load drop scenario. The load gain is introduced at 100ms by increasing the propeller load from 100Nm to 400Nm. The step increase of the load results in a speed drop at the load end of the shaft as shown in Figure 4.8(b) by the trace marked as ‘Load end speed’. This speed drop propagates to the other end of the shaft as well with a slight drop in the magnitude as shown in the same graph by the trace marked as ‘Drive end speed’. The speed controller reacts to this variation and changes the output current to restore the speed to the set value. The two speed variations shown in Figure 4.8(b) is an indication of tight speed regulation which in turn passes load changes in the drive train directly into the motor drive. The speed difference between the two ends of the shaft accounts for the transient energy absorb within the shaft. If the shaft is flexible the

speed difference between the two ends becomes large resulting in more transient energy absorb within the shaft. Nevertheless, flexible shafts introduce torsional oscillations which are detrimental to the shaft life. Therefore, shafts are made to be stiff which, together with the tight speed control, passes the transients straightaway to the motor drive. Moreover, the additional controller mentioned in Section 4.4 reduces the speed difference between the two ends of the shaft by modifying the *q*-axis current reference. Therefore, even if the shaft is flexible, all the transients get passed into the motor drive as will be discussed in Chapter 4(B). The transients in the output current, shown in Figure 4.8(c), is an indication of this transient propagation into the power converter. As a result, the DC link voltage of the frequency converter gets affected as shown in Figure 4.8(d) by the trace marked as 'Normal operation'. The transients can propagate further into the upstream power bus as shown by the rectifier input current shown in Figure 4.8(e). If the generators are not capable of reacting against this kind of fast changes the shipboard power system becomes unstable.

With the proposed method these transients get absorbed by the clamping-capacitors and thus the dc-link voltage changes slowly as shown in Figure 4.8(d) by the trace marked as 'Proposed operation'. As a result, the input currents to the rectifier also show smooth changes as shown in Figure 4.8(f) which gives enough time for generators to react to the changes and thus maintain the stability of the power system. As a result of absorbing the transients, clamping-capacitor voltages get affected. The corresponding clamping-capacitor voltage variations are shown in Figure 4.8(g). As shown in Figure 4.8(c) the modified SPWM method is capable of producing required output currents even under variable capacitor voltage conditions. The THD values of the output current at different places are given in Figure 4.8(c) to show that even if the clamping capacitor voltages vary, THD in output currents still remain at acceptable levels of less than 15 – 20% as specified by relevant standards defining Power Quality in Power Systems such as IEEE 519 (Blooming & Carnovale, 2006; Hoevenaars, 2004; Jewell & Ward, 2002). The a-phase voltage waveform of the inverter output is shown in Figure 4.8(h) to illustrate the capability of the modified modulation method to produce 3-level output voltage waveforms even under unbalanced conditions. System parameters of the simulation setup are given in Table 4.4 which are arbitrarily chosen to demonstrate the operation of the proposed concept.

Table 4.4. System parameters

Parameters	Value
Nominal voltage of the generator (*Vll rms*)	690V
Frequency of the generator output voltage	50Hz
Resistance of the generator (R_{abc})	0.01Ω
Inductance of the generator (L_{abc})	15mH
DC – link capacitance (C_{dc})	0.5mF
Capacitance of the clamping capacitors (C_{abc})	4.7mF
Filter resistance (R_{fout})	0.01Ω
Filter inductance (L_{fout})	1mH
Resistance of the motor (R_m)	0.01Ω
Inductance of the generator (L_m)	1mH
Number of pole pairs in the motor (p)	4
Rotor inertia of the motor (J_m)	0.017kgm^2
Stiffness of the shaft (K)	20000Nm/rad
Damping coefficient of the motor (B)	10Nm/rads^{-1}
IGBT switching frequency	2kHz
Inertia of the load (J_p)	0.025kgm^2

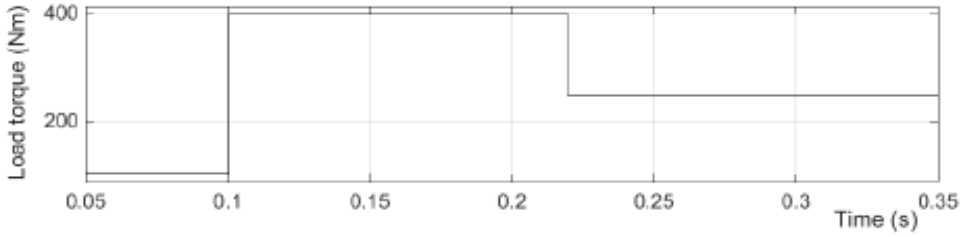

(a)

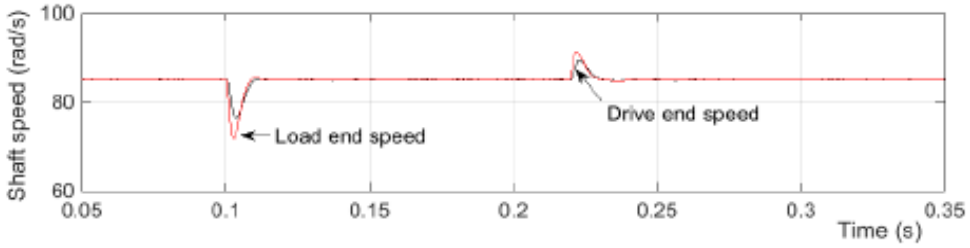

(b)

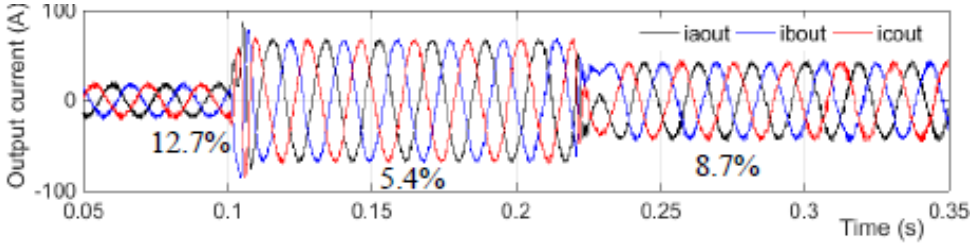

(c)


DC-Link voltage (V)
1000
800
600
Proposed operation
Normal operation
0.05
0.1
0.15
0.2
0.25
0.3
0.35
Time (s)

(d)

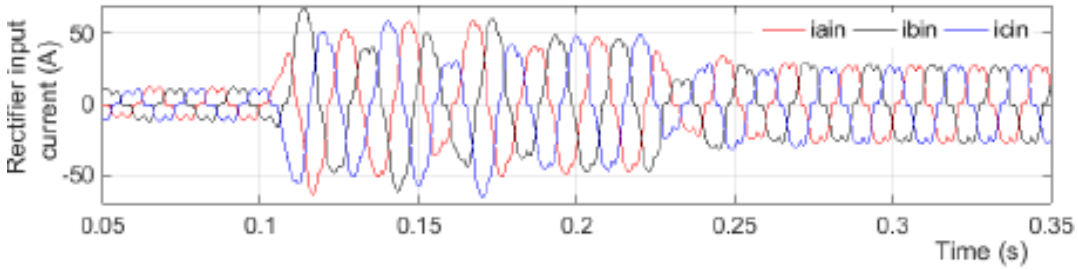
Rectifier input current (A)
50
0
-50
iain
ibin
icin
0.05
0.1
0.15
0.2
0.25
0.3
0.35
Time (s)

(e)

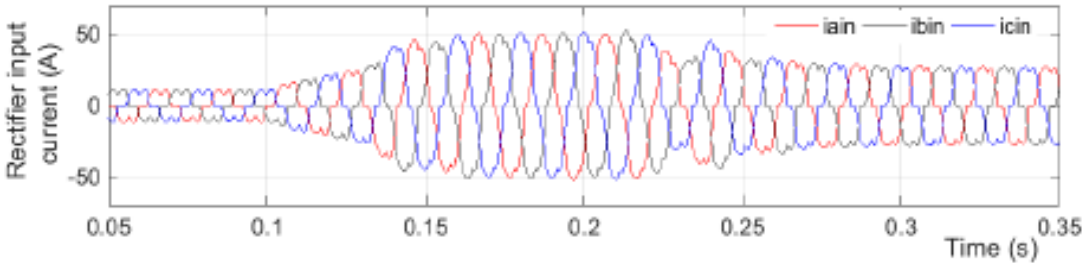
Rectifier input current (A)
50
0
-50
iain
ibin
icin
0.05
0.1
0.15
0.2
0.25
0.3
0.35
Time (s)

(f)

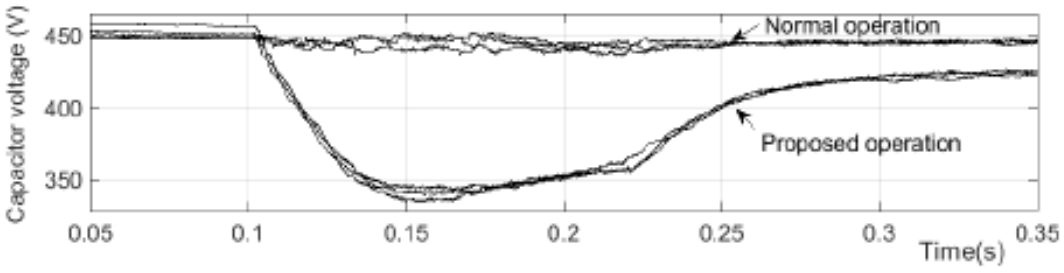
Capacitor voltage (V)
450
400
350
Normal operation
Proposed operation
0.05
0.1
0.15
0.2
0.25
0.3
0.35
Time(s)

(g)

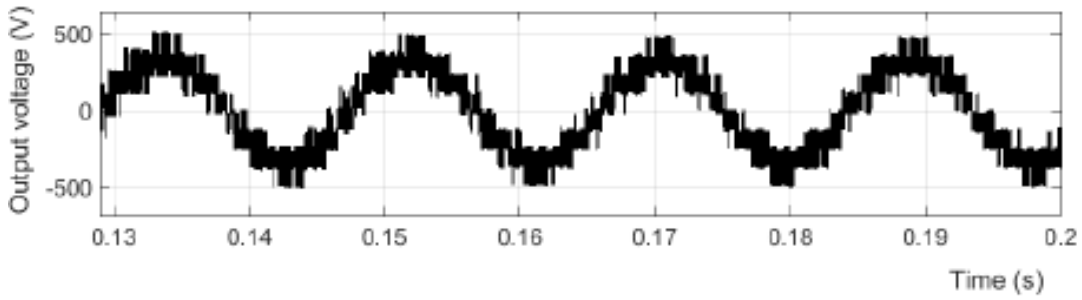

(h)

Figure. 4.8. Simulation results (a) load torque, (b) shaft speed at the drive end and load end, (c) output current, (d) dc-link voltage, (e) rectifier input current in the normal operation, (f) rectifier input current in the proposed operation, (g) clamping capacitor voltage, (h) inverter output voltage (a-phase)

4(A).7 SUMMARY

This paper proposes to use the clamping-capacitors of the capacitor-clamped three-level inverter to absorb load transients in azimuth thrusters and thereby prevent the transient propagation into the shipboard power system. This makes the clamping-capacitors deviate from the balanced condition. The challenge of delivering required output current under unbalanced conditions is achieved through a modified SPWM method. Simulation results verify the ability of the capacitor-clamped inverter to absorb load transients and thereby prevent the propagation into the upstream power bus. Moreover, the results verify the capability of the modified SPWM method in delivering desired current even in unbalanced conditions while keeping the THD level low to suit maritime applications.

CHAPTER 4(B)

A CAPACITOR CLAMPED INVERTER BASED TORSIONAL OSCILLATION DAMPING METHOD FOR AZIMUTH THRUSTER DRIVES

Viknash Shagar, Shantha Gamini Jayasinghe, Hossein Enshaei

Australian Maritime College, University of Tasmania, Launceston, TAS 7250, Australia

Published as '*A capacitor-clamped inverter based torsional oscillation damping method for electromechanical drivetrains*' in the '*MATEC Web of Conferences, 13-14 January 2016, Singapore, pp. 1-5. ISSN 2261-236X (2016)'*

Abstract - A typical electromechanical drivetrain consists of an electric motor, connecting shafts and gears. Premature failures of these shafts and gears have been reported which are mainly due to fatigue caused by extreme loads and torsional oscillations. Overdesign and passive damping are the common approaches taken to increase the fatigue life. Nevertheless, they increase the system cost, weight and volume. Alternatively, active damping through advanced inverter control of the motor drive has been identified as a promising solution that does not require overdesign such as having stiffer shafts or alterations to the existing system. Even with the active damping control, oscillations propagate into the dc side of the power converter and subsequently to the upstream power bus. Generally, a large capacitor or an additional energy storage system is placed to suppress these oscillations. This paper proposes to use the clamping capacitors of the capacitor-clamped inverter as energy storage elements and thereby eliminate the need for a large dc side capacitor or an additional energy storage system. The efficacy of the proposed method has been verified with computer simulations. Simulation results show that the clamping capacitors are capable of containing torsional oscillations within the inverter without passing them to the upstream power bus.

4(B).1 INTRODUCTION

More electric technologies (METs) play an important role in meeting ever growing demands for energy efficiency and emission reduction in the transportation sector (Jayasinghe S. L., 2015). Improved performance and control flexibility are the other advantages that make METs stand out amongst predominantly mechanical technologies. The automobile industry is the first to incorporate METs into vehicles whereas the maritime and aviation industries are catching up fast. As a result, conventional mechanical transmission based propulsion and drive systems in ships and aircrafts are gradually being replaced with electromechanical drive systems. The most prominent MET in ships is the electric propulsion azimuth thrusters or pod propulsion systems (Reusser, 2015).

In a typical electromechanical drive system, there is a power converter to convert the fixed voltage-fixed frequency electrical supply into a variable voltage-variable frequency output to feed the motor. The load is connected to the motor through shafts and gearboxes. The L-drive type azimuth thruster is a good example for this configuration where the motor is connected to the propeller through a vertical shaft, a horizontal shaft and a bevel gear. Depending on the application, the shafts may require being long and thin which results in a certain degree of elasticity. The elasticity leads to torsional oscillations in transient conditions. Unless appropriate control measures are taken, repetition of such oscillations over a period of time leads to fatigue and result in driveline failure (Fonte, 2011). The easiest way to avoid such premature failures is the overdesign with bigger and stiffer shafts and gears. But it increases the weight, volume and cost of the system. Passive damping is another solution that uses additional hardware to suppress oscillation. This also increases the weight, volume and cost of the system.

Alternatively, active damping through advanced power converter control has been identified as a promising solution that can suppress torsional oscillations and thereby increase the fatigue life without hardware modifications (Geng, 2011). Therefore, the size and weight of the drivetrain can be kept at a reasonable level eliminating the need for overdesign.

Even though active damping reduces torsional oscillations, the remaining oscillations in the shaft propagate into the dc-side of the motor drive. These oscillations can propagate further into the main

power system of the ship as well causing damages to the attached equipment. Increasing the dc-link capacitance or adding an energy storage is the common solution to prevent the propagation of oscillations into the power system. However, they require large capacitors or additional hardware. Therefore, as an alternative, this paper proposes to use clamping capacitors of the capacitor-clamped inverter in conjunction with active damping to absorb oscillations and thereby eliminate the need for large dc-link capacitor or an additional energy storage system.

The proposed concept has been verified with computer simulations considering an L-drive azimuth thruster system as an application. The simulations were carried out for three different scenarios. Firstly, the system has been simulated for the normal operation without active damping or clamping-capacitor support to contain oscillations. The results show significant oscillations in the shaft, dc voltage and input current. Secondly, the active damping was added to the control which reduced the oscillation in the shaft. However, the remaining oscillations get propagated into the inverter and appeared in the dc voltage and the input current. Thirdly, both active damping and clamping capacitor support were added to the controller which in turn reduced oscillations in the shaft and smoothened dc voltage and input current. This concept is thus proven to be feasible as the torsional oscillations can be contained within the converter without passing them on to the shipboard power system.

4(B).2 PROPOSED SYSTEM MODEL

The proposed system is shown in Figure 4.9 where a capacitor-clamped inverter is used to drive the propulsion motor of an L-drive type azimuth thruster. In this study, a permanent magnet synchronous motor (PMSM) is used as the propulsion motor. The motor is connected to the propeller through a vertical shaft, horizontal shaft and a bevel gear. For simplicity, in the simulation model, an ideal gear was assumed and the two shafts were represented by a single shaft. Moreover, low values were assigned for the shaft stiffness, K_s, and the damping coefficient, B in order to have a more flexible shaft and hence getting a better illustration of the torsional oscillations. The block diagram of the drivetrain model is shown in Figure 4.4 where m is the angle at the drive end, p is the angle at the load end and J_P is the inertia of the load. The torque transmitted through the shaft, T, varies with the

difference in the twisting angle of the shaft at the drive end and the load end. The corresponding mathematical expression for *T* can be expressed as in (4.8) above.

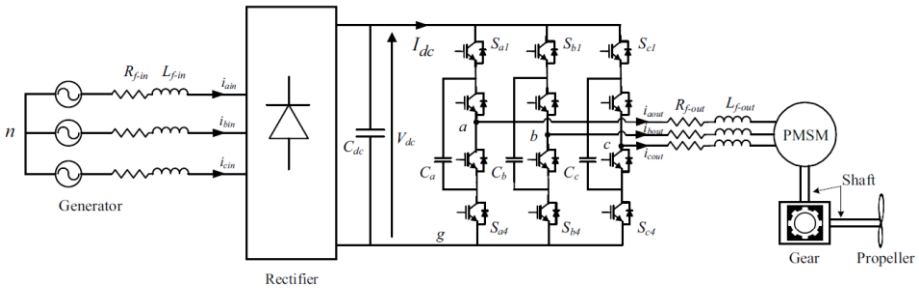

Figure. 4.9. Capacitor clamped inverter based azimuth thruster drive system

4(B).3 CONTROL STRATEGY

4(B).3.1 Motor Controller

A block diagram of the motor controller is shown in Figure 4.7. In the steady state operation, the controller compares the actual motor speed, *m*, with a reference speed, *m**, and the error is then passed through PI controller. The output of the PI controller is the reference torque from which the *q* axis current reference, i_q^*, can be derived. The d axis current reference, i_d^*, is set to zero. The actual *dq* axes currents are compared with the references and the errors are passed through PI controllers which in turn produce references for *dq* axis voltages as shown in Figure 4.7. Finally, using the voltage values of the *dq* axes, the amplitude and angle of the inverter output voltage are generated in the *abc* frame. The PI controller at the bottom left of Figure 4.7 also compares the speed difference between the drive end and the load end of the drivetrain in order for the motor to vary its torque so as to reduce the amount of twisting in the shaft that can occur during wildly fluctuating load conditions. This is the control action that implements active damping. Therefore, a more flexible shaft can have its mechanical stress converted to the electrical equivalent by increasing the gain of the corresponding PI controller. The clamping capacitor charge/discharge controller and modulation technique described

below can then help to absorb and hence damp down the voltage and current oscillations in the inverter.

4(B).3.2 Inverter modulation

Modulation techniques for the capacitor-clamped multilevel inverter have been extensively covered in literature (Li W. L., 2016; Ashraf, 2015; Dargahi, 2015; Kumar, 2015; Ziyou, 2015). However, most of these techniques require balanced capacitor voltages for the operation. In the approach taken in this paper, the goal is for the clamping capacitors to absorb any oscillation in the DC link voltage caused by loading changes. Therefore, the capacitor voltages cannot be assumed to be balanced in such operating conditions. This means that the conventional modulation (PWM) techniques such as carrier based PWM and space vector PWM methods would not be suitable in these capacitor clamped inverters. Hence, the modified PWM method presented in (Vilathgamuwa D. J., 2011) has been adopted as the modulation method for this study.

4(B).3.3 Clamping capacitor charge/discharge controller

The charging and discharging of the clamping capacitors serve to absorb the oscillations in the DC link voltage of the motor drive and thus prevent them from being transferred to the upstream power bus. The clamping capacitor charge/discharge control strategy presented in (Vilathgamuwa D. J., 2011) has been adopted in this study. The corresponding controller block diagram for the capacitor, C_a, is shown in Figure 4.10 where the PI controller at the top of the diagram helps bring the capacitor voltage to half the dc-link voltage value. The second PI controller from the top left corner of Figure 4.10 compares the square of the actual dc-link voltage against a reference generated by passing the same signal through a low pass filter. This reference represents a smooth change in the dc-link voltage and thereby removes the oscillation that occurs during transients. The two PI controllers are designed in a way that the First PI controller is dominant during steady state conditions while the second PI controller is dominant during transient conditions. For instance, if the electrical system experiences more transients reflected as oscillations in the DC link voltage, one way to make it smooth is to make the second PI controller act faster. However, as the effect of the second PI controller is present only during transients it does not bring the capacitor voltage to the balanced condition of half the DC link

voltage after the transient. The first PI controller becomes prominent after the transient and thus it brings clamping-capacitor voltages to the balanced condition. The output function SS_a of the charge/discharge controller shown in Figure 4.10 selects one of the two redundant switching states depending on the polarity of the phase current at the output [10].

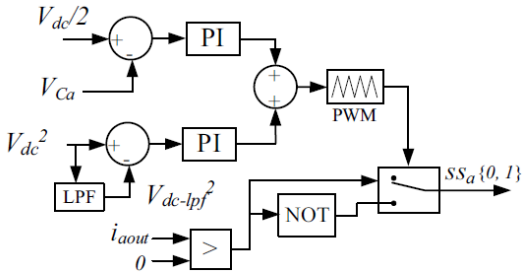

Figure. 4.10. Charge/discharge controller for the capacitor C_a attached to the leg *'a'* of the inverter

4(B).4 SIMULATION RESULTS

Three sets of simulations were carried out on the MATLAB/Simulink platform to verify the efficacy of the proposed torsional oscillation suppression method. Both active damping and clamping capacitor support were not included in the first simulation. Therefore, the results shown in Figure 4.11 correspond to the transient response of the normal system. The load changes introduced to create transients are shown in Figure 4.11(a). These transients excite torsional oscillations in the shaft as shown in Figure 4.11(b). The flexible shaft has a certain damping coefficient and thus these oscillations get damped slowly. Amidst this natural damping, oscillations continue for a significant period of time during which the shaft experiences stresses and resultant fatigue. The output current of the inverter is shown in Figure 4.11(c) where the envelop shows similar oscillations. This is an indication that the oscillations have propagated into the electrical side. The DC side voltage and input current waveforms shown in Figures 4.11(d) and (e) confirm the propagation of oscillations into the DC side and upstream power bus respectively. The clamping capacitor voltages are kept at balanced conditions as shown in Figure 4.11(e) and thus they do not absorb oscillations.

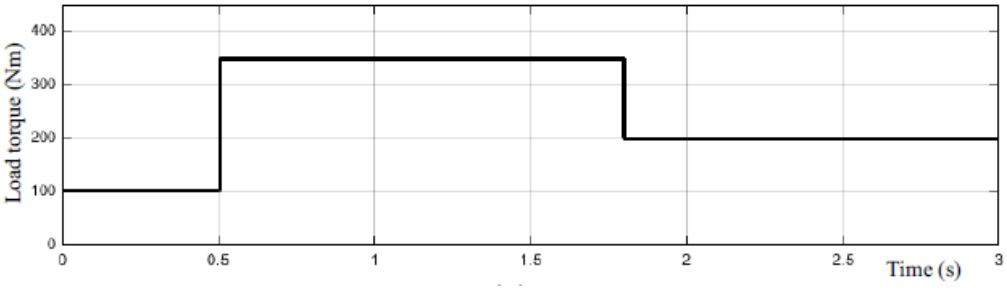
Load torque (Nm)
400
300
200
100
0
0
0.5
1
1.5
2
2.5
3
Time (s)

(a)

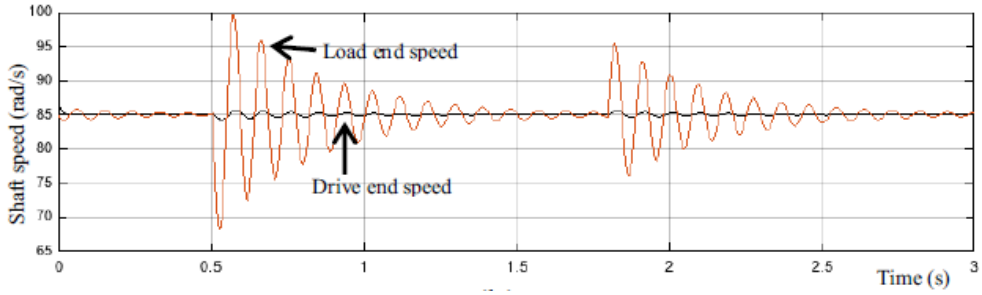
Shaft speed (rad/s)
100
95
90
85
80
75
70
65
Load end speed
Drive end speed
0
0.5
1
1.5
2
2.5
3
Time (s)

(b)

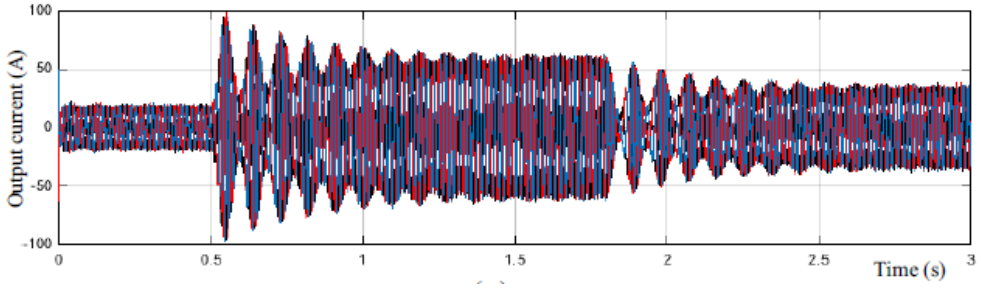
Output current (A)
100
50
0
-50
-100
0
0.5
1
1.5
2
2.5
3
Time (s)

(c)

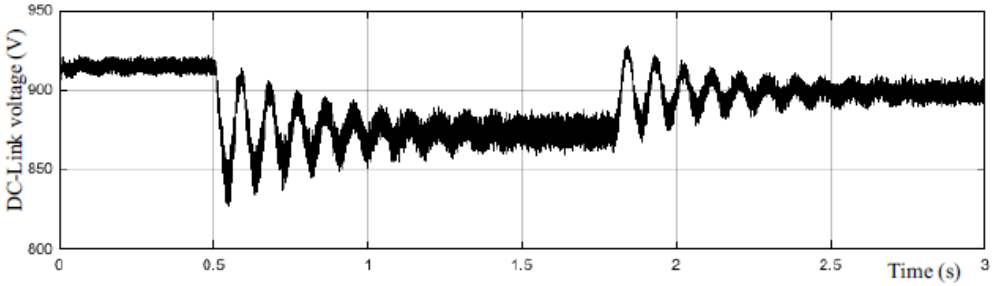
DC-Link voltage (V)
950
900
850
800
0
0.5
1
1.5
2
2.5
3
Time (s)

(d)

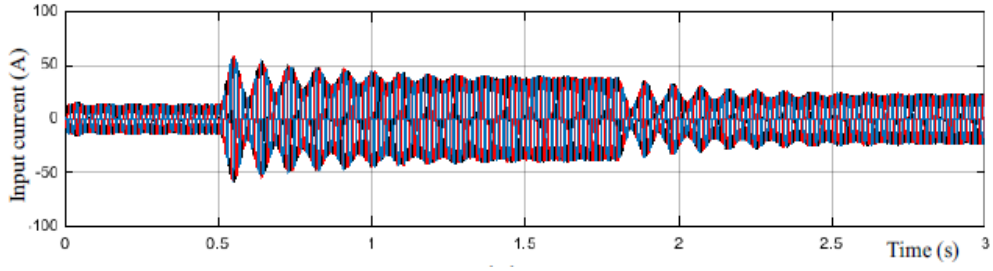
Input current (A)
100
50
0
-50
-100
0
0.5
1
1.5
2
2.5
3
Time (s)

(e)

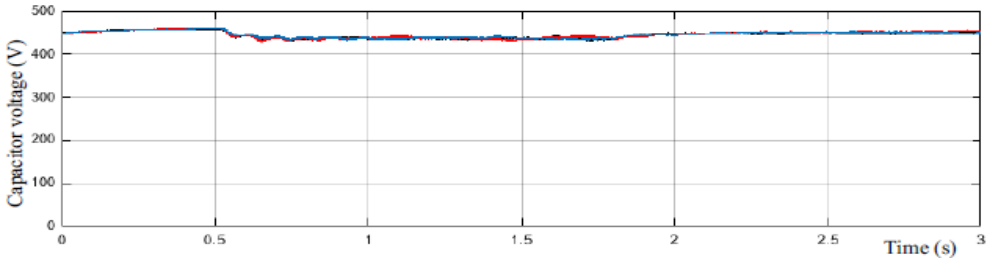

(f)

Figure 4.11. Normal operation: (a) load torque (b) shaft speed at the drive end and load end (c) output current (d) dc-link voltage (e) rectifier input current (f) clamping capacitor voltage

In the second simulation, the active damping was enabled and thus the oscillation in the shaft got damped quickly as shown in Figure 4.12(a). As shown in Figures 4.12(b), 4.12(c) and 4.12(d) the output current, DC link voltage and the input current show the same oscillation, but for a relatively short period of time. As evident from these results active damping is capable of reducing torsional oscillations. Nevertheless, the remaining oscillations still get propagated into the DC side of the inverter and then to the power system.

The proposed method absorbs these oscillations through clamping capacitors of the inverter. The third simulation was carried out to test the performance of this method and thus both active damping and clamping-capacitor support were enabled in the controller. Due to the presence of the active damping controller, the oscillations in the shaft are damped quickly as shown in Figure 4.13(a). This graph and the output current waveforms shown in Figure 4.13(b) are very much similar to the corresponding graphs in Figure 4.12(a) and 4.12(b) respectively. Therefore, torsional oscillation damping on the shaft depends entirely on the active damping controller. In other words, the clamping-capacitor support does not have a significant effect on shaft oscillations.

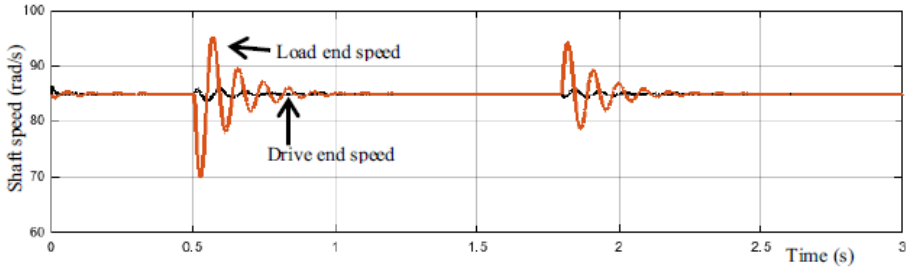
Load end speed
Drive end speed
Shaft speed (rad/s)
Time (s)

(a)

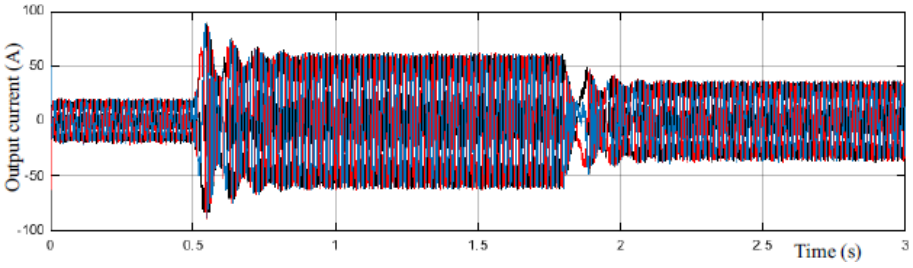
Output current (A)
Time (s)

(b)

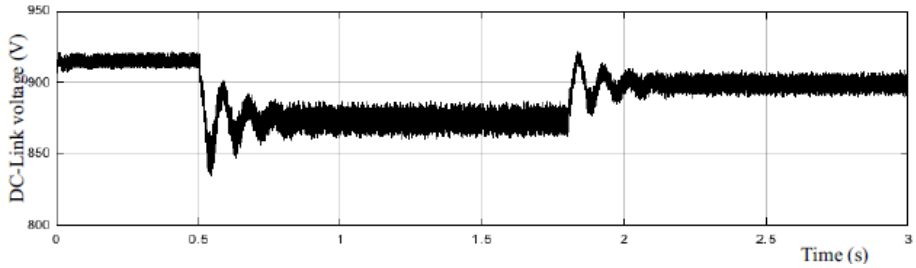
DC-Link voltage (V)
Time (s)

(c)

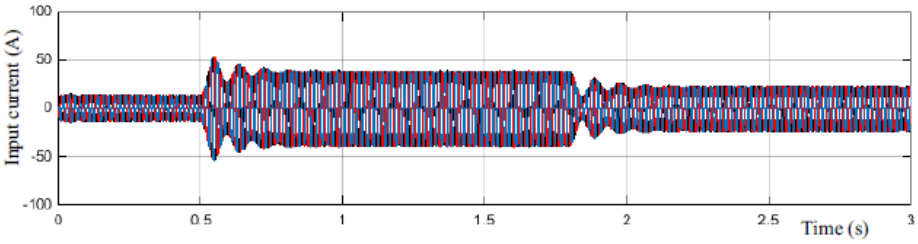
Input current (A)
Time (s)

(d)

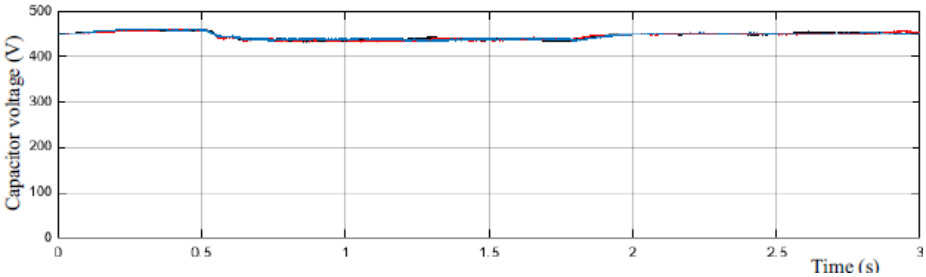
Capacitor voltage (V)
Time (s)

(e)

Figure 4.12. Proposed operation with active damping (a) shaft speed at the drive end and load end, (b) output current, (c) dc-link voltage, (d) rectifier input current, (e) clamping capacitor voltage

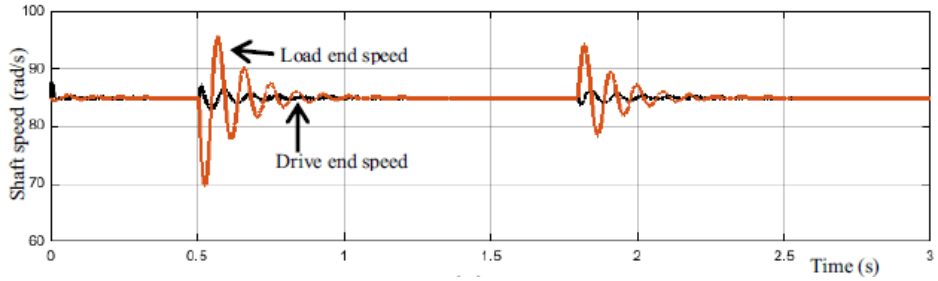

(a)

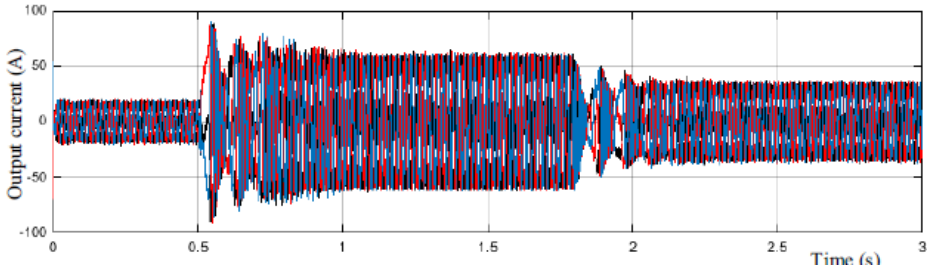

(b)

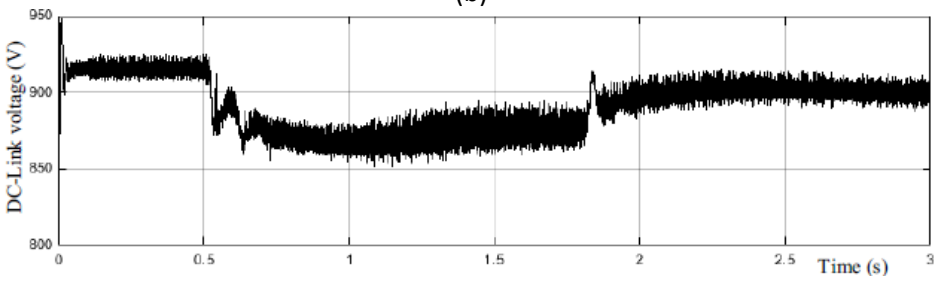

(c)

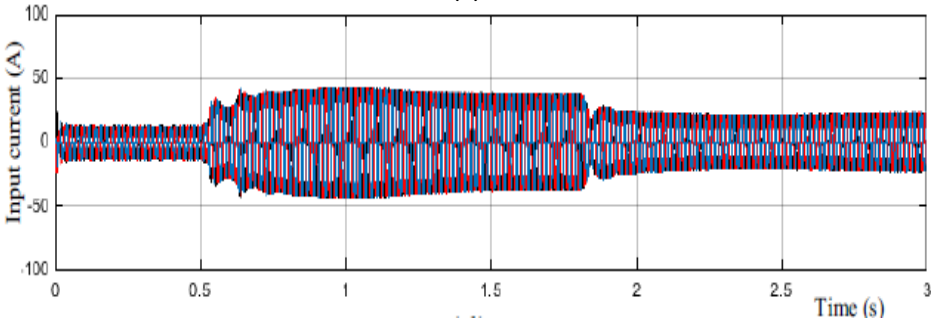

(d)

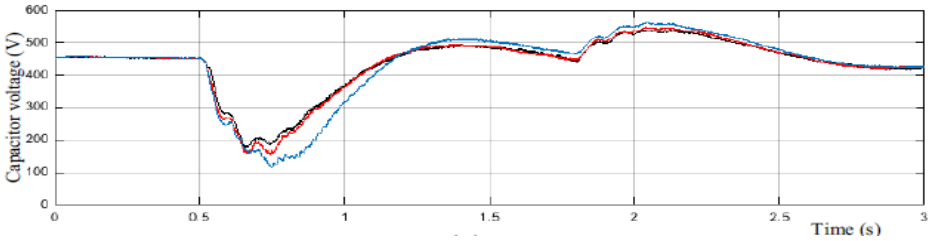

(e)

Figure 4.13. Proposed operation with active damping and clamping capacitor support (a) shaft speed at the drive end and load end, (b) output current, (c) dc-link voltage, (d) rectifier input current, (e) clamping capacitor voltage

As evident from the smooth transients in the DC link voltage and input current waveforms shown in Figure 4.13(c) and (d) respectively, the clamping-capacitor support makes a significant contribution to contain the oscillations within the inverter without passing them to the upstream power bus. The variations in the clamping-capacitor voltage, as shown in Figure 4.13(e), verifies this claim. When the load gain occurs at 0.5s, the clamping capacitors get discharged fast to supply the sudden increase of the load power. Moreover, they absorb the oscillations in the DC link voltage as well. Therefore, the DC link voltage changes smoothly. When the steady state occurs, capacitor voltage rises slowly to the balanced condition. The opposite happens at the load drop.

4(B).5 SUMMARY

This paper demonstrates the effective use of short-term energy storage capability of the capacitor-clamped inverter to contain oscillations within the inverter. Moreover, an active damping controller is used to suppress the torsional oscillations present in electromechanical drivelines with long and flexible shafts. An azimuth thruster with long flexible shafts is used as the example application to assess the efficacy of the proposed method thus eliminating the need for stronger and stiffer shafts. The results show that the proposed method is feasible and the shaft oscillations and vibrations can be damped quickly with the active damping controller. Moreover, the results show that the clamping capacitors are capable of absorbing the resulting transients arising from the shaft oscillations, without passing them on to the upstream power bus.

CHAPTER 5

BATTERY ENERGY STORAGE SOLUTION WITH ADVANCED MODEL PREDICTIVE CONTROL FOR FREQUENCY TRANSIENT SUPPRESSION

Viknash Shagar, Shantha Gamini Jayasinghe, Hossein Enshaei

Australian Maritime College, University of Tasmania, Launceston, TAS 7250, Australia

Published as '*Frequency Transient Suppression in Hybrid Electric Ship Power Systems: A Model Predictive Control Strategy for Converter Control with Energy Storage*' in '*Inventions 2018, 3, 13'*

This chapter presents the work done on a strategy that keeps the main engine power at a pre-defined constant level while applying a Model Predictive Control (MPC) algorithm to the Battery Energy Storage System (BESS) aimed at reducing the transient conditions during load change events. This segment of work focusses on reducing the electrical frequency fluctuations during the transient period.

Abstract - This paper aims to understand how the common phenomenon of fluctuations in propulsion and service load demand contribute to frequency transients in hybrid electric ship power systems. These fluctuations arise mainly due to changes in sea conditions resulting in significant variations in the propulsion load demand of ships. This leads to poor power quality for the power system that can potentially cause hazardous conditions such as blackout on board the ship. Effects of these fluctuations are analyzed using a hybrid electric ship power system model and a proposed Model Predictive Control (MPC) strategy to prevent propagation of transients from the propellers into the shipboard power system. A battery energy storage system, which is directly connected to the DC link of the frequency converter, is used as the smoothing element. Case studies that involve propulsion and service load changes have been carried out to investigate the efficacy of the proposed solution. Simulation results show that the proposed solution with energy storage and MPC is able to contain frequency transients in the shipboard power system within the permissible levels stipulated by the relevant power quality standards. These findings will help ship builders and operators to consider using battery energy storage systems controlled by advanced control techniques such as MPC to improve the power quality on board ships.

5.1 INTRODUCTION

The transportation industry has experienced many technological advancements over the years. One of the key developments is electrification in the form of electric traction or electric propulsion. In view of recent legislation involving the creation of Emission Control Areas (ECAs) (McCoy, 2015), ships with electric propulsion have become more of a reality with more cruise ships, ice breakers and various types of service vessels adopting this technology (Dale, Hebner, & Sulligoi, 2015). However, hybrid propulsion is a convenient waypoint between traditional mechanical propulsion and fully-electric propulsion as it combines the two, thereby reducing the need for a complete revamp of the propulsion system in very large ships such as container vessels. In these ships, propulsion load is the most challenging type of load as it forms the largest proportion of the total load in the electrical system. The propulsion load could vary within a wide range in a matter of seconds, which could result in transient conditions in the hybrid shipboard power system that can include overheating due to high inrush currents in addition to voltage and frequency fluctuations (Kim, et al., 2014; Tetra Tech, n.d.). The load busbar frequency plays an important part in maintaining the power quality due to the relationship between the electrical torque by a synchronous generator and generator speed deviation following a disturbance to the power system (Prabha, 1993). Failure or malfunction of crucial equipment that relies on a high level of power quality at sea such as navigation instruments could result in misinformation and power outages on board, leading to potentially disastrous consequences for lives and property at sea for seaborne vessels (Nielson, 2009; Hall, 1999). Energy storage is effective at reducing such transients due to its ability to exchange active power as required using appropriate control systems resulting in adjustments of the frequency level. This provides a means of reducing frequency transients by controlling power flow from energy storage systems by means of suitable control techniques.

The hybrid electrical shipboard power system considered in this study is shown in Figure 5.1, which contains a Battery Energy Storage System (BESS). The advantages of using a battery as a source of energy storage in power systems is well known. In addition to the reserve energy capacity that it provides, there is considerable literature recommending the use of a BESS to effectively deal with frequency transients, especially in standalone power systems such as terrestrial microgrids, major power grids and in shipboard power systems (Rajapakse, Jayasinghe, Fleming, & Negnevitsky, 2017;

Ceballos, et al., 2015; Vilathgamuwa, Nayanasiri, & Gamini, 2015; Zarghami, Vaziri, Rahimi, & Vadhva, 2013). The BESS integrated with the power system has to be fast in its response to changes in the power system and also have sufficient capacity to bring the state of the power system back to normal operating conditions. Therefore, the BESS control strategy has to be robust in order to act effectively in view of the constantly evolving load conditions of the hybrid ship. The extreme environmental conditions experienced by ships at sea such as sea waves should be taken into account when designing a control strategy for the BESS.

In the system shown in Figure 5.1, the BESS is directly connected to the DC-link of the frequency converter as opposed to the majority of literature, which uses a DC-DC converter to interface the battery to the DC-link (Ceballos, et al., 2015; Vilathgamuwa, Nayanasiri, & Gamini, 2015; Tedeschi, Carraro, Molinas, & Mattavelli, 2011). The absence of this interfacing converter reduces the complexity of the energy storage system while at the same time retaining control of the battery current.

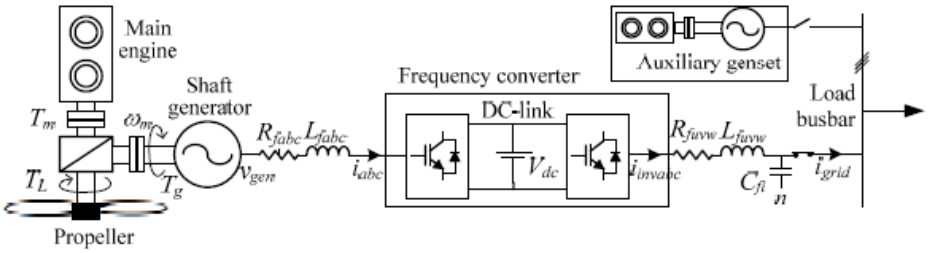

Figure 5.1. Schematic diagram of the hybrid electric ship power system considered in this study

Bi-directional power flow of the frequency converter is an important feature in the hybrid electric ship power system due to the possibility of a battery being charged and discharged in two directions, which could be from the main engine or the auxiliary engine. The main engine supplies mechanical power to the propeller and/or electrical power through the shaft generator to the main busbar of the ship's power system. The auxiliary engine, on the other hand, can supply electrical power to the busbar or further downstream to the shaft machine to be converted to mechanical power needed to meet propulsion load demands if necessary. As these power flows occur across the energy storage system, they can either charge or discharge the battery as required.

Conventional PI control and droop control for the converters have been used in many studies to reduce frequency deviations and improve power tracking for load change studies (Urtasun, Barrios, Sanchis, & Marroyo, 2015; Wenjie, Ådnanses, Hansen, Lindtjørn, & Tang, 2010; Mercier, Cherkaoui, & Oudalov, 2009; Lopes, Moreira, & Madureira, 2006). These control methods have been found to be slower acting and less efficient in rapidly changing loading conditions (Hou, Sun, & Hofmann, 2015). Advanced control strategies such as MPC and adaptive control have also been more recently explored in various research studies as more effective control techniques to reduce frequency transients (Mufti, Iqbal, Lone, & Ain, 2015; Zhang, Li, Cong, & Zhang, 2015; Hou, Sun, & Hofmann, 2014). These strategies, while reacting faster to changes in system operation as compared to feedback control techniques such as PI, have the added benefit of reducing charging and discharging current for batteries and improving the power tracking capabilities of the energy storage system by reducing tie power deviations. Furthermore, they are found to be suitable for highly non-linear problems with multiple constraints as in applications such as isolated power systems. However, most of the work in this area has not targeted the growing area of hybrid electric ship power systems, which presents a unique configuration involving interconnections of both mechanical and electrical components. Furthermore, though the results in the vast majority of work in this area show that the transient effects on electrical parameters have been reduced through the use of various control methods, they still exist to some extent, especially in hybrid electric ships mainly due to the above-mentioned unique configuration. A comprehensive background review of energy storage as a potential solution to load changes in hybrid ships has been reported in (Shagar, Jayasinghe, & Enshaei, 2017; Shagar, Gamini, & Enshaei, 2016). In contrast to the published work, an important objective of this work is to give a clear picture of the modelling of a hybrid propulsion shipboard power system with battery energy storage capability that is controlled by an MPC strategy. The effects that varying mechanical propulsion loads and electrical service loads in different combinations can have on the mechanical aspect of generator speeds and the electrical aspect of load busbar frequency have not been studied in sufficient detail for vessels that utilize hybrid propulsion. The aim of this study is to gain a clearer understanding of the mechanical and electrical dynamics of this complex power system. The extent to which the electrical frequency deviations are evident in terms of the observed transient magnitudes and settling times of the transients due to various loading conditions will also be investigated in this paper.

The rest of the paper is organized as follows. Section 5.2 presents the modelling aspects of the hybrid electric ship power system and its various modes of operation. Section 5.3 introduces the Model

Predictive Control (MPC) strategy and explains how it has been modified and adopted in the hybrid shipboard power system. Section 5.4 explains the load change scenarios simulated using the developed hybrid shipboard power system model under different operating conditions and the results obtained. An analysis of the results will follow in Section 5.5. Finally, Section 5.6 concludes the study.

5.2 HYBRID SHIPBOARD POWER SYSTEM AND MODELLING

The modelling of the hybrid power system closely follows the schematic shown in Figure 5.1. MATLAB-Simulink® software has been used to run the simulations. The five major components to be modeled are the shaft generator, auxiliary engine-generator set (genset), BESS, source side converter and grid side converter. It is to be noted that the source side converter is located near the shaft machine, while the load side converter is located next to the service loads and the load busbar as shown in Figure 5.1. In Figure 5.1, both of these converters are jointly called the frequency converter, as it converts the variable voltage-variable frequency output of the shaft generator to be connected to the constant voltage-constant frequency ship power system.

The main engine torque value has been set to the optimum value based on the specific fuel oil consumption versus load characteristics of the main engine (Shagar, Gamini, & Enshaei, 2016). The advantage of constant speed operation is two-fold. Firstly, the speed can be set at the most efficient point for the main engine. This results in fuel savings. Additional torque can be supplied by the auxiliary generator or the battery energy storage. Secondly, since the output torque of the engine is not changing, the transients passed along by the main engine to the rest of the system are reduced. This is highly desirable as lesser speed transients mean that the electrical frequency transients due to the main engine operation can be eliminated, thus reducing the overall frequency transients as seen in the electrical system. The propeller dynamics have been ignored in this study, although the propulsion loading profile is represented as a step load profile. A step load profile is generally considered to be the worst case loading due to the rapid rate of load increase and decrease. Therefore, loading profiles similar to a step load profile of the propulsion load are used in this study in order to understand the transient effects that these have on the system frequency. Service loads have been taken to be resistive and inductive in nature, and portions of this load will be switched in and out of the system to

examine their effects on the resulting transients. The effects of varying both the propulsion and service loads will be explored in this study.

The modelling of the main and auxiliary engines, as well as the shaft generator and the auxiliary generator remains the same as in a previous work done in (Shagar, Jayasinghe, & Enshaei, 2017) by the authors. The modelling of the Permanent Magnet Synchronous Generator (PMSG) with the IEEE Type 1 excitation system is well known and has been used widely in various other studies (Shagar, Gamini, & Enshaei, 2016; MatLab , n.d.; Saadat, 2004; Hall, 1999). However, it is important to note that in this case, the shaft generator can also act as a motor. Thus, this device is also called the shaft machine. When the main engine is supplying power to the load busbar to feed the ship's service loads, the shaft machine is acting as a generator. However, when the auxiliary generator and/or the battery is supplying power to the propulsion load, then the shaft machine carries out motor operation.

The system parameters of the model are given in Table 5.1. It is worth noting that the set point capacity of the main engine is fixed at 85% of its maximum capacity assuming that it is the point of maximum efficiency of the engine. The capacity of the auxiliary generator is kept at 20% of that of the main generator.

Table 5.1. Electrical parameter values for the power system model.

Parameters	Value
Bus voltage	400V
Main engine active power capacity	440kW
Main engine set point power capacity	374kW
Auxiliary genset active power capacity	88kW
Frequency	50Hz
Main engine reference speed	68rad/s
Auxiliary engine reference speed (4 pole)	78.5rad/s

Lithium ion batteries have been used in this study. They have been used commercially for a long time, and their high efficiency and high energy and volume density coupled with low cost per usable kWh per cycle have made them suitable for use in energy storage systems. These batteries have been used in high power applications involving pulse loads, which can be considered similar to environmental conditions such as sea waves that hybrid ships can potentially face in high seas that demand a quick response from the shipboard power system and its associated energy storage (Kim, Suharto, & Daim, 2017; Farhadi & Mohammed, 2016; Ma, Cintuglu, & Mohammed, 2015). Lithium ion

batteries have also been successfully integrated in the energy storage system of power systems that use bidirectional converters and utilize MPC to control these converters (Morstyn, Hredzak, Aguilera, & Agelidis, 2017; Ma, Cintuglu, & Mohammed, 2015). The lithium ion battery model used in this study has been adopted from models available in the MATLAB-Simulink software. The reader is encouraged to refer to (Thirugnanam, Joy, Singh, & Kumar, 2014; Rahmoun & Biechl, 2012) for the mathematical representation of the battery including the charging and discharging rate formulation. The specification of the battery used in the model is shown in Table 5.2.

Table 5.2. Battery specifications

Parameters	Value
Nominal Voltage	1000V
Fully charged voltage	1048V
Rated capacity	832Ah
Maximum capacity	1000Ah
Capacity at nominal voltage	1050Ah
Initial state of charge	65%
Nominal discharge current	361A
Cut-off voltage	800V

5.3 PROPOSED MPC STRATEGY

5.3.1 The MPC Concept

The general algorithm used for the MPC strategy will be introduced and explained below. This will be aligned with the modification and application of the MPC strategy to the hybrid ship power system in Section 5.3.2. Note that $u(k + i/k)$ and $x(k + i/k)$ refer to the input and state vectors at time $k + i$, which are predicted at time k. $x(k + i)$, and will then evolve as per a prediction model.

The optimization stage involves minimization of a cost function $J(k)$ that includes relevant input parameters, $u(k)$, and state parameters, $x(k)$, of the system under consideration in order to maximize performance. Constraints on the input, $u(k)$, can also be imposed as appropriate for the application to be solved simultaneously with the cost function.

The optimal input sequence of $u(k)$, $u^*(k)$ would be the one that minimizes $J(k)$. MPC utilizes the receding horizon implementation technique. Receding horizon implementation means that only the first element of $u^*(k)$ is fed to the plant model, and following that, the process of minimizing the predicted cost is then repeated again in the next time instant for the next set of $u^*(k)$ to be determined. This process of optimization is known as online optimization. The length of the prediction horizon remains the same at each time instant giving rise to the receding horizon concept portrayed in Figure 5.2. The measurement of the current state is required to compute $u^*(k)$, and this element of feedback that exists in the MPC law increases the robustness of this control strategy (Shaosheng & Yaonan, 2004; Cannon M. , n.d.). One of the main advantages of the MPC strategy is that it can be applied to a wide range of plant models. These can be linear or non-linear. The prediction model could be deterministic, stochastic or fuzzy in nature and discrete or continuous. Discrete time prediction models perform optimization periodically at times $t\ (=kT)$, and at each time instant k, T has to be sufficiently large to take into account the computation time at each iteration. However, the sampling interval, T_{samp}, could be a fraction of T if the optimal input sequence from the previous computation is to be used for further analysis. Continuous time prediction models are only used when the plant dynamics do not have a closed form discrete time representation such as in the case of non-linear plant models, and the previous optimal trajectory is accessible when the controller is computing the current optimal trajectory. In deterministic prediction models, the output of the prediction model is determined by fully-defined parameter values and initial conditions. Stochastic prediction models have inherent randomness that gives a variety of outputs for each run given the same set of parameters and initial condition values. Fuzzy prediction models rely on creating fuzzy rules based on the clustering effect of the existing data to make predictions of the future trajectory of plant operation (Cannon & Kouvaritakis, 2016; Maciejowski, 2000).

This study looks into improving the MPC concept and adopting it into the hybrid shipboard power system. As mentioned in Section 5.1, bidirectional converters are essential for controlling power flow between the battery and the loads, as well as the main and auxiliary power sources. As the converters perform rectifier and inverter operations, proper switching of the power electronic elements is essential to ensure expected power flow that is in line with power supply and demand in the system. This can be achieved if certain key control objectives are met when predicting the switching sequence in the converters ahead of time. As mentioned in Section 5.2, regulating the speed of the main generator is

the control objective for the source side converter. To ensure high energy sufficiency and preventing overheating and flux weakening, current flow should not exceed the desired value that is just sufficient to meet the power requirements. Finally, the predicted amount of active and reactive power flow to the electrical load side should be as close as possible to the actual power flow to avoid additional stress to the system, which can result in worse transient conditions. Section 5.3.2 will look into how the implementation of the MPC concept into the converters can optimize the above-mentioned objectives.

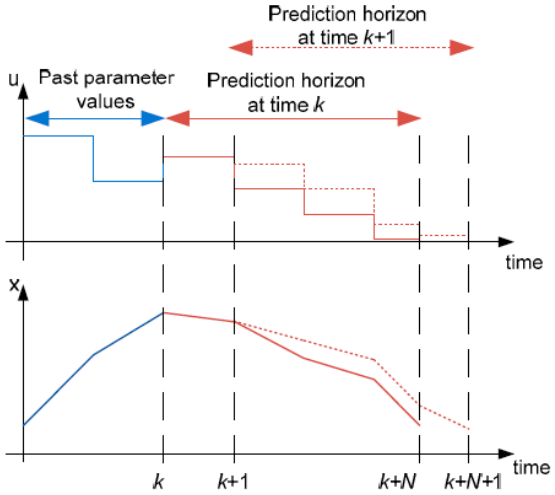

Figure 5.2. Receding horizon in Model Predictive Control (MPC).

5.3.2 MPC Implementation in the Hybrid Shipboard Power System

An MPC with a short prediction horizon has been chosen as the control strategy for converter control in the hybrid shipboard power system operation due to its advantages of rapid response and ease of implementation even in cases of non-linearity and multiple constraint optimization. The literature suggests that it is less complex to implement compared to conventional converter control techniques such as Voltage Control-based Pulse Width Modulation (PWM) with better reference tracking capabilities (Rajapakse, Jayasinghe, Fleming, & Negnevitsky, 2017; Parvez, Tan, & Akagi, 2015; Rodriguez & Cortés, 2012). The major disadvantage of using MPC would be the high computational burden in the algorithm. However, with the rapidly increasing processing power of microprocessors, this is unlikely to be a huge deterrent and is one that is common to most advanced control techniques (Rajapakse, Jayasinghe, Fleming, & Negnevitsky, 2017). MPC has been applied to two different components in the converter control system. They are the source side converter and the grid (load)

side converter. A schematic diagram of the proposed converters in the electrical system of the hybrid ship is shown in Figure 5.3, and their operation is described below.

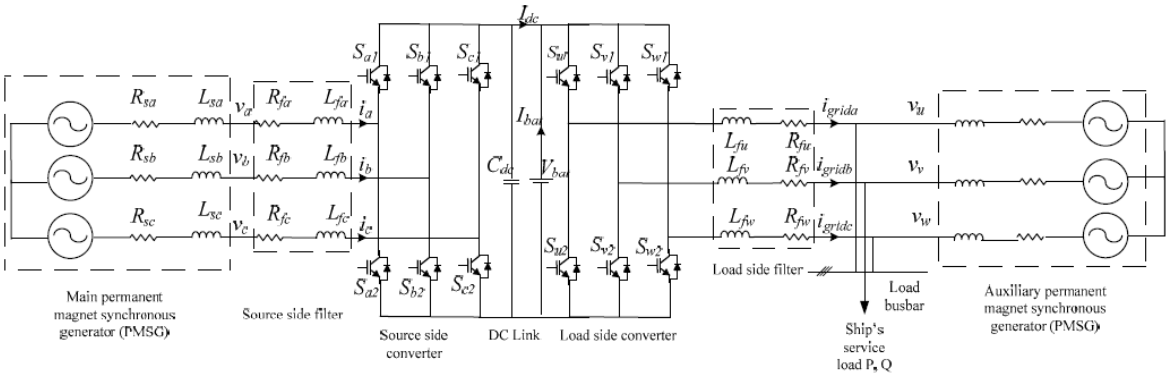

Figure 5.3. Schematic diagram of converters in the electrical portion of the hybrid shipboard power system

5.3.2.1 Source side converter modelling with the MPC Strategy

This converter is directly connected to the shaft machine AC supply via series inductors and resistors that act as filters. It has the capability of bidirectional operation depending on the direction of power flow from the main generator or from the auxiliary generator. It consists of six Insulated Gate Bipolar Transistor (IGBT) diode switches as shown in Figure 5.3. The switching configuration is such that no two switches in the same branch will be on or off simultaneously in order to prevent short circuiting in the system. As each switch in each phase can have two states of either being on or off, the three signals from the three phases would produce eight possible switching states that can be represented by a switching function vector, $\underset{S}{\rightarrow}$ This would result in eight different voltage space vectors. Using Kirchoff's voltage law, the source side converter's space vector can be found. The input current dynamics can then be derived, and since the MPC controller works in a discrete time domain, this is written in discrete time form as in Equation (5.1):

$$\frac{di_s}{dt} = \frac{i_s(k+1) - i_s(k)}{T_s} \tag{5.1}$$

where it is to be noted that i_s is the source side converter input current vector, *k* is the sampling instant and T_S is the sampling time. From Equation (5.1), the current at the *(k + 1)* − th time instant can be predicted as:

$$i_s(k+1) = \left(1 - \frac{R_S T_S}{L_S}\right) i_s(k) + \frac{T_S}{L_S}(v_s(k) - v_{AFE}(k)) \tag{5.2}$$

where v_s is the generated three-phase voltage vector, v_{AFE} is the converter output voltage and R_s and L_s are the total resistance and inductance of the PMSG and filter. The future value current, $i_s(k+1)$, is predicted for each of the eight switching states. Each of these current values is then converted into the *dq* frame. This is used to predict the future generator electromagnetic torque, $T_s(k+1)$, which in turn is used to compute the future predicted mechanical angular speed of the generator, $\omega^p = \omega_m(k+1)$, as per Equations (5.3) and (5.4):

$$T_e(k+1) = 1.5 p \psi i_q(k+1) \tag{5.3}$$

$$\omega_m^p = \omega_m(k) + \frac{T_S}{J}(T_m - T_e(k+1)) \tag{5.4}$$

Note that T_m is the mechanical torque applied on the generator, i_q is the *q* axis current, *p* is the number of poles and ψ is the PMSG flux. The values ω^p and $i_s(k+1)$ are then used in the cost function, g_{rec} as in Equation (5.5), to deduce the switching state that gives the minimum value for the function.

$$g_{rec} = |\omega^* - \omega^p| + K.\left|i_{d_{ref}}(k+1) - i_d(k+1)\right| \tag{5.5}$$

where ω^* is the reference speed, $i_{d_{ref}}(k+1)$ is the reference *d*-axis current and $i_d(k+1)$ is the predicted future value *d*-axis current. The speed variation is to be kept as close to zero as possible due to the aforementioned strategy to keep the output torque of the main generator constant at its most optimal level. The constant, *K*, has been added to further reduce the *d* axis current in the generator and thus prevent flux weakening and overheating effects in the generator. A flowchart of the MPC control algorithm used for the source side converter is shown in Figure 5.4. The software program for the gate control of this converter is given in Appendix AI.

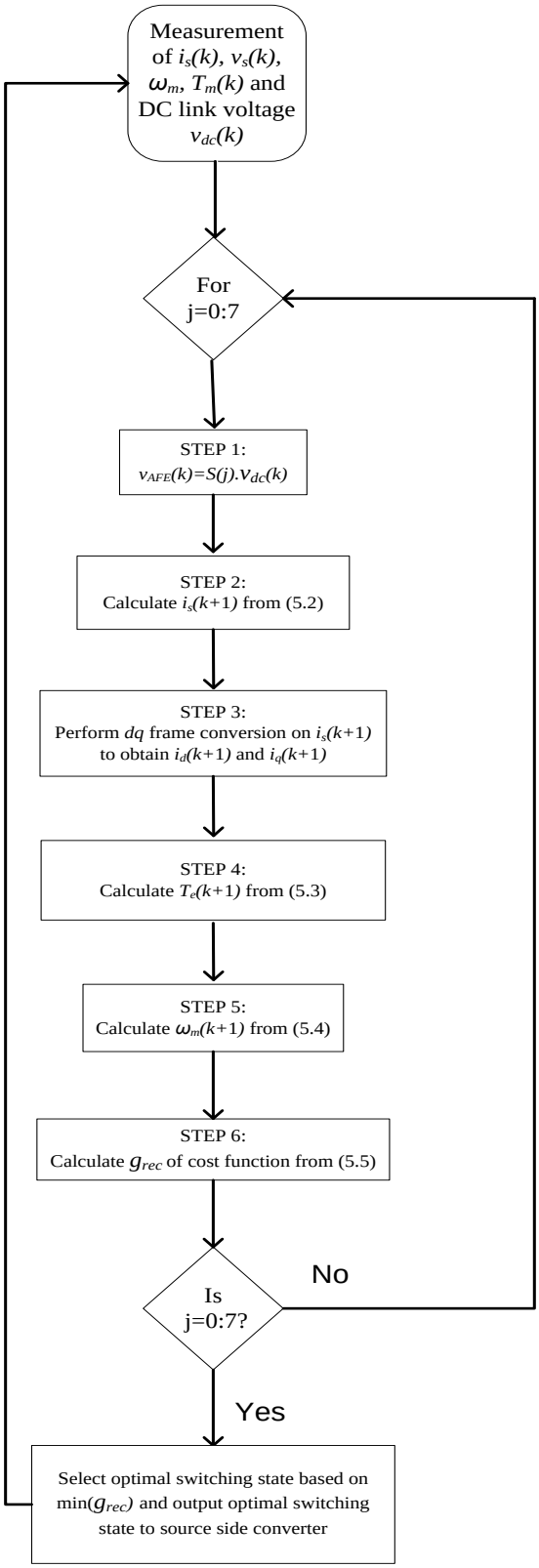

Figure 5.4. MPC algorithm flowchart for the source side converter

5.3.2.2 Grid (Load) Side Converter Modelling with the MPC Strategy

This converter connects the BESS to the load busbar through filters. The load busbar serves the service loads for ships and also receives power from the auxiliary generator and main generator if needed to supply service or propulsion load increases. Therefore, this converter has bidirectional operation where it can act as a rectifier or an inverter depending on the direction of power flow. The objective of the grid side converter control is to limit the active and reactive power needed by the loads to the required levels. The MPC concept achieves this objective in an efficient manner using a predictive control strategy. The switch operation of this converter is similar to the source side converter. The mathematical relation between the converter input voltage, v_{VSI} , and the three phase load busbar voltage derived from Kirchhoff's law applied to the output side of the converter is explained in (Rajapakse, Jayasinghe, Fleming, & Negnevitsky, 2017). The input current dynamics to the converter is as follows:

$$\frac{di_g}{dt} = -\frac{R_g i_g}{L_g} - \frac{v_g}{L_g} + \frac{v_{VSI}}{L_g} \tag{5.6}$$

where i_g, v_g and v_{VSI} are the load busbar current, voltage and inverter input voltage vectors, respectively. The inductive and resistive filter components are denoted by L_g and R_g. Equation (5.6) can then be discretized to predict the grid current at the *(k + 1)-th* time instant in the proposed MPC strategy as shown in Equation (5.7):

$$\mathrm{i_g(k+1)} = \left(1 - \frac{\mathrm{R_g T_g}}{\mathrm{L_g}}\right)\mathrm{i_g(k)} + \frac{\mathrm{T_s}}{\mathrm{L_g}}(\mathrm{v_{VSI}(k) - v_g(k)}) \tag{5.7}$$

From Equation (5.7), the apparent power and hence the real and active power prediction for the converter at the next time instant, *S(k + 1)*, can be calculated as in Equation (5.8):

$$S^P(k+1) = P^P(k+1) + jQ^P(k+1) = [Re(v(k)).Re(i(k+1)) + Im(v(k).Im(i(k+1) + j[Im(v(k)).Re(i(k+1)) - Re(v(k)).Im(i(k+1))] \tag{5.8}$$

The difference between the reference active and reactive power denoted by P^* and Q^*, and the predicted values for the *(k + 1)-th* time instant as denoted by P^P and Q^P, is then calculated for all the switching states in the cost function as shown in Equation (5.9). The P^* value is set depending on the variation of the measured speed of the auxiliary generator, $\omega_{measured}$ from the reference speed ω^* as stated in Table 5.1. P^* can also be considered to be the power that the battery supplies to the system and is calculated as in Equation (5.10). Q^* is zero in all cases. The switching state that gives the minimum g_{INV} value for this cost function is then chosen to be implemented in the next time instant. It is worth noting that the same control strategy for the converters is employed when the battery is not in operation. The flowchart illustrating the MPC control algorithm used for the grid (load) side converter is displayed in Figure 5.5 and the software program for the converter control is given in Appendix AII.

$$g_{INV} = |Q^* - Q^P|^2 + |P^* - P^P|^2 \tag{5.9}$$

$$P^* = 4000(\omega^* - \omega_{measured}) - 1500\frac{d\omega_{measured}}{dt} \tag{5.10}$$

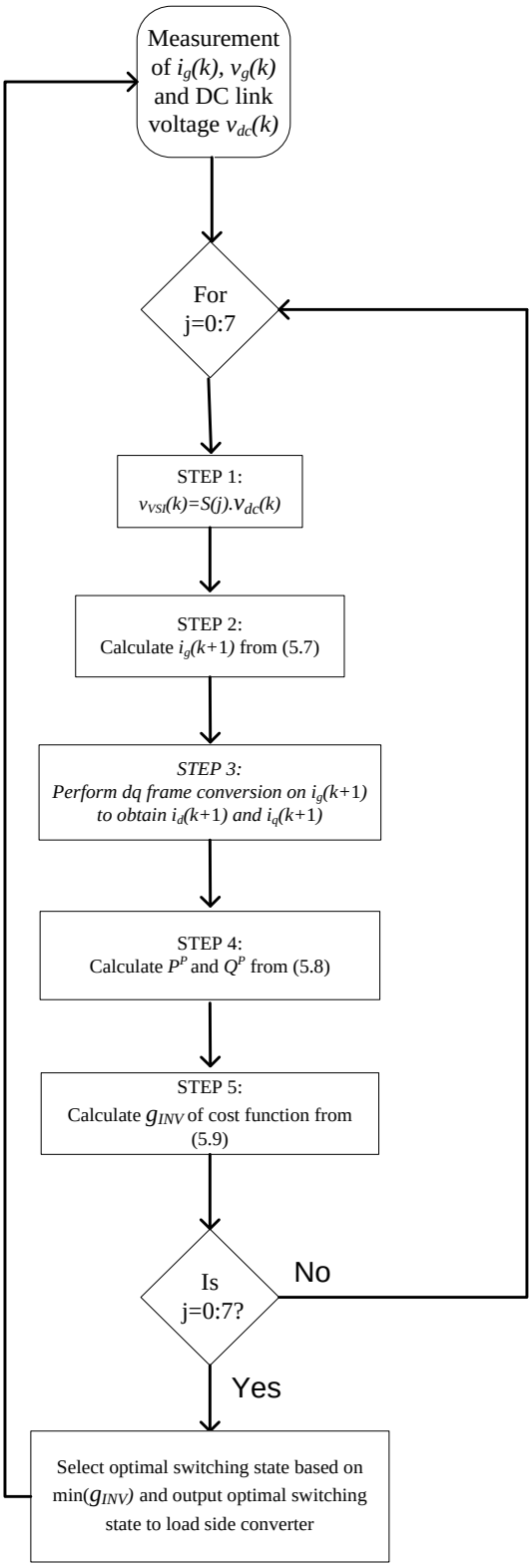

Figure 5.5. MPC algorithm flowchart for the grid (load) side converter

5.4 SIMULATION RESULTS

In order to assess the performance of the proposed solution in reducing the propagation of transients from the propulsion load to the electrical load busbar and frequency transients caused by service load changes, step changes are applied to the loads as shown in Figure 5.6(a),(b). These load changes and corresponding simulations are grouped into four scenarios, namely 1a, 1b, 2a and 2b, for the clarity of the discussion. Simulation results of these scenarios are combined and plotted together in corresponding waveforms in Figure 5.6 for the simplicity of the comparison. Scenarios 1a,b are without BESS, while Scenarios 2a,b use a BESS. Propulsion load changes have been applied in Scenarios 1a and 2a as shown in Figure 5.6(a) during the 0–30-s period. In order to keep the main engine speed constant as explained in Section 5.2, it is set to deliver a constant torque of 5500 Nm, which is termed the 'main generator set point torque'. Service load changes applied for Scenarios 1b and 2b are shown in Figure 5.6(b) during the 30–60-s period. The steady state is considered to be achieved when the parameter being considered is within 2% of the steady state value. These variations would be ±1.36 rad/s and ±1 Hz for the main generator speed and load busbar frequency, respectively, based on the reference values in Table1. The International Electrotechnical Commission (IEC) has recommended ranges for frequency excursions for both permanent and temporary conditions. As transient conditions are considered temporary in nature, the maximum allowable variation of the frequency amplitude is 10% with a maximum settling time period of 5s (Shagar, Jayasinghe, & Enshaei, 2017).

In order to focus the study only on load changes that occur during steady state operation of the system, any initial speed transients of the engines due to engine start up dynamics are not considered. In Scenarios 1a and 2a, propulsion load is increased to 5800 Nm, reduced to 5200 Nm and then brought back to 5500 Nm at 3 s, 13 s and 25 s, respectively, while service load remains constant at 50 kW. A Resistive-Inductive (RL) load is chosen for the service with 5 kVAR reactive power to reflect commonly-used loads in ship power systems. The corresponding variations of the shaft generator speed and load busbar frequency are shown in Figure 5.6(c),(d), respectively. The shaft generator speed variations for both scenarios are the same, and thus, the two traces coincide. Nevertheless, the load busbar frequency has significant differences in the two scenarios, and they are marked as 'without battery' and 'with battery' for Scenarios 1a and 2a, respectively. The upper limit and lower limit for frequency transients are also marked in Figure 5.6d to identify unacceptable scenarios. The DC-link

voltage is indirectly controlled by the converter controllers in Scenario 1a, and the corresponding variations under load change scenarios are shown in Figure 5.6e by the trace marked as 'without battery'. In the same figure, DC-link voltage variation for Scenario 2a is marked as 'with battery' where the BESS governs the voltage instead of converters controlling it. The corresponding variations in inverter power, auxiliary engine power and service load are shown in Figure 5.6f.

In Scenarios 1b and 2b, service load is increased from 50 to 80 kW and then brought back to 50 kW at 35 s and 45 s, respectively, while propulsion load remains constant at 5500 Nm. Similar to the above description, the corresponding variations in the shaft generator speed and load busbar frequency are shown in Figure 5.6(c), (d), respectively. The DC-link voltage is shown in Figure 5.6(e). The corresponding variations in inverter power, auxiliary engine power and service load are shown in Figure 5.6(g).

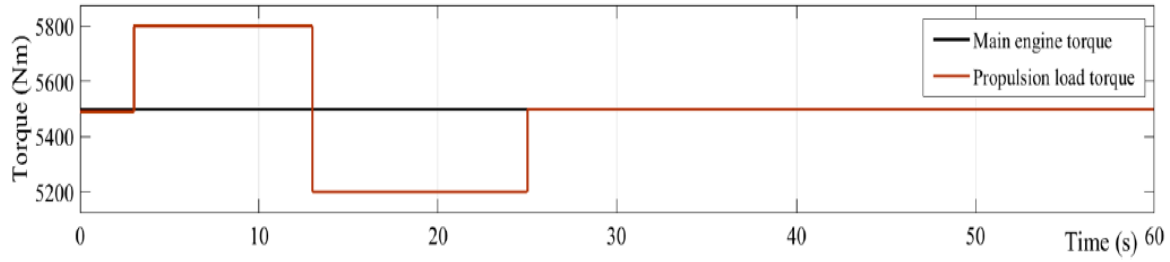

(a)

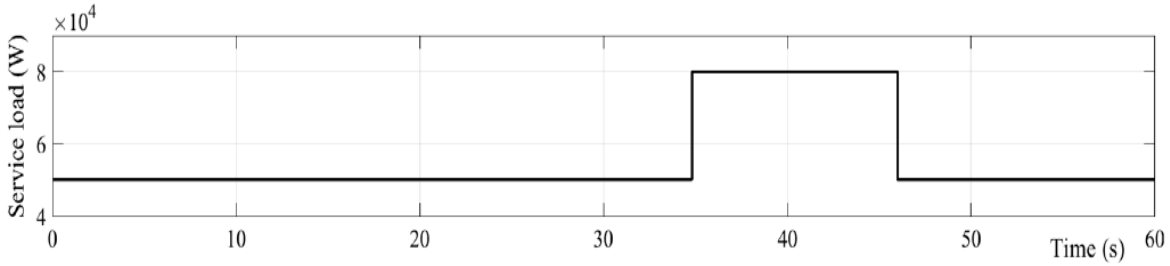

(b)

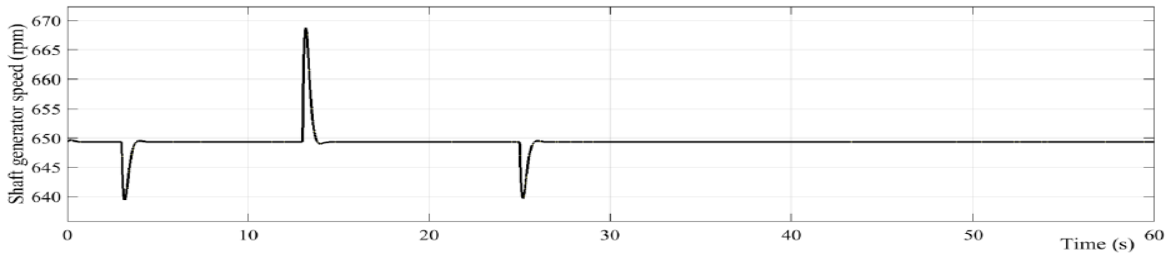

(c)

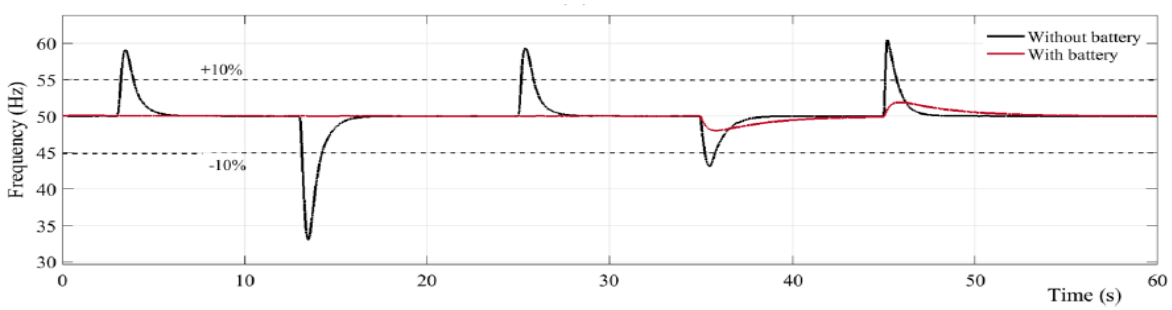

(d)

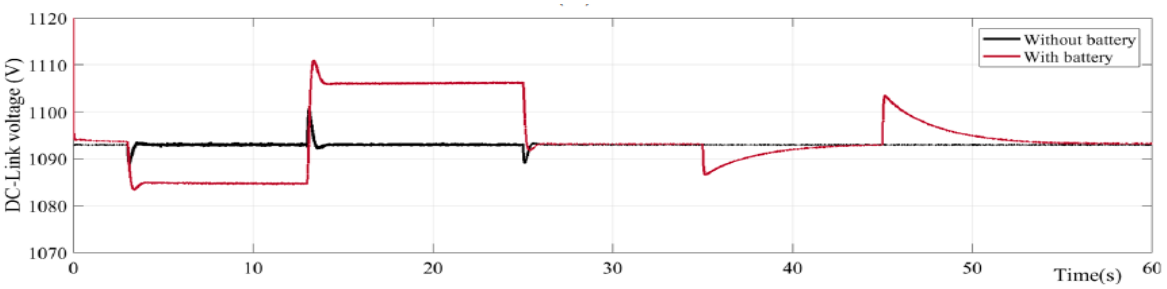

(e)

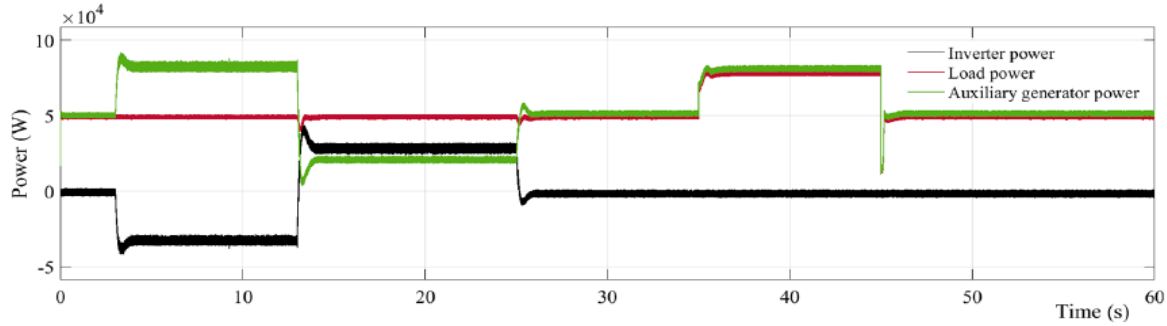

(f)

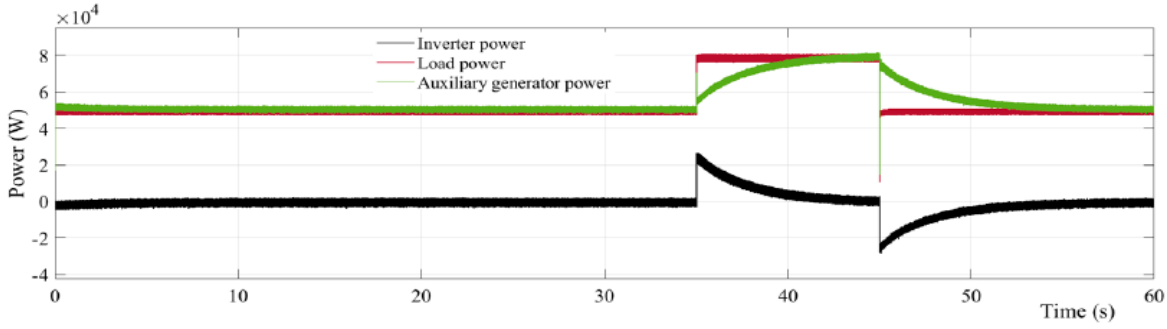

(g)

Figure 5.6. (a) Main engine torque and load torque (b) service load (c) shaft generator speed (d) load busbar frequency (e) DC-link voltage (f) inverter power, auxiliary engine power and service load without BESS (g) inverter power, auxiliary engine power and service load with BESS.

5.5 DISCUSSION OF RESULTS

The main objective of this study in using energy storage with MPC control to reduce speed and frequency transients is two-fold. Firstly, the propagation of transients from the main engine to the electrical load busbar due to changing propulsion load conditions is to be reduced. Secondly, the overall transients in the system are to be decreased. Excessive frequency transients indicate poor power quality and can affect the operation of other electrical equipment that draw power from the load busbar. Therefore, it is crucial that any load changes that occur at the mechanical part of the system that involves propulsion or the electrical part of the system supplying the service loads result in minimal speed fluctuation to the auxiliary generator speed. From the above discussion and due to the fact that the auxiliary generators are directly connected to the load busbar, it becomes clear that speed fluctuations at the auxiliary generators are more crucial as they have more implications for electrical power quality for other electrical components of the hybrid shipboard power system as compared to the main generator. Moreover, while propellers and connecting shafts do suffer from fatigue over time due to speed fluctuations, electrical components malfunction much more quickly and are more difficult to detect especially when sensitive technology such as navigation equipment is involved.

The scenario studies and results from Section 5.4 are structured in such a way so as to clearly highlight the effects of changing propulsion and service loading conditions separately on the main and auxiliary generator speeds and observing how these parameters are affected by adding battery energy storage. The load changes are applied as step changes to simulate the most challenging load changes. This would be the most appropriate type of loading profile encountered due to the fact that the waves and wind conditions that a ship experiences in rough weather are unpredictable and have a high impact on the load level of a ship in a short period of time. Service load changes can also be considered as step load changes as the resistive and inductive loads are switched in through a circuit breaker in the system, while they are directly being fed by the load busbar, thereby creating the highest possible impact.

The results in general indicate that speed and frequency settling times remain at or within 5 s for all of the cases. However, it is clear from the frequency plots that the rate of recovery of the system is much slower with battery energy storage. In Scenario 1b where battery energy storage is not used, the

frequency recovery rate is much higher compared to the corresponding rate in Scenario 2b. Nevertheless, this is not a significant disadvantage as the frequency sag or swell in Scenario 2b is much smaller than 10% and returns to the ±2% range within 5 s. This would be acceptable for satisfying the recovery time requirement following transient conditions in most standards including the IEC. As evident in Figure 6b, shaft generator speed transients do not vary even if a BESS is used. Therefore, the BESS reduces transients only in the load busbar side. Frequency transient amplitudes arising from propulsion load changes present the biggest transient conditions at the load busbar as they fluctuate more than 45% from their steady state values when there is no BESS used in the system. Therefore, propulsion load changes are more potent in causing major transients at the electrical part of the system because a 10% increase in propulsion load is causing more than a 45% change in frequency at the load busbar. This is due to the relatively smaller capacity in the electrical power system compared to the mechanical system. In practice, the transient conditions could be much higher at the auxiliary generator as load changes could be more severe than the 13% propulsion load change that has been applied in this study. In comparison, service load changes do not affect the speed of the main engine irrespective of whether a BESS is used or not. Therefore, service load transients do not propagate upstream to the main engine, but instead bring about a more than 10% frequency transient at the load busbar. Therefore, service load changes can be considered to be less impactful to the hybrid propulsion power system due to the following three reasons. Firstly, they allow the system to reach the steady state more quickly. Secondly, they do not propagate to the main generator, and lastly, since the transient amplitude is approximately equal to the load change magnitude, it is easier to predict its effect on the electrical frequency of the system.

The integration of an energy storage battery has massively reduced the transient frequency amplitude at the load busbar in all of the cases regardless of the type of load applied. For the case where only propulsion load was added with energy storage present in Scenario 2a, the transient amplitude at the load busbar of 45% seen in Scenario 1a was completely absorbed by the battery resulting in no noticeable transient on the load busbar frequency. This implies that the electrical frequency at the load busbar is completely unaffected by the step-like change in the propulsion load. The transient amplitude at the busbar caused by only a service load change as in Scenario 1b was reduced by 10% after energy storage was added to the system as in Scenario 2b. All the amplitudes of the transients with energy storage are far below the 10% level set by the IEC for allowable frequency fluctuation during the transient period. Settling times are also negligible since the speed fluctuations are very minimal in

nature. It should be noted that SoC management of the BESS is not included in this study as the focus is on reducing frequency transients, but this will be presented in future publications.

5.6 SUMMARY

This paper has illustrated the integrated modelling of the hybrid shipboard power system comprised of both the mechanical propulsion system and the electrical power system. This model has served as the platform for load change studies involving both propulsion and service loads and the transient effect that they have on the main generator speed and the electrical frequency. Further work has been done at the next stage to reduce these transient effects using battery energy storage. The main engine torque has been kept constant, and an MPC technique is used to control the power converters. It is observed that propulsion load changes have a bigger impact on the busbar frequency profiles as compared to service load changes. The biggest challenge encountered using this strategy is the propagation of the propulsion load change transients from the main engine to the load busbar where they have been magnified, hence creating massive fluctuations to the load busbar frequency. These frequency transients can be reduced by integrating battery energy storage into the system. It is believed that this paper would set a precedent for further work on load change studies on the hybrid shipboard power system with advanced energy storage control. While light to moderate loading conditions have been used in this study, more severe loading conditions can be applied to the system in future work to determine the resulting transient levels while improving the robustness of the energy storage control strategy further to ensure that transient conditions continue to be maintained at negligible levels.

CHAPTER 6

CONCLUSION AND FUTURE WORK

This chapter gives an overview of this thesis and provides the flow of work done throughout the study. The key findings gained as well as their implications in the area of hybrid propulsion shipboard power systems have been explained. Potential extensions to this study as well as other possible avenues for future work in this area have been discussed.

6.1 SUMMARY OF WORK PERFORMED

This study aims to investigate the effect that load changes have on the power system of a ship with hybrid propulsion. The first stage of the study involves creating a model of the hybrid shipboard power system and analyzing the existing effects that load changes have on the power system without implementation of any control measures. The representation of the hybrid shipboard power system forms the basis of the study therefore, a simulation model of the power system was developed. The extent of the effect of load changes to the power system can be quantified by observing the transients that follow load change events in the power system. The key parameters to be considered during this transient period are the electrical frequency and main engine speed behavior. As the loading of a ship can be broadly classified into propulsion and service loads, the effects of changes in each of these types of loads have been investigated separately. Furthermore, the effect that different magnitudes of single and consecutive load changes can have on the system parameters has been analyzed. The unique feature of hybrid propulsion in a ship lies in the fact that it can supply power both mechanically and through electrical means. Therefore, the impact of electrical and mechanical load changes on the nature of system wide key electromechanical parameters during the course of operation of both the main and auxiliary power generation sources was an essential avenue of the study.

The second stage of the study aims to reduce the electrical and mechanical oscillations that arise due to propeller shaft oscillations at the thruster drive train connecting to the electric motor. The electric motor is part of the electrical propulsion portion of the hybrid propulsion system. The first part of the study focusses on reducing the electrical transients arising from the load changes. A three level capacitor clamped inverter with a modified space vector PWM has been developed to reduce transients from affecting the DC link and travelling further upstream into the power bus. PWM has been used to control the net charging and discharging rate of the capacitor. The reference signal is generated by two PI controllers whose gains are selected such that one of the controller dominates during steady state condition while the other has prominent action during the transient condition. This allows the clamping capacitors to deliver the desired current despite unbalanced clamping capacitor voltages. The motor speed control uses a synchronous reference based controller that is PI based. In the second part of the study, the assumption of having stiff shafts has been relaxed. The long and thin shafts will therefore experience much greater oscillations during the propulsion load changes

experienced by the thruster. This leads to significant torsional oscillations that can lead to shaft fatigue if not controlled. In addition to the conventional PI-based speed control for Permanent Magnet Synchronous machines, an additional speed control component has been added that changes the *q*-axis current reference, thereby altering the torque reference in order to reduce the speed difference between the drive end and the load end of the shaft. This allows the motor to vary its torque resulting in reduced amounts of twisting by the shaft during the fluctuating load conditions thus reducing the torsional oscillations. This is the active damping component of the motor controller. The controller, thus, allows the conversion of the torsional oscillations which are mechanical in nature into the electrical transients that will then be reduced at the capacitor clamped inverters. Huge step load changes in the torque were applied to the system which was run under three control conditions. The first case was the control case, with neither the active damping feature nor the capacitor clamping support was enabled. The second case had only the capacitor clamping feature enabled while the third case had both the features in operation during the load change events. The variations and distortion observed in the shaft speed difference between the load and the drive ends, DC voltage oscillation and the input current wave were then analyzed.

The third stage of the study focusses on developing an advanced Model Predictive Control strategy (MPC) for the Battery Energy Storage System (BESS). The BESS is designed to reduce the frequency transients that occur during load changes for the hybrid shipboard power system and also supply additional load when applicable while the main engine power supply has been kept constant. Separate MPC algorithms have been developed to control the source and the load side converters with the aim of reducing the transient conditions. Both RL-service and propulsion step load changes have been applied to the system to separately analyze their effects and the improvements in transient response to MPC application on battery energy storage.

6.2 FINDINGS

The major findings of the study have been summarized below.

6.2.1 LOAD CHANGE PHENOMENA ON HYBRID SHIPBOARD POWER SYSTEM

- Fluctuations in the Main engine speed due to propulsion load changes are propagated and amplified at the electrical portion of the propulsion system as proven by extensive frequency transients at the main busbar
- Speed and frequency transient profiles have been found to be largely symmetrical during the load application and removal events, thereby, making prediction of transients possible and especially useful in the event of unexpected load change such as those due to fluctuating propulsion demands at sea
- Simultaneous service and propulsion load change result in slightly higher fluctuation magnitude for the Main engine speed transients but the frequency transients are increased significantly as compared to separate loading events for the service and propulsion loads
- Electrical transient limits stipulated by the relevant standards for marine vessels have been found to be exceeded by relatively low levels of propulsion or service load changes
- Relationship between the amount of load change and the severity of transients increases non linearly
- Multi-stage propulsion loading leads to reduced transients to the system as compared to equivalent single stage load change events of the same magnitude

6.2.2 CAPACITOR CLAMPED INVERTER SOLUTION

- Stiff shafts for thrusters with tight speed control pass reduce mechanical shaft oscillations but pass huge electrical transients to the electric motor drive train when step load torque change occurs
- Large variations in motor drive output current and resulting DC link voltage is a sign of electrical transients due to load change
- Electrical transients can travel upstream thus affecting the rectifier input current

- Addition of clamping capacitors to the inverter reduces the electrical transients by decreasing the rate of change of DC link voltage and smoothening the rectifier input current
- Due to absorption of the transients, voltages of the clamping capacitors vary widely
- Modified SPWM for the capacitor clamped inverter enables delivery of the required current without large distortions under unbalanced and varying clamping capacitor voltage conditions

6.2.3 CAPACITOR CLAMPED INVERTER BASED ACTIVE DAMPING METHOD

- Three cases involving capacitor clamped inverters and active damping feature carried out
- Flexible shaft used results in higher speed variation between load and drive end speeds which excite torsional oscillations
- Active damping reduces the speed difference between the drive and load ends of the shaft thus reducing the shaft speed oscillations passed into the system
- Case 1: Both capacitor clamped support (clamping capacitor voltages kept at balanced condition) and active damping support turned off
    - Torsional oscillations are damped slowly
    - Torsional oscillations have propagated to the electrical circuit because output current of inverter show similar transient conditions
    - Oscillations in DC link voltage and input current waveforms show propagation of electrical transients to DC side and upstream power bus
- Case 2: Active damping was enabled and capacitor clamping support remain turned off
    - Output current, DC link voltage and input current show similar oscillations but the transient period is shorter as compared to Case 1
- Case 3: Both active damping and capacitor clamping support are turned on
    - Torsional oscillations in the shaft have been damped the quickest due to active damping effect
    - Transients in the DC link voltage and the input current have been reduced further due to clamping capacitor action, thus, transient propagation upstream has been limited
    - Clamping capacitor action evident due to rapid variation in its voltage upon load change to supply load power and absorb DC link voltage

6.2.4 MPC IMPLEMENTATION IN BESS FOR THE HYBRID SHIPBOARD POWER SYSTEM

- Auxiliary generator speed is closely tied to electrical frequency as it draws power from the main (load) busbar
- Generator speed and frequency settling times are at or below 5s for the step load change scenarios investigated that involve light to moderate propulsion and service load changes
- Rate of recovery of frequency is much slower when BESS has been used although the frequency transient amplitude is lower with application of BESS
- Frequency transient levels due to propagation of mechanical transients from the mechanical propulsion load changes to the electrical system are very significant relative to the amount of propulsion load increase but they are almost completely eliminated when BESS was added to the system
- Service load changes are less impactful to the system than propulsion load changes because of the following reasons:
    - System reaches steady state condition quicker after service load changes
    - Service load changes do not propagate upstream as they do not affect the speed of the main engine regardless of BESS application
    - Transient amplitude is approximately equal to magnitude of load change, thus, making prediction of transient effect on system more possible
- All transient amplitudes are below IEC limits and settling times are negligible when BESS has been used

Having gone through the entire sequence of work that has been detailed in this thesis, perhaps the most significant contribution of this study has been the ability to have been able to contribute to a wide array of areas in the hybrid propulsion power system during transient events. These range from reducing mechanical oscillations at the mechanical aspect of the system through to improving the transient profiles of the DC link voltage, drive current and finally the main bus supply frequency at the electrical side of the system. The myriad of approaches used to tackle these parameter fluctuations include energy storage devices like batteries and capacitors separately controlled by a variety of measures that can be conventional in nature such as PI to more advanced algorithms such as MPC.

6.3 IMPLICATIONS OF THE STUDY

The study has, as part of its main objective conceived and developed a software model of the hybrid propulsion shipboard power system for analysis of the system behavior and also built a hardware test rig for experimentation and validation. This can be a precursor for improved models developed for further studies in this area. The variety of different loading conditions applied to the hybrid propulsion power system gives an idea of the susceptibility of the system to load change. This can be a point of consideration for hybrid ship operators to develop load scheduling and other load management strategies for their power system onboard in order to reduce the transient effects on the power system due to load changes. These findings can be particularly effective if the approximated levels of loading on the ship power system throughout the journey can be predicted beforehand.

A different approach to reducing transient conditions resulting from torsional oscillations of the shaft linking the motor drive and the propeller has been undertaken. The speed oscillations at the mechanical side of the system have been reduced by reducing the twisting effect between the ends of the shaft through speed control. The control strategy which relies more on PI control, thus aims to tackle the transient conditions as well as reduce propagation of transients upstream from a point in the system that is closer to the source of the changing load conditions which, in this case is the load end of the shaft connecting to the propeller because the propeller is the main point of contact for the changing environmental conditions that impose the varying load demands on the power system of the ship. Subsequently, capacitive energy storage elements have been used at the motor drive inverter to absorb the DC link and motor drive output current transients from the electrical side of the system. Therefore, through this combined 2-way approach, the shaft is being protected from excessive mechanical oscillations and in addition, the power system also encounters reduced electrical transients that have propagated into the electrical system from the drive shaft or have originated from electrical load changes. This solution which has been developed considering both the electrical and mechanical aspect of the hybrid propulsion power system can be highly effective as opposed to a solution consisting solely of energy storage measures applied to the electrical portion of the hybrid power system, as evident in the majority of the literature pertaining to this issue. Thus, this consideration illustrates a paradigm shift into the way the load change phenomena can be viewed in the case of hybrid ships.

In addition to capacitive energy storage, battery energy storage has been implemented on the hybrid ship power system. MPC as a more advanced control strategy has been applied to the Battery Energy Storage System to reduce frequency transients. It is observed that although this strategy reduces the amplitude of the transients, the settling time of the transients is longer. However, this is unlikely to be a major concern as settling times have been observed to be minimal in cases with no control measures. The major contribution through this approach has been the almost complete removal of transients propagating upstream of the power system to the electrical side following propulsion load changes. It has also been shown that the main engine supply power can be kept constant at its point of highest efficiency despite changing load conditions when the energy storage system is in operation. This results in fuel savings in the long term. It has also been found that the effect of service load changes are less severe and the extent of transients that they create can be estimated. This means that the capacity of energy storage necessary to absorb transients especially from service loads can be predicted without excessive redundancies and it indicates that additional equipment that are resistive and inductive in nature and not directly related to propulsion can be connected to the power network without concerns for excessive transient conditions that may propagate to other segments of the power system. Most importantly, this part of the study has illustrated the capability of BESS with MPC control to decrease both the amplitudes and settling times of the transients significantly. It has been proven that this approach can effectively deal with transient conditions resulting from any kind of load changes that have rapid ramp rates such as step load changes. It is to be noted that modelling of loading conditions as step load changes can be considered to be the worst case scenarios for load changes and as such, are very relevant to conditions experienced at sea where the wind and wave that contribute to propulsion loads can be unpredictable and can have a sudden impact on the power system.

6.4 LIMITATIONS OF STUDY AND SCOPE FOR FUTURE WORK

This work has endeavored to shed more light on hybrid propulsion shipboard power systems and the dynamics of how load changes experienced by the hybrid ship can affect key parameters of the power system. However, due to constraints of time and scope of the study, there are further avenues in this area where more work can be undertaken. Firstly, although the load change phenomena is the issue of concern, only low load levels have been considered in system modelling. Also, various other

configurations of the hybrid propulsion system utilizing only one source of power generation can be modeled and their sensitivity to load changes analyzed in further detail. The main modes of operation of hybrid propulsion considered in this study for in-depth investigation has been the PTI modes. However, other modes of operation such as the PTO, PTH, Parallel mode where the main engine runs at partial load together with the auxiliary generators and the cold ironing mode which involves shore power connection have not been explored. Although these modes of operation are not as commonly mentioned in the literature, they might still prove advantageous during load change conditions at specific scenarios such as maneuvering and while docked at port. This further reinforces the uniqueness of the hybrid power system that makes it possible to continue the study with different power system configurations. Subsequently, the efficacy of energy storage systems to reduce transient conditions in response to higher level loading conditions and other configurations of the hybrid propulsion power systems can be explored using a similar methodology adopted by this thesis.

The main body of work has focused on using different control strategies to reduce the transient conditions for different system parameters. Although, these strategies have been found to be hugely effective it might be worth using similar strategies to bring down the transient levels for other system parameters. As an example, the DC link voltage and the motor drive input current transients have been decreased using the capacitor clamped inverter based active damping method while the MPC based BESS approached has been successfully implemented against engine speed and electrical frequency transients. These strategies could be modified appropriately to investigate if the MPC based BESS can be effective against distortion and fluctuations in the motor drive input currents and the DC link voltage during load changes.

It has been noted that addition of energy storage can result in longer recovery times for system parameters following a load change. While this was not deemed severe enough to violate existing standards on transient conditions, the issue could be of more concern when much heavier changes in load conditions are applied. In such cases, additional measures such as State of Charge (SOC) management of the energy storage systems might have to be implemented. This could be yet another area for further extension of the work that could refine the overall control strategy and make the proposed solution against transient conditions in the hybrid propulsion power system more comprehensive.

A possible schematic of a test rig for the experimental setup to represent the hybrid shipboard power system is as shown in Figure 6.1. It is to be noted that the power capacity of the model might have to be scaled down due to the limitation in Power generation capabilities and the power handling capacities of the converters.

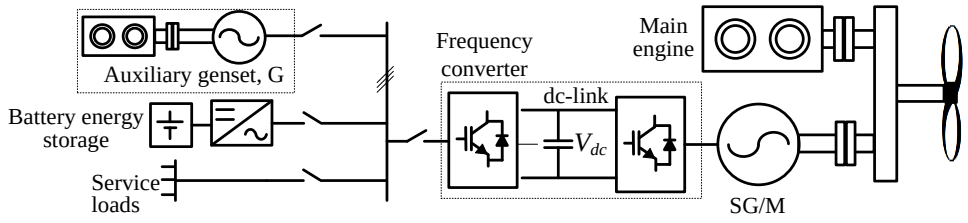

Figure 6.1. Schematic of laboratory test rig experimental setup

The system schematic shown in Figure 6.1 depicts a hybrid propulsion system that is powered by one main engine and one auxiliary electrical generator, denoted as G. A shaft machine is represented by the block labelled as SG/M. The main engine can supply mechanical propulsion power to the propeller load or electrical power to the ship service loads via the shaft machine which acts as a generator. The auxiliary electrical generator is connected to the main bus bar and can directly supply electrical power to the ship service loads or send power to the propeller loads through the shaft machine which acts as an electrical motor in this case. A Battery Energy Storage System (BESS) will be connected to the main bus bar of the system to control the frequency transients in the power system when there is a load change.

There are three main modes of operation to be studied under various loading conditions. They are as follows:

1. Power Take In (PTI) Mode – The auxiliary electrical generator and the main engine are operating. Main engine supplies power to the propeller. The auxiliary generator is supplying power to ship service loads and propeller.
2. Power Take Out (PTO) Mode – Only the main engine is supplying power to the propulsion and ship service loads.
3. Power Take Home (PTH) Mode – Only the auxiliary electrical generator is working to supply the propulsion loads and ship service loads.

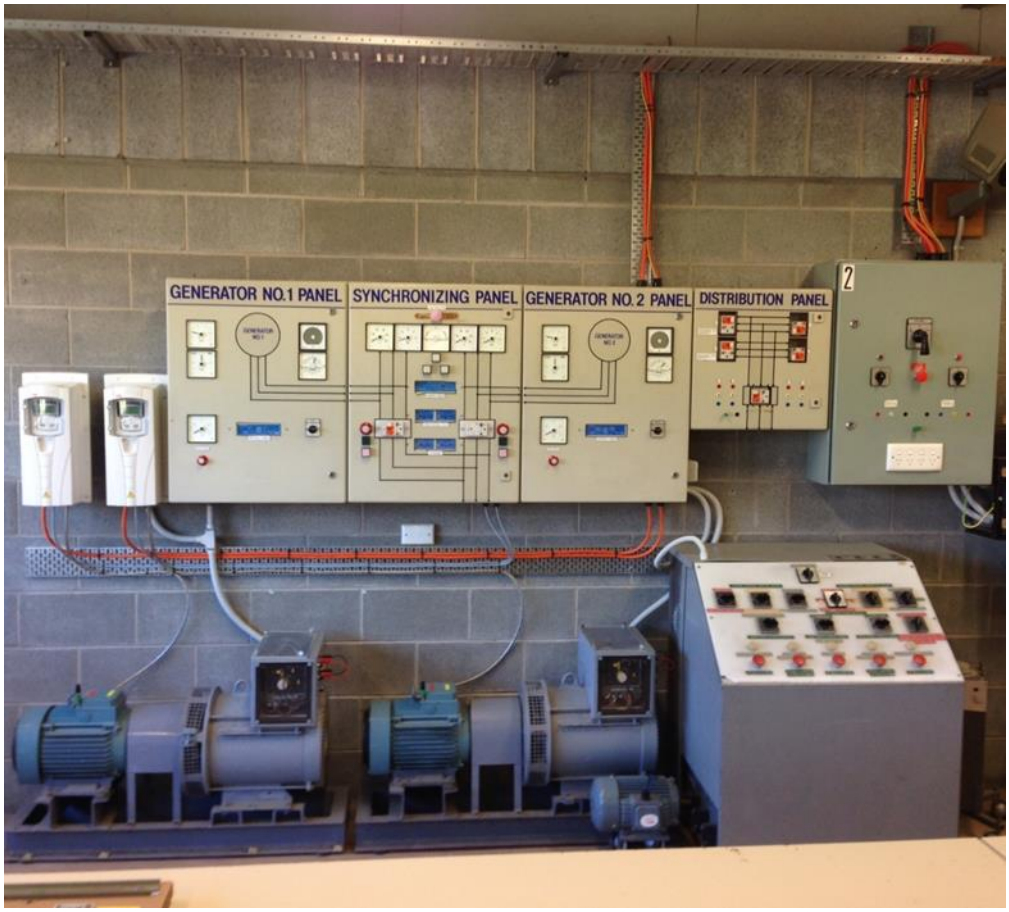

Figure 6.2. Laboratory Equipment – Gensets and Load bank

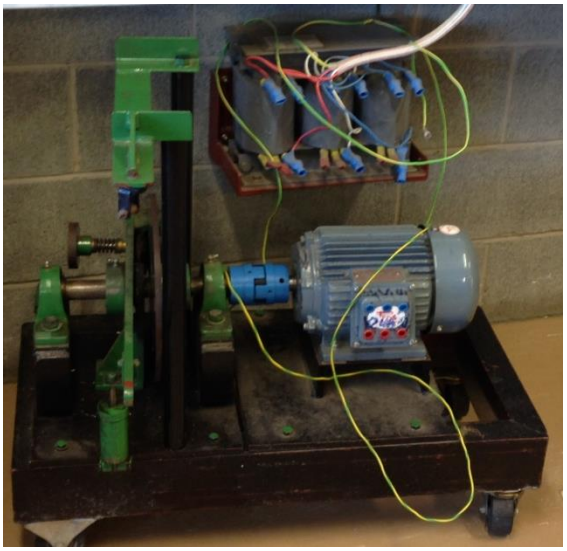

Figure 6.3. Laboratory Equipment – Shaft motor and related apparatus

There are two Motor-Generator sets. One of the two motor-generator set is used as the shaft generator while the other is used as the auxiliary generator. A load disc can be used to mimic the propeller load. The block diagram describing the link between the concept shown in Figure 6.1 and the lab equipment shown in Figures 6.3 and 6.4 is displayed in Figure 6.4.

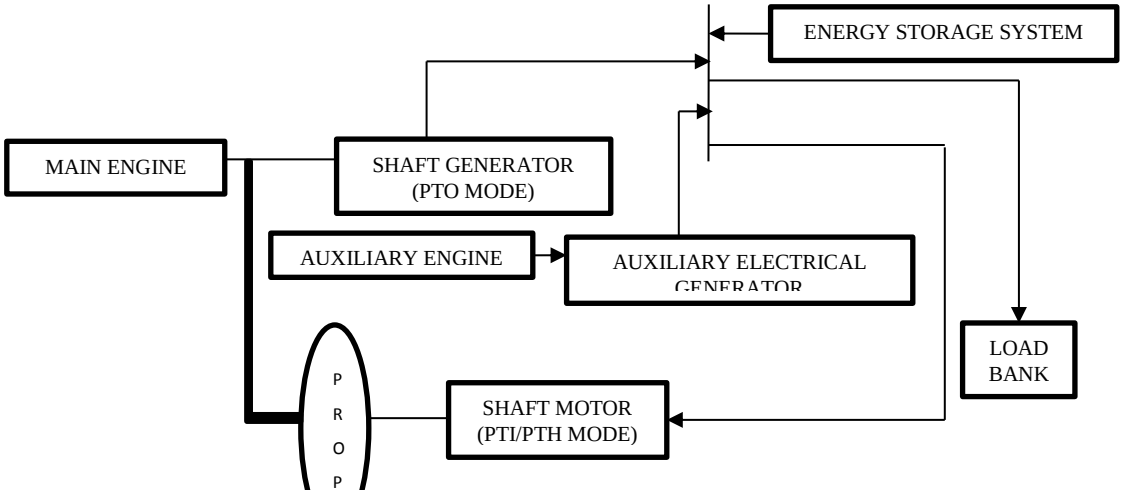

Note: The bold line linking the Propeller and the shaft connecting the Main Engine to the Shaft Generator is the belt that is added to simulate the mechanical connection between the Main Engine and metal disc representing the propulsion load

Figure 6.4. Relationship between hardware equipment and schematic diagram

The operation of the hybrid power system in different modes in the context of the laboratory testrig detailed above is explained as follows:

1. The shaft machine shown in the schematic of Figure 6.1 can act as a motor and generator depending on its mode of operation. However, due to technical limitations, this is not possible in the laboratory setup. Therefore, a separate motor with a load disc, as shown in Figure 6.3, are used. During the Power Take Out mode, the Shaft Generator is in operation to supply power to the load bank while during the Power Take In and Power Take Home mode, the Shaft Motor is running to supply power from the Auxiliary Electrical Generator to the propeller load labelled as 'PROP' in Figure 6.4.
2. The propeller load in Figure 6.1 will be represented as a load disc during the lab experiments as shown in Figure 6.3. The load has been applied by the loading mechanism which includes a brake pad attached to the disc. The disc screw can be used prior to load application to set

the amount of load to be added by the brake pad onto the disc. The lever attached to the disc can be used to allow the brake pad to clamp onto and release the disc thereby delivering and removing the required propulsion load. The braking mechanism has been designed such that the load is applied as an impulse to the system. The disc has to be mechanically connected to the shaft, thus, linking the Main Engine and the Shaft Generator to this representation of the propulsion load. This has been done as shown in Figure 6.2 through a belt. This belt connection is shown as the thick black strip in the schematic of Figure 6.4. Uneven loads can be attached magnetically to the rotating disc to induce mechanical vibrations at the shaft.

3. The Auxiliary Engine drives the Auxiliary Electrical Generator.
4. The values of an RLC load bank representing the ship service loads can be changed in steps while the lever shown in Figure 6.3 allows one to vary the resistance on the spinning disc thus changing the propulsion load with a step load change profile.

Figure 6.5 shows validation for the hardware testrig described above with the Simulation result for a PTO mode of operation. A 75N propulsion step load has been applied to the test rig at 1s and removed at 3.5s while the service load is been kept constant at 200W. The resulting frequency transient has been observed to have a reasonably good match with the simulation result.

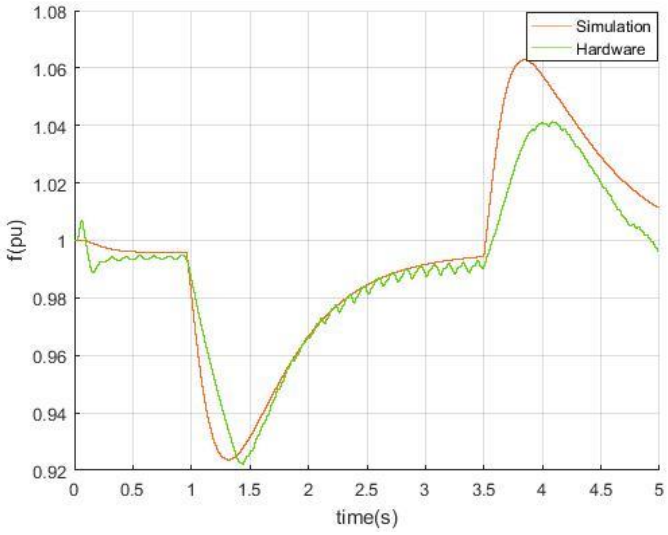

Figure 6.5. Experimental validation for Hardware testrig

A BESS can developed to provide an additional source of power in a controlled manner to the hybrid shipboard power system as required. As explained in Chapter 5, frequency transients have been observed due to load changes experienced by the power system and hence, the periods following the load changes are the crucial times when the energy storage system engages in an exchange of power with the hybrid shipboard power system. However, charging of the batteries can occur at other times of operation. A 2kW 3 phase phase demonstration board, such as the STEVAL – IHM028V1 that features the STGIPS20K60 IGBT power module can be used for motor control. The capacitor clamped inverter design can be implemented in the demonstration board. The algorithm for the Clamping capacitor charge and discharge controller as well as the PI based motor controller described for the 'Capacitor clamped inverter based torsional oscillation damping method' in Chapter 4 can be implemented MPC strategy explained in Section 5.3 can be utilized for the converter control in the BESS is using a microcontroller such such as the Tiva C series Launchpad by Texas Instruments. Similarly, the MPC strategy explained in Section 5.3 can be implemented using the microcontroller. Tachometers can be used to measurement, recording and providing feedback of the motor speed at the shaft, ZMPT 101B Voltage Sensor Modules can be used for voltage measurement for each phase while current transducers such as the HO8 NSM/SP33 can been used for current measurement for all three phases. Two STGIPS20K60 IGBT modules can be used as a rectifier and an inverter for AC-DC conversion. Possible specifications for the Li –ion Polymer battery used have been summarized in Table 6.1.

Table 6.1. Battery specifications for BESS

Parameters	Value
Nominal capacity (Ah)	40.0
Nominal voltage (V)	24.0
Discharge cutoff voltage (V)	19.0
Charge voltage (V)	29.4
Maximum charge voltage (V)	30.0
Maximum charge current (A)	10.0
Recommended charge current (A)	5.00
Continuous discharge current (A)	40.0
Maximum discharge current (A)	80.0
Maximum pulse discharge current (A)	80.0
Maximum AC impedance resistance (ohms)	150
Weight (kg)	6.20
Dimensions (mm)	250*98*155

An illustration of the BESS system that can be developed for testing and verification is as shown in Figure 6.6. It's worth noting that the BESS system described in this section would then be been

integrated as the ‘Energy Storage System’ into the main Hybrid propulsion testrig illustrated by the schematic in Figure 6.4.

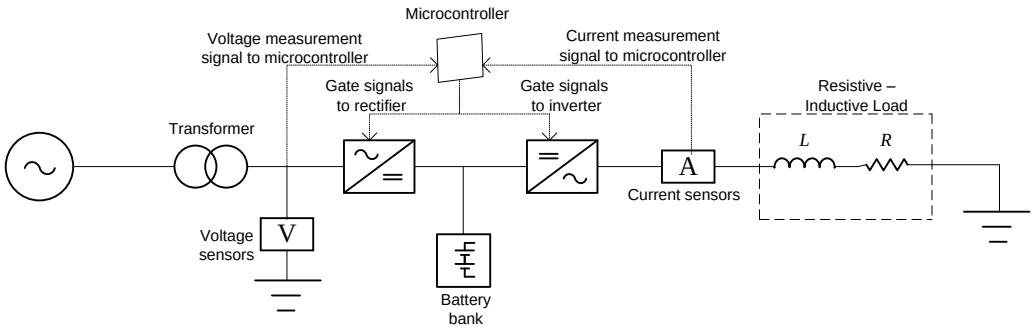

Figure 6.6. BESS schematic

In conclusion, the extent of coverage of the work firstly shows that there are many areas in such a power system that can be improved during transient conditions. It also proves that there are multiple ways to improve a particular area in the hybrid propulsion power system both with Simulation work that can be validated by hardware experimentation. Hence, it is hoped that the reader is convinced and motivated in realizing that there are potentially countless other possibilities to improve the hybrid propulsion shipboard power system performance in multiple areas that might not have been covered in the thesis.

References

Al-Barazanchi, S., & Vural, A. (2015). Modeling and intelligent control of a stand-alone PV-Wind-Diesel-Battery hybrid system. *International Conference on Control, Instrumentation, Communication and Computational Technologies.* Kumaracoil, India.

Arani, M., & El-Saadany, E. (2013). Implementing virtual inertia in DFIG-based wind power generation. *IEEE Trans. Power Syst., 28*, 1373-1384.

Ashraf, A. G. (2015). Control strategy applied on double flying capacitor multi-cell inverter for increasing number of generated voltage levels. *IET Power Electronics, 8*(6), 887-897.

Bennabi, N., Charpentier, J., Menana, H., Billard, J., & Genet, P. (2016). Hybrid propulsion systems for small ships: Context and challenges . *2016 XXII International Conference on Electrical Machines.* Lausanne, Switzerland.

Blooming, T. M., & Carnovale, D. J. (2006). Application of IEEE std 519-1992 Harmonic limits. *Conference Record of 2006 Annual Pulp and Paper Industry Technical Conference*, (pp. 1-9). Appleton.

Bø, T., & Johansen, T. (2017). Battery power smoothing control in a marine electric power plant using nonlinear model predictive control. *IEEE Trans. Control Syst. Technol., 25*, 1449-1456.

Bolognani, S., Zordan, M., & Zigliotto, M. (2000). Experimental fault-tolerant control of a PMSM drive. *IEEE Transactions on Industrial Electronics, 19*(4), 1134-1141.

Butler, K., & Sarma, N. (2000). General reconfiguration methodology for AC radial shipboard power systems. *Proceedings of the Power Engineering Society Winter Meeting.* Piscataway, USA.

Cannon, M. (n.d.). *Model Predictive Control*. Retrieved December 26, 2017, from http://www.eng.ox.ac.uk/~conmrc/mpc/mpc_lec1.pdf (accessed on 26 December 2017

Cannon, M., & Kouvaritakis, B. (2016). *Model Predictive Control—Classical, Robust and Stochastic.* New York, USA: Springer.

Caterpillar. (n.d.). *Caterpillar 3516B HD-2500kVA datasheet*.

Ceballos, S., Rea, J., Robles, E., Lopez, I., Pou, J., & O'Sullivan, D. (2015). Control strategies for combining local energy storage with wells turbine oscillating water columns. *Renew. Energy, 83*, 1097-1107.

Chin, H., Su, C., & C, L. (2016). Estimating Power Pump Loads and Sizing Generators for Ship Electrical Load Analysis. *IEEE Transactions on Industry Applications*, 4619-4627.

Cupelli, M., Ponci, F., Sulligoi, G., Vicenzutti, A., Edrington, C., El-Mezyani, T., & Monti, A. (2015). Power Flow Control and Network Stability in an All-Electric Ship. *Proc. IEEE , 103*, 2355-2380.

Dae-Wook, K. B.-K. (2005). A symmetric carrier technique of CRPWM for voltage balance method of flying-capacitor multilevel inverter. *IEEE Trans. Ind. Electron.*, 879-888.

Dale, S., Hebner, R., & Sulligoi, G. (2015). Electric Ship Technologies. *Proc. IEEE*, *2.* , pp. 2225–2228.

Dargahi, V. S. (2015). A New Family of Modular Multilevel Converter Based on Modified Flying-Capacitor Multicell Converters. *IEEE Transactions on Power Electronics, 30*(1), 138-147.

Das, D., Roy, A., & Sinha, N. (2011). PSO based frequency controller for wind-solar-diesel hybrid energy generation/energy storage system. *International Conference of Energy, Automation, and Signal.* Bhubaneswar, India.

Dempa Shimbun. (n.d.). *Long Life Technology for Aluminium non-solid Electrolytic Capacitors*. Retrieved November 2015, 15, from http://www.rubycon.co.jp/en/products/topics/img/t003_04.pdf

EVOX RIFA PASSIVE COMPONENTS,. (2001). *Life-Limiting factors in Electrolytic Capacitors*. Retrieved from http://www.efo-power.ru/pub/power/Capacitors/articles/kak_otsenit_srok_cond.pdf

Farhadi, M., & Mohammed, O. (2016). Energy Storage Technologies for High-Power Applications. *IEEE Trans. Ind. Appl., 52*, 1953-1961.

Fonte, M. R. (2011). Failure analysis of a gear wheel of a marine azimuth thruster. *Engineering Failure Analysis, 18*, 1884-1888.

Fuchs, F. (2003). Some diagnosis methods for voltage source inverters in variable speed drives with induction machines - a survey. *Industrial Electronics Society, 2003. IECON '03.*

Gayatri, M., Parimi, A., & Kumar, A. (2016). Utilization of Unified Power Quality Conditioner for voltage sag/swell mitigation in microgrid . *2016 Biennial International Conference on Power and Energy Systems.* Bangalore, India.

General Electric. (n.d.). *(Product Catalogue Style) Capacitors, Arrestors and Harmonic Filters, General Electric*. Retrieved from

http://www.geindustrial.com/catalog/buylog/24_BuyLog2013_Capacitrs ArrestrsHarmonFiltrs.pdf?omni_key=PG-BL24

Geng, H. X. (2011). Active Damping for PMSG-Based WECS With DC-Link Current Estimation. *IEEE Trans. Industrial Electronics, 58*(4), 1110-1119.

Gilles, T., AVX, A Kyocera Group Company. (n.d.). *Film Technology to replace Electrolytic Technology in Wind Power Applications*. Retrieved from http://web.arrownac.com/sites/default/files/pdfs/FilminWindPower.pdf

Hall, T. (1999). *Practical Marine Electrical Knowledge .* Livingston, UK: Witherby Publishers.

Hoevenaars, T. E. (2004). New marine harmonic standards. *IEEE Ind. Appl. Mag., 16*(1), 16-25.

Hou, J., Sun, J., & Hofmann, H. (2014). Mitigating power fluctuations in electrical ship propulsion using model predictive control with hybrid energy storage system. *Proceedings of the 2014 American Control Conference.* Portland, USA.

Hou, J., Sun, J., & Hofmann, H. (2015). Interaction analysis and integrated control of hybrid energy storage and generator control system for electric ship propulsion. *American Control Conference.* Chicago, USA.

Hou, J., Sun, J., & Hofmann, H. (2017). Mitigating Power Fluctuations in Electric Ship Propulsion with Hybrid Energy Storage System: Design and Analysis. *IEEE J Ocean Eng.*, 1-15.

IEEE. (n.d.). *IEEE Recommended Practice for Electrical Installations on Shipboard—Electrical Testing.* Retrieved july 19, 2017, from http://ieeexplore.ieee.org/document/7865875/

Jayasinghe, S. L. (2015). Electro-technologies for Energy Efficiency Improvement and Low Carbon Emission in Maritime Transport. *IAMU AGA.*

Jayasinghe, S. V. (2013). Flying Supercapacitors as Power Smoothing Elements in Wind Generation. *IEEE Trans. Ind. Electron.*, 2909-2918.

Jayasinghe, S., Meegahapola, L., Fernando, H., Jin, Z., & Guerrero, J. (2017). Review of Ship Microgrids: System Architectures, Storage Technologies and Power Quality Aspects. *Inventions, 2*(4).

Jayawardena, A., Meegahapola, L., Robinson, D., & Perera, S. (2015). Low-voltage ride-through characteristics of microgrids with distribution static synchronous compensator (DSTATCOM). *2015 Australasian Universities Power Engineering.* Wollongong, Australia.

Jewell, W., & Ward, D. J. (2002). Single phase harmonic limits. *PSERC EMI, Power Quality, and Safety Workshop* (pp. 1-7). Wichita: Wichita State University.

Jing Huang, K. A. (2006). Extended operation of flying capacitor multilevel inverters. *IEEE Trans. Power Electronics*, 140-147.

Journee, J. (n.d.). *Prediction of Speed and Behaviour of a Ship in a Seaway*. Retrieved July 19, 2017, from http://shipmotions. nl/DUT/PapersReports/0427-ISP-76.pdf

Kanellos, F., Tsekouras, G., Prousalidis, J., & Hatzilau, I. (2011). An effort to formulate frequency modulation constraints in ship-electrical systems with pulsed loads. *IET Electr. Syst. Transp, 1*, 11-23.

Kanellos, F., Tsekouras, G., Prousalidis, J., & Hatzilau, I. (2012). Effort to formulate voltage modulation constraints in ship-electrical systems with pulsed loads. *IET Electr. Syst. Transp, 2*, 18-28.

Kang, D. L. (2004). Carrier-rotation strategy for voltage balancing in flying capacitor multilevel inverter. *IEE Trans. Electric Power Appl.*, 239-248.

Kim, J., Suharto, Y., & Daim, T. (2017). Evaluation of Electrical Energy Storage (EES) technologies for renewable energy: A case from the US pacific Northwest. *J. Energy Storage, 11*, 25-54.

Kim, S., Ock, Y., Heo, J., Park, J., Shin, H., & Lee, S. (2014). CFD simulation of added resistance of ships in head sea for estimating energy efficiency design index. *Proceedings of the OCEANS* . Taipei, Taiwan.

Krause, P. (1986). *Analysis of Electric Machinery.* McGraw Hill.

Kristensen, H., & Marie, L. (n.d.). *Prediction of Resistance and Propulsion Power of Ships; Project No. 2010-56; Emissionsbeslutningsstøttesystem Work Package 2, Report No. 04.*

Kumar, P. K. (2015). Seventeen-Level Inverter Formed by Cascading Flying Capacitor and Floating Capacitor H-Bridges. *IEEE Transactions on Power Electronics, 30*(7), 3471-3478.

Li, S. (2012). Research on grid-connected operation of novel Variable Speed Constant Frequency (VSCF) shaft generator system on modern ship. *2012 15th International Conference on Electrical Machines and Systems (ICEMS)*, (pp. 1-5). Sapporo.

Li, W. L. (2016). Flying-Capacitor Based Hybrid LLC Converters with Input Voltage Auto-Balance Ability for High Voltage Applications. *IEEE Trans. Power Electron, 31*(3), 1908-1920.

Lin, B. H. (2006). Implementation of a Three-Phase Capacitor-Clamped Active Power Filter Under Unbalanced Condition. *IEEE Trans. Ind. Electron*, 1621-1630.

Lopes, J., Moreira, C., & Madureira, A. (2006). Defining control strategies for MicroGrids islanded operation. *IEEE Trans. Power Syst., 21*, 916-924.

Ma, T., Cintuglu, M., & Mohammed, O. (2015). Control of hybrid AC/DC microgrid involving energy storage, renewable energy and pulsed loads. *2015 IEEE Industry Applications Society Annual Meeting Meeting* . Addison, USA.

Maciejowski, J. (2000). *Predictive Control with Constraints.* London, UK: Pearson Education.

MAN Diesel & Turbo. (n.d.). *Hybrid Propulsion - Flexibility and Maximum efficiency optimally combined*. Retrieved july 19, 2017, from https://marine.man.eu/docs/librariesprovider6/4-Stroke-Engines/hybrid-propulsion.pdf?sfvrsn=6

MarelliGenerators . (n.d.). *MarelliGenerators MJRM 630 MB 8 datasheet*. Retrieved from http://www.powertechengines.com/MarelliData/Data%20Sheet/COMM.DSG.001.6%20GB.pdf

MatLab . (n.d.). *MatLab demo: Excitation System,l*. Retrieved from https://au.mathworks.com/help/physmod/sps/powersys/ref/excitationsystem.html

MATLAB. (n.d.). *MatLab demo: Emergency Diesel-Generator and Asynchronous Motor*. Retrieved from https://au.mathworks.com/help/physmod/sps/examples/emergency-diesel-generator-and-asynchronous-motor.html

McCoy, T. (2015). Electric Ships Past, Present, and Future [Technology Leaders]. *Electrification Magazine, 3*(2), 4,11.

Mercier, P., Cherkaoui, R., & Oudalov, A. (2009). Optimizing a Battery Energy Storage System for Frequency Control Application in an Isolated Power System. *IEEE Trans. Power Syst., 24*, 1469-1477.

Mindykowski, J., Szweda, M., & Tomasz, T. (2005). Voltage and frequency deviations in exemplary ship's network—Research for ship owner. *Electri. Power Qual. Util., 1*, 61-68.

Miroševic´, M., & Maljkovic´, Z. (2015). Effect of sudden change load on isolated electrical grid. *Conference on Electrical Systems for Aircraft, Railway, Ship Propulsion and Road Vehicles (ESARS).* Aachen, Germany.

Morstyn, T., Hredzak, B., Aguilera, R., & Agelidis, V. (2017). Model Predictive Control for Distributed Microgrid Battery Energy Storage Systems. *IEEE Trans. Control Syst. Technol.*, 1-8.

Mufti, M., Iqbal, S., Lone, S., & Ain, Q. (2015). Supervisory Adaptive Predictive Control Scheme for Supercapacitor Energy Storage System. *IEEE Syst. J., 9*, 1020-1030.

Murty, D. M. (n.d.). *Diesel Engine Governor Model*. Retrieved from http://www.sari-energy.org/PageFiles/What_We_Do/activities/CEB_Power_Systems_Simulation_Training,_Colombo,_Sri_Lanka/Course_ppts/Lecture_29_Modeling_Diesel_Engine_Gov_Sys.pdf

Nesje, J. R. (2013). *Patent No. Hybrid Shaft Generator Electric System for Shaft Generators Patent Number NO 332138.*

Nielson, B. (2009). *8500 TEU Container Ship Concept Study.* Munkebo, Denmark: Odense Steel Shipyard Ltd.

Parvez, M., Tan, N., & Akagi, H. (2015). An Improved Active-Front-End Rectifier Using Model Predictive Control. *IEEE Applied Power Electronics Conference and Exposition (APEC).* Charlotte, USA.

Prabha, K. (1993). *Power System Stability and Control.* New York, USA: McGraw-Hill.

Prousalidis, J., Hatzilau, I., Michalopoulos, P., Pavlou, I., & Muthumuni, D. (2005). Studying Ship Electric Energy Systems with Shaft Generator. *Proceedings of the IEEE Electric Ship Technologies Symposium.* Philadelphia, USA.

Radan, D., Sorensen, A., Adanes, A., & Johansen, T. (2008). Reducing power load fluctuations on ships using power redistribution. *Control Mar. Tecnol., 45*, 162-174.

Rahmoun, A., & Biechl, H. (2012). Modelling of Li-ion batteries using equivalent circuit diagrams. *Przegla¸d Elektrotechniczny, 88*, 152-156.

Rajapakse, G., Jayasinghe, S., Fleming, A., & Negnevitsky, M. (2017). A Model Predictive Control-Based PowerConverter System for Oscillating Water Column Wave Energy Converters. *Energies, 10*, 1631.

Rauti, T. (2013). Gear failures: Lessons learned. *6.Proc. Dynamic Positioning Conference.*

Report on the investigation of the catastrophic failure of a capacitor in the aft harmonic filter room on board RMS Queen Mary 2. Dec. 2011. (n.d.). Retrieved November 15, 2015, from https://assets.digital.cabinet-office.gov.uk/media/547c6fa6ed915d4c10000031/QM2Report.pdf

Reusser, C. Y. (2015). Full electric ship propulsion based on a flying capacitor converter and an induction motor drive. *International Conference on Electrical Systems for Aircraft, Railway, Ship Propulsion and Road Vehicles.*

Review of Maritime Transport . (2014). *United nations conference on trade and development (UNCTAD 2014)*, (pp. 27-48).

Roa, M. (2009). ABS Rules for Integrated Power Systems (IPS). *IEEE Electric Ship Technologies Symposium7.* Baltimore, USA.

Rodriguez, J., & Cortés, P. (2012). *Predictive Control of Power Converters and Electrical Drives.* Chichester, UK: JohnWiley & Sons Ltd.

Rolls Royce . (n.d.). *Report on Evaluation of a 50% constant-power load step using the "V01" Bergen model.* Glasgow, UK: University of Strathclyde.

Rolls Royce Power Electric Systems. (2010). *Hybrid Shaft Generator Propulsion System Upgrade-Making Fixed Engine Speed History .*

Saadat, H. (2004). *Power system analysis.* McGraw-Hill Education.

Shagar, V., Gamini, S., & Enshaei, H. (2016). Effect of load changes on hybrid electric ship power systems. *IEEE 2nd Annual Southern Power Electronics Conference.* Auckland.

Shagar, V., Jayasinghe, S., & Enshaei, H. (2017). Effect of Load Changes on Hybrid Shipboard Power Systems and Energy Storage as a Potential Solution. *Inventions, 2*(21).

Shaosheng, F., & Yaonan, W. (2004). Fuzzy model predictive control for alternating current excitation generators. *4th International Power Electronics and Motion Control Conference.* Xi'an, China.

Shen, Q., Ramachandran, B., Srivastava, S., Andrus, M., & Cartes, D. (2011). Power and Energy Management in Integrated Power System. *Electric Ship Technologies Symposium.* Piscataway, USA.

Smogeli, Ø. (2006). *Control of Marine Propellers: From Normal to Extreme Conditions.* Trondheim: Norwegian University of Science and Technology.

Srivatchan, N., Rangarajan, P., & Rajalakshmi, S. (2015). Control Scheme for Power Quality Improvement in Islanded Microgrid Operation. *Procedia Technol., 21*, 212-215.

Sun, Z., Wang, J., & Dai, Y. (2011). Modeling and control system design of a marine electric power generating system. *2011 6th IEEE Conference on Industrial Electronics and Applications.* Beijing, China.

Tedeschi, E., Carraro, M., Molinas, M., & Mattavelli, P. (2011). Effect of Control Strategies and Power Take-Off Efficiency. *IEEE Trans. Energy Convers, 26*, 1088-1098.

Tetra Tech. (n.d.). *Use of Shore Side Power for Ocean Going Vessels*. (American Association of Port Authorities) Retrieved july 2017, 2017, from http://wpci.iaphworldports.org/data/docs/onshore- power-supply/library/1264151248_2007aapauseofshore-sidepowerforocean-goingvessels.pdf

Thantirige, K. R. (2015). Medium voltage multilevel converters for ship electric propulsion drives. *Proc. Intl. Conf. on Elec. Sys. for Aircraft, Railway, Ship Prop. and Road Vehicles,*, (pp. 1-7).

Thirugnanam, K., Joy, E., Singh, M., & Kumar, P. (2014). Mathematical Modeling of Li-Ion Battery Using Genetic ALgorithm Approach for V2G Applications. *IEEE Trans. Energy Convers. , 29*, 332-343.

UN Framework Convention on Climate Change. (2011). *Control of greenhouse gas emissions from ships engaged in international trade*. Retrieved from http://unfccc.int/resource/docs/2011/smsn/igo/142.pdf

Urtasun, A., Barrios, E., Sanchis, P., & Marroyo, L. (2015). Frequency-Based Energy-Management Strategy for Stand Alone Systems with Distributed Battery Energy Storage. *IEEE Trans. Power Electron., 30*, 4794-4808.

Vilathgamuwa, D. J. (2011). A unique battery/supercapacitor direct integration scheme for hybrid electric vehicles. *Proc. IEEE Ind. Electron. Society Conf.*

Vilathgamuwa, D. J. (2011). Battery clamped three-level inverter for renewable energy systems. *Proc. IEEE Ind. Electron. Society Conf.*, (pp. 3105-3110).

Vilathgamuwa, M., Nayanasiri, D., & Gamini, S. (2015). *Power Electronics for Photovoltaic Power Systems.* San Rafael, USA: Morgan & Claypool Publishers.

Völker, T. (n.d.). *Hybrid Propulsion Concepts on Ships.* . Retrieved july 19, 2017, from zeszyty.am.gdynia.pl/.../Hybrid% 20propulsion%20concepts%20on%20ships_200.pdf

Welchko, B. L. (2004). Fault tolerant three-phase AC motor drive topologies: a comparison of features, cost, and limitations. *IEEE Trans. Power Electronics, 19*(4), 1108-1116.

Wenjie, C., Ådnanses, A., Hansen, J., Lindtjørn, J., & Tang, T. (2010). Super-capacitors based hybrid converter in marine electric propulsion system. *Proceedings of the Electrical Machines (ICEM), 2010 XIX International Conference.* Rome, Italy.

Xiaomin, K. K. (2004). A unique fault-tolerant design for flying capacitor multilevel inverter. *IEEE Trans. Power Electron.*, 979-987.

Zarghami, M., Vaziri, M., Rahimi, A., & Vadhva, S. (2013). Applications of Battery Storage to Improve Performance of Distribution Systems. *Green Technologies Conference.* Denver, USA.

Zhang, J., Li, Q., Cong, W., & Zhang, L. (2015). Restraining integrated electric propulsion system power fluctuation using hybrid energy storage system. *IEEE International Conference on Mechatronics and Automation.* Beijing, China.

Zhang, L. W. (2007). Capacitor voltage balancing in multilevel flying capacitor inverters by rule-based switching pattern selection. *IET Trans. Electric Power Appl.*, 339-347.

Ziyou, L. M. (2015). Modular-Cell Inverter Employing Reduced Flying Capacitors With Hybrid Phase-Shifted Carrier Phase-Disposition PWM. *IEEE Trans. Ind. Electron, 62*(7), 4086-4095.

APPENDICES

(AI) Model Predictive Control (MPC) MATLAB algorithm for Source Side Converter Control

```
function [Sa,Sb,Sc] = fcn(iqref,Vdc,I_labcgen,V_phasegen,Theta)
Tsample = 1e-5;
% Load parameters
R = 0.01;       % Resistance [Ohm]
L = 5e-3;       % Inductance [H]
%pole pairs
Polepairs =4;
%flux
flux=0.6667;
%inertia

J=2;
% Switching states
states = [0 0 0;1 0 0;1 1 0;0 1 0;0 1 1;0 0 1;1 0 1;1 1 1];
states2 = [0 0 0;2 -1 -1;1 1 -2;-1 2 -1;-2 1 1;-1 -1 2;1 -2 1;0 0 0];
vinv = Vdc*states2/3;
% Optimum vector and measured current at instant k-1
g_opt = 1e10;
x_opt = 1;
Ome1=0;

for i = 1:8
      % Current prediction at instant k+1
      ik1a = (1 - R*Tsample/L)*I_labcgen(1) - Tsample/L*(vinv(i,1)-
V_phasegen(1));
      ik1b = (1 - R*Tsample/L)*I_labcgen(2) - Tsample/L*(vinv(i,2)-
V_phasegen(2));
      ik1c = (1 - R*Tsample/L)*I_labcgen(3) - Tsample/L*(vinv(i,3)-
V_phasegen(3));
   % Calculate idk1 and iqk1
   idk1 =2*(ik1a*sin(Theta)+ik1b*sin(Theta-
2*pi/3)+ik1c*sin(Theta+2*pi/3))/3;
   iqk1 =2*(ik1a*cos(Theta)+ik1b*cos(Theta-
2*pi/3)+ik1c*cos(Theta+2*pi/3))/3;
```

```
  %Te=1.5*Polepairs*flux*iqk1;
 % Omegak1 = Omega + Tsample*(Torque-Te)/J;

   % Cost function
   g = abs(idk1)+ abs(iqref-iqk1);
   %g = abs(Omegaref-Omegak1)+ 5e-5*abs(idk1);
     % Selection of the optimal value
     if (g<g_opt)
        g_opt = g;
       x_opt = i;
     end
end
% Output switching states
Sa = states(x_opt,1);
Sb = states(x_opt,2);
Sc = states(x_opt,3);
```

(All) Model Predictive Control (MPC) MATLAB algorithm for Grid Side Converter Control

```
function [Sa,Sb,Sc,P,Q] = fcn(Vdc,P_ref,I_abcgrid,V_abcgrid)
Tsample = 1e-4;
% Load parameters
R = 0.01;       % Resistance [Ohm]
L = 10e-3;       % Inductance [H]
% Voltage vectors
v0 = 0 + 1j*0;
v1 = 2/3*Vdc + 1j*0;
v2 = 1/3*Vdc + 1j*sqrt(3)/3*Vdc;
v3 = -1/3*Vdc + 1j*sqrt(3)/3*Vdc;
v4 = -2/3*Vdc + 1j*0;
v5 = -1/3*Vdc - 1j*sqrt(3)/3*Vdc;
v6 = 1/3*Vdc - 1j*sqrt(3)/3*Vdc;
v7 = 0 + 1j*0;
v = [v0 v1 v2 v3 v4 v5 v6 v7];
% Switching states
states = [0 0 0;1 0 0;1 1 0;0 1 0;0 1 1;0 0 1;1 0 1;1 1 1];
% Optimum vector and measured current at instant k-1
g_opt = 1e10;
x_opt = 1;

% Read power reference inputs at sampling instant k
Pk_ref = P_ref(1) + 1j*P_ref(2);

% Read current and voltage measurements at sampling instant k
ik = (2/3*(I_abcgrid(1)- I_abcgrid(2)/2 - I_abcgrid(3)/2)) +
1j*(0.57735*(I_abcgrid(2) - I_abcgrid(3)));
vk = (2/3*(V_abcgrid(1)- V_abcgrid(2)/2 - V_abcgrid(3)/2)) +
1j*(0.57735*(V_abcgrid(2) - V_abcgrid(3)));

%Read power measurements at sampling instant k
```

```
Pk = (real(vk)*real(ik) + imag(vk)*imag(ik)) + 1j*(imag(vk)*real(ik) -
real(vk)*imag(ik));
for i = 1:8
    % i-th voltage vector for current prediction
     v_inv = v(i);
    % Current prediction at instant k+1
      ik1 = (1 - R*Tsample/L)*ik + Tsample/L*(v_inv - vk);
      Pk1 = (real(vk)*real(ik1) + imag(vk)*imag(ik1)) +
1j*(imag(vk)*real(ik1) - real(vk)*imag(ik1));
    % Cost function
    g = (abs(real(Pk_ref - Pk1)))*(abs(real(Pk_ref - Pk1))) +
(abs(imag(Pk_ref - Pk1)))*(abs(imag(Pk_ref - Pk1)));

    % Selection of the optimal value
     if (g<g_opt)
        g_opt = g;
       x_opt = i;
    end
end
% Output switching states
Sa = states(x_opt,1);
Sb = states(x_opt,2);
Sc = states(x_opt,3);
P = real(Pk);
Q = imag(Pk);
```